UNIVERSIDADE DE LISBOA

FACULDADE DE CIÊNCIAS

DEPARTAMENTO DE QUÍMICA E BIOQUÍMICA

New Pathways Involved in The Regulation of Epithelial Chloride Transport

Maria Carolina Borges da Silva

Mestrado em Bioquímica e Biomedicina

Dissertação orientado por:
Prof. Doutor Peter Jordan
Doutor Paulo Henrique Carrasquinho de Matos

2023

Agradecimentos

Entre todas as pessoas que tenho de agradecer, começo pelo meu orientador Paulo Matos. Foi o Paulo que me deu o apoio e disponibilidade fundamental para a conclusão desta dissertação. Esteve sempre presente quando necessário.

Estou ainda muito grata pela oportunidade que me foi dada de realizar o meu trabalho de dissertação de Mestrado no Laboratório de Oncobiologia e Vias de Sinalização do Departamento de Genética humana do Instituto Nacional de Saúde Doutor Ricardo Jorge (INSA). Assim quero aqui deixar expressos os meus profundos agradecimentos a esta instituição, nas pessoas do Dr. Fernando de Almeida, presidente do Conselho Directivo do INSA, da Dr.ª Glória Isídro, Coordenadora do Departamento de Genética Humana, e do Prof. Doutor Peter Jordan, Coordenador do Laboratório de Oncobiologia e Vias de Sinalização.

Agradeço ainda ao Prof. Peter, também meu orientador interno na FCUL, por todo o apoio e acompanhamento durante este percurso. Não me posso esquecer, também, de todas as colegas de bancada do laboratório de acolhimento, Ana, Vânia, Patrícia, Márcia, Joana, Cláudia, e as ajudas que me deram tantas vezes. Agradeço em particular à Ana, que não só me guiou por todas as técnicas e me ensinou a trabalhar no laboratório, mas ainda teve a paciência de responder a todas as minhas perguntas.

Aos meus pais, que nunca desistiram de mim: deram sempre importância aos meus estudos e foram o meu pilar durante este trabalho.

Resumo*

A Fibrose Quística (FQ) é uma doença hereditária que afecta cerca de 105 000 indivíduos em todo o mundo. Estima-se que, em populações com descendência europeia, 1 em cada 3000 a 6000 recém-nascidos tenha a doença. A FQ tem origem em mutações do gene CFTR (do inglês, *Cystic Fibrosis Transmembrane Conductance Regulator*). A proteína CFTR codifica um canal de cloreto (Cl^-), expresso maioritariamente na membrana de células epiteliais. Quando o gene sofre mutações, ocorre uma secreção deficiente de Cl^- que provoca alterações eletrolíticas e manifestações patológicas no epitélio de vários órgãos. A FQ é uma doença progressiva, que apresenta um grande número de sintomas e de severidade variável, dependendo do tipo de mutação do gene CFTR e de outras influências genéticas e ambientais. Os sistemas pulmonar e gastrointestinal, são os mais afectados, onde ocorre uma acumulação de muco viscoso que facilita infecções e inflamações pulmonares e obstrução pancreática com consequente malnutrição. A doença pulmonar progressiva, acaba por ser a maior causa de morbidade e mortalidade nos doentes, sendo que a esperança média de vida se encontra actualmente entre os 30 e os 45 anos de idade. O tratamento primário da doença envolve a prevenção e atenuação dos sintomas, e complicações provocadas pela FQ. Mas para aumentar a esperança média de vida é também necessário corrigir a causa molecular da FQ (o defeito da proteína CFTR), e esta vai depender do tipo de mutação do gene que o portador tenha.

Até há data estão identificadas mais de 2000 mutações do gene CFTR. A maioria destas mutações encontra-se associada à doença. A delecção de um único aminoácido, fenilalanina, na posição 508, designada por Phe508del, é a mutação mais comum. Esta mutação é detectada em pelo menos um alelo, em cerca de 70% dos pacientes de FQ. A proteína com a mutação Phe508del apresenta um processamento (*folding)* incorrecto e é alvo do controlo de qualidade do retículo endoplasmático (RE). Durante este processo, a proteína mutante é ubiquitinada e direccionada para degradação, impedindo que a esta chegue à membrana plasmática (MP). As moléculas de CFTR-Phe508del que chegam à superfície das células, apresentam defeitos na função de secreção, devido à abertura deficitária do poro do canal. Adicionalmente, a CFTR-Phe508del na MP apresenta um tempo de vida reduzido (estabilidade deficitária na MP). Actualmente, as terapias direcionadas para o canal com a mutação Phe508del incluem correctores (como VX-809, VX-661, VX-445) e potenciadores (VX-770). Estes moduladores actuam melhorando o *folding*, processamento e tráfego da proteína mutante para a membrana (corrector), bem como a sua função ao potenciarem a abertura do canal na MP (potenciador). No entanto, até á conclusão desta dissertação, não existe nenhum composto aprovado que aumente significativamente o tempo de vida da CFTR-Phe508del na MP. Existe assim, uma necessidade de encontrar novos interactores da CFTR que possam modular a estabilidade do mutante CFTR-Phe508del resgatado farmacologicamente na superfície da célula.

As proteínas que interagem com CFTR são necessárias para a regulação não só do tráfego do canal como da sua função. E, embora vários estudos proteómicos tenham sido realizados para identificar o interactoma global da CFTR, estas abordagens não direcionadas poderão não identificar moduladores com baixa abundância que interajam seletivamente com CFTR localizado na MP, envolvidos na sua estabilização à superfície das células. Nesse sentido, o laboratório de acolhimento tem vindo a realizar vários trabalhos para a identificação de novos interactores que se liguem à CFTR localizada especificamente na superfície da célula. Recentemente, o grupo de trabalho identificou vários potenciais interactores selectivos que evidenciaram novos mecanismos de regulação da ancoragem e tráfego da CFTR na MP. Estes incluem a regulação da estabilidade da CFTR na MP por fosforilação

* Escrito de acordo com o antigo acordo ortográfico.

pela cinase SYK, a regulação da função da CFTR por proteínas moduladas por cAMP. e a regulação da estabilidade da CFTR-Phe508del resgatada na MP por acção da GTPase de baixo peso molecular Rac1 e pela protéase Calpaina. Para uma melhor compreensão destes novos mecanismos e identificação de todos os interactores envolvidos, o grupo de trabalho realizou uma análise proteómica extensa. Desta resultou uma lista de potenciais novos moduladores da estabilidade da CFTR-Phe508del farmacologicamente resgatada na MP de células das vias respiratórias. Neste sentido, o principal objectivo deste trabalho foi a validação e caracterização do impacto de algumas das proteínas candidatas identificadas na abundância, resgate farmacológico, estabilidade na MP e função de transporte de Cl^- da proteína CFTR-Phe508del em células epiteliais brônquicas.

Foi observado que a regulação negativa das proteínas candidatas TCP-1-Theta e FLT-1 não afectaram a abundância do canal CFTR-Phe508del na MP, após o resgate farmacológico do mesmo. Este resultado está em conformidade com o esperado, visto que as funções conhecidas para TCP-1-Theta (uma subunidade da chaperona CCT) e Flt-1 (um receptor de factores angiogénicos), não estão relacionadas com o canal CFTR. Quando foi realizada a regulação negativa da proteína Calgranulina (uma molécula *DAMP*), foi observado uma redução ligeira dos níveis de CFTR-Phe508del maturo (proteína glicosilada, banda C) nos níveis totais da célula. O resultado indica que a redução de Calgranulina poderá interferir com o tráfego do RE para o complexo de Golgi da proteína imatura (não glicosilada, banda B) de CFTR ou a sua maturação no complexo de Golgi. No entanto a abundância do canal resgatado CFTR-Phe508del na superfície da célula não se alterou. Estas observações geraram interesse para estudos posteriores, pois é conhecido que Calgranulina encontra-se regulada positivamente em várias condições patológicas, nomeadamente em pacientes com FQ.

A redução dos níveis da proteína Tenascina-C (glicoproteína da matriz da célula), reduziram a abundância do canal na MP, sugerindo assim um papel desta proteína na estabilidade de CFTR-Phe508del na superfície da célula. Foi também demonstrado que Enigma (proteína scaffold) e Coronin 1C (regulador do citoesqueleto) afectam os níveis totais de CFTR-Phe508del maturo na célula e na MP, sugerindo que estas proteínas possam afectar o tráfego RE-Golgi de CFTR imaturo. Confirmamos que este resultado é específico para CFTR-Phe508del, pois a regulação negativa das proteínas Enigma e Coronin 1C não afetaram a abundância de CFTR-wt na totalidade da célula ou na MP. Foi ainda observado que a depleção da proteína Ku86 (subunidade de DNA-PK) parece fazer decrescer os níveis de mRNA de CFTR-Phe508del e, por conseguinte, a abundância do canal resgatado na membrana plasmática. Estes resultados ainda requerem confirmação. O mesmo foi observado para as proteínas βII Espectrina (citoesqueleto), PTRF (factor de transcripção e componente de caveolae), Lamin (componente da lamina) e TG2 (transglutaminase). O que sugere um papel destas proteínas na regulação da transcrição ou estabilidade do mRNA do canal. Sugerimos também, que βII Espectrina tenha um papel no tráfego para a membrana e na abundância de CFTR-Phe508del na membrana.

Resumindo, foi observado que algumas proteínas em estudo estão envolvidas na manutenção da abundância de CFTR-Phe508del resgatado farmacologicamente, no total da célula e na membrana plasmática. No entanto, nenhuma pareceu constituir um bom alvo para o resgate farmacológico do canal CFTR ou a sua retenção na MP. Contudo, não deve ser ignorado a realização de estudos posteriores para compreender o mecanismo pelo qual estas proteínas aparentam afectar a abundância do canal CFTR-Phe508del. E perceber se as proteínas ou a sua desregulação poderá estar envolvida na patologia da doença Fibrose Quística, ou contribuir para uma resposta diferencial de drogas moduladoras de CFTR para pacientes com genótipos de CFTR equivalentes. A continuação da

investigação poderá também identificar novos interactores de CFTR-Phe508del que podem ser interessantes para a descoberta de novos moduladores de CFTR.
Palavras-chave:

Fibrose Quística, CFTR, Phe508del, abundância de CFTR na membrana plasmática, interactoma da CFTR

Abstract

Cystic Fibrosis (CF) is an autosomal recessive disorder caused by mutations on the cystic fibrosis transmembrane conductance regulator (CFTR) gene. The gene encodes a chloride channel (Cl^-) expressed at the plasma membrane (PM) of epithelial cells. The deletion of phenylalanine 508 (Phe508del) is the most common mutation, it causes the protein to misfold and be prematurely degraded, failing to reach the PM. The use of recently clinically approved CFTR modulator drugs has changed CF management, enabling the rescue of several CFTR mutant proteins, including Phe508del-CFTR folding, trafficking, and function at the PM. However, these rescued channels still exhibit evidence of a reduced half-live at the PM, indicating space for improvement in CF therapeutic strategies. Previous work of the host lab identified new cellular pathways and key interactor proteins that were shown to influence the retention of rescued Phe508delCFTR at the PM. The group identified a short list of candidate proteins that could constitute new targets for pharmacological modulation of rescued Phe508del-CFTR stability at the PM of airway cells. Therefore, the objective of this project was to validate and characterize the effect of 11 of these candidate proteins on the pharmacologically rescued Phe508del-CFTR. We found that downregulation of Calgranulin, TCP-1-Theta and FLT-1 did not change the abundance of rescued Phe508del-CFTR at the PM, but Tenascin-C downregulation did. We suggest a role for Tenascin-C in regulating Phe508del-CFTR permanence at the PM. We observed a reduction of rescued Phe508del-CFTR after Coronin 1C and Enigma knockdown, suggesting that they affect CFTR ER-Golgi traffic. We saw a reduction on CFTR mRNA levels for Ku86 knockdown, however this result still needs confirmation. We also demonstrated that βII Spectrin, PTRF, TG2 and Lamin affected Phe508del-CFTR expression, and propose an additional role for βII Spectrin in Phe508del-CFTR traffic to, and abundance at the PM.

Keywords:

Cystic Fibrosis, CFTR, Phe508del, CFTR abundance at the plasma membrane, CFTR interactome

Table of Contents

List of Figures

List of Tables

Abbreviations

ABC transporter	ATP-Binding Cassette Transporter
ADLD	Autosomal Dominant Leukodystrophy
ATP	Adenosine Triphosphate
ASL	Airway Surface Liquid
ASOs	Antisense Oligonucleotides
CAL	CFTR-Associated Ligand
cAMP	cyclic Adenosine Monophosphate
CAP70	CFTR-Associated Protein 70
CCT	Chaperonin Containing T-complex Polypeptide
cDNA	complementary DNA
C-ERMAD	C-terminus ERM association domain
CF	Cystic Fibrosis
CFTR	Cystic Fibrosis Transmembrane Conductance Regulator
Cl^-	Chloride
Coro 1C	Coronin 1C
C-Terminal	Carboxyl Terminal
DAMP	Damage-Associated Molecular Pattern
DNA-PK	DNA-dependent Protein Kinase
DTT	Dithiothreitol
EBD	Ezrin-Binding Domain
ECL	Enhanced Chemiluminescence
ECM	Extracellular Matrix
ENaC	Epithelium Sodium Channel
ER	Endoplasmatic Reticulum
ERAD	ER-Associated Degradation
ERM	Ezrin-Radixin-Moesin
ERQC	ER Quality Control
F-actin	Filamentous Actin
FBS	Foetal bovine serum
GITC	Guanidine Isothiocyanate

$HCO3^-$	Bicarbonate
HRP	Horseradish Peroxidase
Hsc70	Heat shock cognate 70-kD protein
InsR	Insulin Receptor
MCC	Mucociliary Clearance
MEM	Minimal Essential Medium
MSD	Membrane-Spanning Domain
Na^+	Sodium
NBD	Nucleotide-Binding Domain
N-ERMAD	N-terminus ERM association domain
NHERF1	Na/H Exchanger Regulatory Factor 1
NHS	N-hydroxysuccinimide
NSAIDs	Nonsteroidal Anti-Inflammatory Drugs
N-Terminal	Amino Terminal
PDZK1	PDZ Domain-Containing in Kidney 1
PIGF	Placenta Growth Factor
PIP	1-phosphatidyl-1D-myo-inositol-4-phosphate
PIP2	1-phosphatidyl-1D-myo-inositol-4,5-bisphosphate
PIP5K	Phosphatidylinositol-4-phosphate-5-inase
PKA	Protein Kinase A
PKC	Protein Kinase C
PM	Plasma Membrane
Pol I	RNA Polymerase I
PPQC	Peripheral Protein Quality Control
PTC	Premature Stop Codon
PTRF	Polymerase I and Transcript Release Factor
PVDF	Polyvinylidene Fluoride
QPol2	RNA polymerase II
QR	Quenching Rate
RD	Regulatory Domain
RISC	RNA-Induced Silencing Complex

rPhe508del-CFTR	Rescued Phe508del-CFTR
RT	Reverse Transcription
RT-PCR	Reverse Transcription-Polymerase Chain Reaction
SA	Streptavidin
SDS-PAGE	Sodium dodecyl sulphate – polyacrylamide gel electrophoresis
Shank2	SH3 and ankyrin repeats containing protein 2
siRNA	Short Interference RNA
TCP-1-theta	T-Complex Protein 1 subunit theta
TNC	Tenascin-C
TBE	Tris-Borate with EDTA
TG2	Transglutaminase 2
Tm	melting temperature
VEGF	Vascular Endothelial Growth Factor
WB	Western Blot
YAP	Yes Associated Protein
βII Spectrin	Spectrin Beta chain, non-erythrocytic 1

1. Introduction

1.1. Cystic Fibrosis

Many epithelial cells regulate chloride (Cl^-) secretion trough modulating cystic fibrosis transmembrane conductance regulator (CFTR) channel activity [1–3]. The CFTR channel creates an electric driving force (lumen-negative) for paracellular sodium secretion, and this movement generates an osmotic driving force for water flow necessary for epithelial function [1,2,4]. The disruption of genes encoding proteins that mediate epithelial processes can result in disease [1]. Cystic fibrosis (CF) is an example of a disease caused by mutations on the chloride channel CFTR [5].

Cystic fibrosis is an autosomal recessive disorder [5]. Being the most common life-threatening disease in Caucasians, it affects about 105 000 people worldwide [†], with an estimated incidence of 1 in 3000-6000 new-borns in European descendent populations [6,7]. Birth prevalence has recognized heterogeneity in the geographic distribution [7]. In fact, within Europe, United kingdom, Germany and France are three of the countries with more CF patients reported. While worldwide it is Europe, North America and Australia who have the highest birth prevalence, and Africa and Asia have low birth frequencies [7–9].

Mutations in the CFTR gene are the fundamental cause of CF [10]. In cystic fibrosis, CFTR channel is missing or defective, impairing secreted fluid volume and composition in several organ systems [2,11]. CF presents itself with a wide range in severity and manifestation [10].

1.1.1. CFTR Protein - Structure and Function

CFTR is a glycoprotein, found primarily in epithelial tissues where it localizes to the apical cellular membrane [2,5,11]. It functions as an anion channel with the capacity for regulating secretion of Cl^-, bicarbonate (HCO_3^-) and small amounts of other anions, being determinant to maintain ion and fluid homeostasis [2,10,11].

The CFTR gene is found in chromosome 7 and encodes a 1480-amino-acid protein (~160 kDa) member of the ATP-Binding Cassette (ABC) transporter family. The protein is composed by two transmembrane domains (MSD1 and MSD2, both containing six membrane-spanning alpha helixes), each followed by a cytosolic nucleotide-binding domain (NBD1 and NBD2). And, located between two MSD-NBD complexes is a regulatory domain (RD) that contains multiple consensus phosphorylation sites (see Figure 1.1). The MSDs regions contribute to the formation of the pore, the R domain phosphorylation controls channel activity, and the NBDs bind and hydrolyse ATP to regulate channel gating (opening and closing) [1,5,10–12].

[†] https://www.cff.org/intro-cf/about-cystic-fibrosis
Site accessed at 18th September 2023

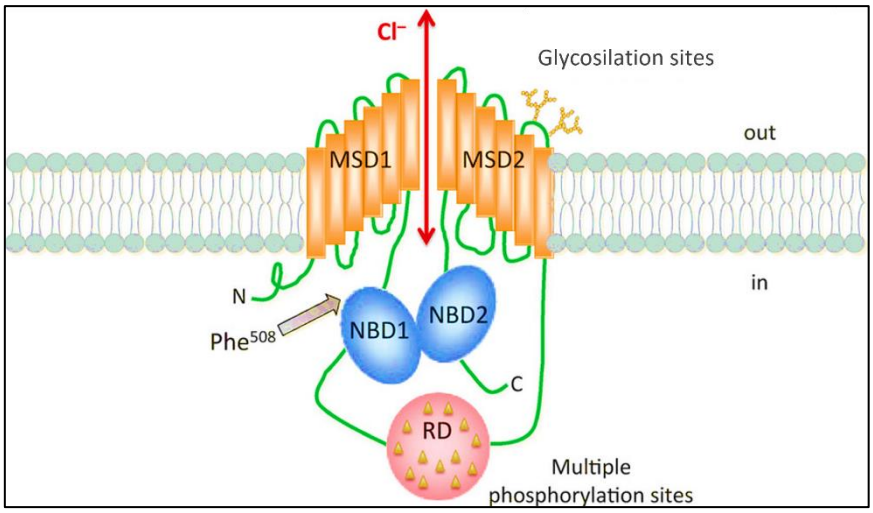

Figure 1.1 – Structure of CFTR inserted into the plasma membrane. The representation shows CFTR domains: the membrane-spanning domains MSD1 and MSD2, the regulatory domain RD, and the nucleotide-binding domains, NBD1 and NBD2. It is also indicated the position of the most frequent mutation (Phe508del) in NBD1, as well as glycosylation and phosphorylation sites at MSD2 and R domain, respectively. [Adapted from [13]].

CFTR is regulated by protein kinase A (PKA) in a cAMP-dependent way [10–12]. First, the increase of cAMP activates PKA, which in turn phosphorylates multiple serine residues within the R domain, enabling channel gating. The extent of R domain phosphorylation controls the probability of channel opening (i.e., the level of activity). Then channel gating is regulated by a cycle of ATP hydrolysis at the NBDs. ATP binding leads to the dimerization of NBD and opening of the channel while ATP hydrolysis translates into the separation of the NBDs, decreasing the frequency of chloride channel opening [10,11,14,15]. The channel returns to its quiescent state when phosphatases dephosphorylate the R domain [10,11]. Cl^- secretion is regulated by modulating not only channel activity, but also by regulating the total number of CFTR channels in the membrane. Mutations in CFTR affect the number of channels in the plasma membrane (PM), channel activity and the protein intracellular trafficking [16].

CFTR also regulates several transport proteins, including the epithelium sodium channel (ENaC), potassium channels, ATP-release mechanisms, anion exchangers, sodium-bicarbonate transporters, and aquaporin water channels [10–12,16]. In the airways, CFTR is an inhibitor of ENaC, limiting sodium reabsorption, and thus in CF there is sodium (Na^+) hyperabsorption [1,16].

The single residue deletion of phenylalanine in position 508 (Phe508del), detected in at least one allele in ~70% of CF patients is located in the surface of the first NBD [5,10,12].

1.1.2. Pathophysiology

Mutations in the CFTR gene are the fundamental cause of the CF autosomal recessive disease [10,17]. CF is a progressive multisystem disease, presenting a wide range of manifestations and varying severity dependent on the type of mutation of the CFTR gene and other genetic and environmental influences [10,18–20]. CF most common symptoms include progressive lung disease and chronic digestive conditions, with pulmonary complications being the major cause of morbidity and mortality for patients [18,20].

CFTR and ENaC help to regulate homeostasis of the epithelium by controlling the movement of water. However, with the impairment of CFTR, there is hyperabsorption of Na^+ and subsequent dehydration of the epithelial surface, leading to abnormal mucus with altered concentration of its components (e.g., mucins) and biophysical properties. Bicarbonate, an alkalising agent that helps in pH buffering and mucin expansion, also has decreased secretion in CF pathophysiology, resulting in a lower epithelial

surface pH, and defective mucin expansion that results in the formation of a sticky and dense mucus [20]. Mucins, one of mucus components, are large O-linked glycoproteins produced by specialised secretory cells, that are stored and compacted in intracellular granules with high concentrations of Ca^{2+}. These cations shield mucins negative charge preventing their expansion. After mucin exocytic release, HCO_3^- ions sequester $Ca^{2+}$and promote alkalinisation, facilitating mucin expansion and hydration on mucus formation. Because of all this aspects, the disease pathogenesis is characterized by accumulation and obstructing of thick mucus in multi mucin producing organs, such as lungs, sinuses, intestine, pancreas and reproductive organs [20–22].

In the airways, dehydration leads to airway surface liquid (ASL) volume depletion, increasing mucus concentration and reduced mucociliary clearance (MCC), facilitating bacterial growth and infection and triggering inflammation [20]. In the intestine, plugging of the terminal ileum, referred to as meconium ileus, is one of the earliest manifestations of CF and may lead to ischaemic necrosis of the ileus wall [18]. Also, the prolonged acidity following food uptake and dehydrated intestinal mucus facilitates bacterial growth in the gastrointestinal tract. In the pancreas, the obstruction of ducts by mucus causes autodigestion by pancreatic enzymes. About 85% of CF patients have severe loss of pancreatic tissue and the inadequate secretion of digestive enzymes leads to malabsorption of proteins and fat-soluble vitamins A, D, E and K [18–20].

Fertility is affected in both male and female CF patients. Approximately 97-98% of males with CF are infertile due to absent or atretic vas deferens and dilated or absent seminal vesicles that lead to azoospermia [18,21,23,24]. And while infertility in woman is not so recurrent, only ~50% of woman with CF are able to conceive a child [24]. While mucus gland hyperplasia, cervical erosions and cervicitis are common, altered ion and fluid transport throughout the female reproductive track, endocrine abnormalities and menstrual irregularities may also account for infertility in CF woman [18,21,24]

Pharmacological and non-pharmacologic treatment exists to relief symptoms and complications caused by the disease [25]. This primary therapy does not treat the molecular cause of the disease (i.e., defective CFTR protein), but allows the prevention and progression of the symptoms (i.e., management of CF), and extends life expectancy into adulthood [25–27]. It includes the use of antibiotics, nonsteroidal anti-inflammatory drugs (NSAIDs), mucolytics, physiotherapy, pancreatic enzyme and vitamin supplements, and attention to the diet [19,25,26,28]. To treat the disease beyond the symptoms means to further increase the life expectancy of CF patients [26]. Recently, new drugs have been developed that target the basic defects associated with CFTR gene mutations, enabling rescue of the mutated protein expression and function in CF patients (see below). However, this approach is still dependent on the type of mutations carried by the patient and only the most common mutations have successfully addressed [19,20,25,28].

1.1.3. Class Mutations and Current Therapeutic

There are over 2100 CFTR gene mutations reported to this date [‡], with most of them being disease-causing mutations [§]. The large number and variety of mutations imposes the classification of each CFTR mutant into one of six established functional classes (see Figure 1.2), in which the same therapeutic strategy may be effective. Nevertheless, many of the molecular and cellular defects underlying each of the multiple disease-causing mutation identified still require further clarification,

[‡] http://www.genet.sickkids.on.ca/StatisticsPage.html
Site accessed at 27th September 2022
[§] https://www.cff.org/What-is-CF/Genetics/Types-of-CFTR-Mutations/
Site accessed at 27th September 2022

which has limited not only their classification but also the development of mutation-specific corrective therapies [26,29].

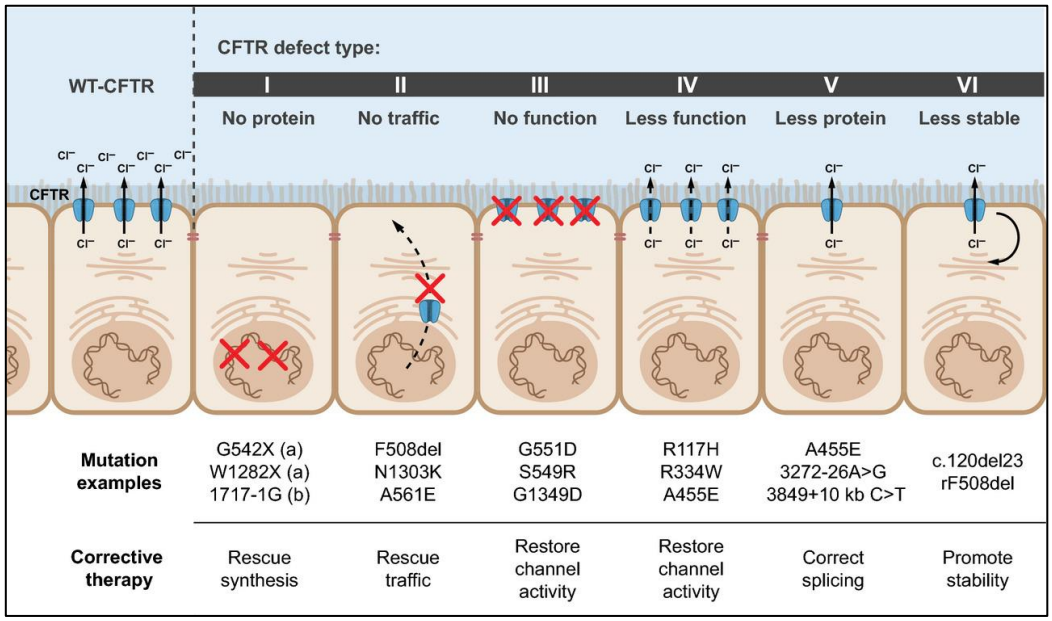

Figure 1.2 - Classes of CFTR gene mutation. CFTR mutations are classified into one of six established functional classes, where the same therapeutic correction can be applied. Examples of mutations of each class are shown. [Adapted from [26]].

Class I, also called "no protein" class, includes mutations (e.g., G542X, R553X, R1162X and W1282X) that generate a premature stop codon (PTC) into the CFTR mRNA because of splice site abnormalities, frameshifts due to insertions or deletions, or nonsense mutations [26,29–31]. These mutations, abrogate CFTR protein synthesis or result in translation of shortened, truncated forms. The current therapeutic strategy for class I mutants comprises the use of read-through compounds. These agents induce a ribosomal "over-reading" of a PTC, enabling the continued translation to the normal end of the transcript. ELX-02 (NB124; Eloxx Pharmaceuticals) is a synthetic glycoside that can restore CFTR expression and function in cells expressing PTC mutations and, its currently undergoing phase II clinical trials (NCT04126473 and NCT04135495, https://www.eloxxpharma.com/pipeline/) [32,33]. For the class I mutants that involve small deletions/insertions, there is no therapeutic strategy except the bypass therapies that target other channels (non-CFTR) [26].

Class II, also called "no traffic protein" class, comprises mutants that fail to traffic to the cell surface, due to misfolding and premature degradation by the endoplasmatic reticulum (ER) quality control (ERQC) [26]. Therapy for this class uses correctors (chemical chaperones or protease modulators) that rescue folding, processing and trafficking to the plasma membrane of CFTR class II mutants [26,30]. These compounds usually enhance protein conformational stability during the ER folding process. This class includes the most common CF-causing mutation, Phe508del and, given its frequency, much effort has been put into identification of chemical and molecular chaperones that rescue folding of these mutant proteins [29]. Lumacaftor (VX-809; Vertex Pharmaceuticals), Tezacaftor (VX-661; Vertex Pharmaceuticals) and Elexacaftor (VX-445; Vertex Pharmaceuticals) are all correctors approved for clinical use for patients with Phe508del mutation, in a combinatory therapy with a potentiator (see below). The co-treatment with Lumacaftor/Ivacaftor (Orkambi®) is approved for Phe508del-homozygous patients, and co-treatment with Tezacaftor/Ivacaftor (Symdeko®) is approved for Phe508del-homozygous and -heterozygous (with residual function mutations in trans) patients. The triple combination Tezacaftor/Ivacaftor/VX-445 (Trikafta®) has been recently approved for the

treatment of CF patients with Phe508del in at least one allele. Other correctors are also under study and already in phase II clinical trials, ABBV-2222 (Galicaftor; Abbvie/Galapagos) or VX-121 (Vertex Pharmaceuticals) [30].

Class III it is called "no function" and includes CFTR mutants (e.g., G551D) that reach the plasma membrane but exhibit defective channel gating (i.e., the channel pore does not properly open) due to impaired response to channel agonists[1,2]. When Phe508del-CFTR is promoted to reach the plasma membrane by corrector compounds, it still has a partial gating defect, and thus, corrector-rescued Phe508del proteins can also be considered to be class III mutants. Class IV mutants (e.g., R334W) show substantially reduced conductance (i.e., decreased flow of ions), with a resulting decrease in net Cl^- channel activity. The class is also called "less function". The gating defects of class III and IV mutants can both be overcome with potentiators, compounds that restore or even enhance the channel open probability [26,30]. Several class III mutations, including G551D have approved clinical use of potentiator Ivacaftor (VX-770, Kalydeco®, Vertex Pharmaceuticals). The drug binds and potentiates CFTR function by promoting decoupling between ATP hydrolysis and gating cycles. Treatment with Ivacaftor has shown to improve clinical condition of patients, reducing sweat chloride levels to near normal values and slowing deterioration of lung function. As discussed above, Ivacaftor is also used in co-treatment with other correctors for patients with Phe508del mutation, because even after rescue of intracellular retention by corrector drugs, the mutant protein still presents a gating defect [29]. Several other potentiators have demonstrated promising effects and are currently under experimental and clinical investigations [e.g., VX-561 (deutivacaftor; Vertex Pharmaceuticals)].

Class V, also called "less protein" class, includes mainly alternative splicing mutants (e.g. 3272-26A>G) that allow synthesis of some normal CFTR mRNA (and functional protein), albeit at very low levels [26]. The therapeutic strategy for these mutants is either to enhance the activity of normal channels already at the cell surface or to achieve correct splicing [26,30,31]. The treatment with Ivacaftor for some splicing mutations was shown to improve the average open probability and conductance of CFTR channels present at the PM [26,30]. The use of antisense oligonucleotides (ASOs) is understudy and appears to be promising to correct some of the splicing defects [30]. Class V also includes promoter mutations that reduce transcription (e.g. -94G>T) and amino acid substitutions that cause inefficient protein maturation (e.g., A455E). Therapies under investigation include compounds that increase expression of CFTR mRNA (i.e., amplifiers). PTI-428 (Nesolicaftor; Proteostasis Therapeutics) is an amplifier, with phase I and II clinical trials completed, that in combination with other correctors and potentiators was shown to improve lung function [30].

Class VI is also called "less stability" class and includes CFTR mutants that although are present at the PM and are functional, they have intrinsic plasma membrane instability (i.e., reduced half-life) [26,30]. As such, proper therapeutic approaches will require the use of compounds that enhance CFTR retention/anchoring at the cell surface (tentatively called stabilizers), to reduce or prevent the mutant proteins' removal from the PM and their degradation by lysosomes [26,30]. Due to its intrinsic instability, Phe508del-CFTR also behaves as a class VI mutant when rescued by correctors to the cell surface.

The therapy with use of modulators for the correction of the molecular defects of mutant CFTR proteins is, at present, not sufficiently effective to be used as stand-alone treatments [27]. Thus, conventional symptomatic therapies remain important until disease manifestations can be prevented by eliminating the cause of the disease and blocking the pathophysiological cascade. Currently, there are several promising approaches under-investigation to restore CFTR channel function regardless of the

type mutation. These include not only new modulator compounds but also gene therapy, gene-editing using CRISPR/cas9 technology, RNA therapy, and therapeutic miRNAs [25].

1.2. CFTR Interactions

A variety of proteins have been identified to interact directly or indirectly with CFTR, impacting the channel function, localization and processing within cells [34,35]. These proteins include transporters, ion channels, receptors, kinases, phosphatases, signalling molecules, and cytoskeletal elements [35]. CFTR interactions mostly occur between the cytosolic amino or carboxyl (N- or C-) terminal tails of CFTR and its binding partners, either directly or mediated/regulated through various adptor proteins, including PDZ-domain containing proteins [34,35]. PDZ domains are conserved protein-interaction modules, that typically mediate interactions with the C-termini of target proteins containing a PDZ motif, such as CFTR [34,36]. Different PDZ proteins have been reported to bind with various affinities to the C-terminal tail of CFTR at the apical membrane: NHERF1 (Na/H exchanger regulatory factor 1), NHERF2 (also called NHE3 kinase A regulatory protein, E3KARP), PDZK1 (PDZ domain-containing in kidney 1, also called NHERF3 and CFTR-associated protein 70 [CAP70]), PDZK2 (also called NHERF4 and intestinal and kidney-enriched PDZ protein [IKEPP]), and Shank2 (SH3 and ankyrin repeats containing protein 2, also called Cortactin-binding protein 1 [CortBP1]) [34–36]. CFTR-associated ligand (CAL) is also a PDZ domain-binding protein that interacts with the CFTR C-terminus, but is primarily localized to the Golgi [37]. CAL is an overall negative modulator of surface expression of CFTR. It was suggested that CAL retains CFTR in the cell and target CFTR for degradation [38]. Shank2 is also a negative regulator of CFTR, inhibiting the cAMP-induced phosphorylation and activation of the channel [35].

NHERF1 and NHERF2 both contain two PDZ domains and a ERM-binding domain within their C-terminal tails that tethers them to the actin cytoskeleton via binding to ezrin in a phosphorylation-dependent manner [35,39,40]. Previous studies have shown that the interaction between CFTR, NHERF1 and ezrin is responsible for the anchoring of the channel to the cortical actin cytoskeleton, which is critical for CFTR's retention at the PM (see below) [40]. NHERF2 was also reported as being able to functionally stabilize CFTR at the cell-surface [35,40], and ezrin was also described to function as an anchoring protein for PKA, a regulator for CFTR activity in epithelial cells [4,41]. It has been argued that CFTR can forms a multicomplex with several proteins at the PM, including NHERF proteins, ezrin, and PKA [42].

1.2.1. PM Anchoring of CFTR

Like described above, various PDZ domain proteins may stabilize and retain CFTR in the apical plasma membrane as well as regulate the exocytic and endocytic trafficking of CFTR by interacting with the C-terminal PDZ-motif of CFTR [43]. NHERF1 stabilizes and enhances the half-life of CFTR at the apical membrane. NHERF1 anchors CFTR to the apical membrane by interacting with actin cytoskeleton via interaction with ezrin [40], leading to up to 50% of surface CFTR existing in an immobile pool, tethered to filamentous actin (F-actin) [44].

NHERF1 is a scaffold protein with two tandem PDZ domains (PDZ1 and PDZ2) at the N-terminus, and an ezrin-binding domain (EBD) at its C-terminus [45]. Both PDZs have bidding affinity for the PDZ-binding motive at the C-terminal tail of CFTR [46,47]. NHERF1 can also be held in a partially inactive conformation through intramolecular interactions between PDZ2 and the C-terminus [48]. This conformational constrain is relieved upon binding of ezrin, which not only allows its anchoring to F-

actin but also enables the binding of CFTR to NHERF1's PDZ2 with a higher affinity [48–50]. This strengthens the retention of CFTR at the apical membrane [51].

Ezrin is a member of the ezrin-radixin-moesin (ERM) protein family, with a N-terminus FERM domain (also known as N-ERMAD domain) and C-terminus ERM association domain (C-ERMAD) that can associate with plasma membrane proteins or membrane protein adaptors and the F-actin cytoskeleton, respectively [45,52]. It is through N-ERMAD that ezrin interacts with the C-terminal ERM-binding domain of NHERF1 [45,52]. However, in the cytoplasm, ezrin is held inactive through an intramolecular interaction between N-ERMAD and C-ERMAD, masking membrane and actin F-actin binding sites [53]. Activation of ezrin is a several-step process. Briefly, Rac1 stimulation of phosphatidylinositol-4-phosphate-5-kinase (PIP5K) leads to the conversion of 1-phosphatidyl-1D-myo-inositol-4-phosphate (PIP) at the membrane to 1-phosphatidyl-1D-myo-inositol-4,5-bisphosphate (PIP2) [54]. PIP2 binding to ezrin, activates the protein, and induces conformational change allowing the phosphorylation of threonine 567 (T567) in the C-ERMAD. These events unmask both membrane protein and actin binding sites and leading to ezrin correct apical localization [55]. Other kinases implicated in ezrin phosphorylation are Rho-kinase, protein kinase C (PKC) α and PKC θ [56–58].

1.2.2. CFTR PM Regulation

CFTR is subjected to a quality control whilst traveling through the secretory pathway. Regulating its folding, stabilization, or degradation and eventually its functional protein levels [59,60]. CFTR proteins that do not reach full maturation are removed by ER-associated degradation (ERAD). Misfolded proteins are recognized by ER-associated molecular chaperones, ubiquitinated and transported to the proteasome for degradation [61–63]. After reaching the cell surface, CFTR is also the substrate of peripheral protein quality control (PPQC), that regulates its endocytosis [64].

In the apical plasma membrane, CFTR can be found both at the cell surface and in the endosomal compartments at subapical region. The distribution is regulated through endocytosis and recycling/exocytic pathways [65–67]. Briefly, CFTR endocytosis is clathrin-dependent, and occurs through Rab5-positive endosomes [65,68,69]. It is mediated by the recognition of multiple endocytic motifs of CFTR C-terminal tail by the endocytic adaptor complex AP-2 [67,70,71]. CFTR residing in endosomes can either be selected for lysosomal degradation, or recycled to the plasma membrane [64,69,72]. Endocytic recycling of CFTR from early endosomes to the plasma membrane occurs through Rab11-positive vesicles, and is facilitated by Rme-1 and NHERF-1 PDZ domain interaction [50,69,72,73]. In addition, CAL, syntaxins, and Rho family GTPase TC10 affect the endocytic trafficking and plasma membrane expression of CFTR [38,50,73]. Misfolded CFTR, such as Phe508del-CFTR, has a decreased apical membrane half-life [61,73]. It is recognized by the PPQC and targeted for lysosomal degradation, preventing the channel from recycling [61,62,64,69]. The unfolded cytoplasmic regions of CFTR are recognized by heat shock cognate 70-kD protein (Hsc70) in concert with co-chaperone DNAJA1 and possibly by the Hsp90 machinery. The interaction with chaperone-cochaperone complex recruits E3 ubiquitin ligase CHIP, leading to ubiquitination of the misfolded CFTR its endocytosis and subsequent lysosomal degradation [62].

1.2.3. CFTR Interactome Research

CFTR research already led to the therapeutic development of modulators that rescue the basic defect in CF. But there is a continuous interest in studying CFTR molecular disease mechanisms for additional therapeutic options. This will entail a better understanding of, for instance, the mechanisms through which protein-protein interactions affect CFTR biogenesis, trafficking, and function. Finding

which interactions are critical to rescue CFTR and which are altered by modulators or CFTR mutations [64]. Several studies are using proteomics to assess global CFTR protein interactions (the CFTR interactome), identifying new and previously documented interactors of CFTR, be it direct or indirect, while focusing on the key differences in wt and Phe508del proteomes [74,75].

In ongoing effort to determine the CFTR interactome at the PM, my host lab used proteomics to characterize CFTR's protein interacting network with the aim of identifying novel pharmacological targets to rescue CFTR function in CF [76]. The group used three complementary approaches: capturing and identifying proteins binding SYK kinase-phosphorylated CFTR, protein complexes involved in cAMP-mediated CFTR stabilization at the PM, and proteins selectively interacting at the PM with rescued Phe508del-CFTR but not wt-CFTR [76]. The network analysis was focused on proteins never described to interact with or regulate CFTR. The host group identified candidate proteins that are involved in the regulation of CFTR membrane traffic and/or its retention at the PM. The proteins encoded by the Calpain1, GABARAP, NOS2, and SMURF1 genes were validated for their robust interaction with CFTR-containing protein complexes and for their ability to modulate the amount of CFTR expressed at the cell surface of bronchial epithelial cells [76].

However, the host lab identified an additional shortlist of candidate proteins that could also participate in the modulation of rescued Phe508del-CFTR stability at the plasma membrane of airway cells. Eleven of these proteins were selected to be validated during this MSc dissertation project, namely: Tenascin-C, Calgranulin-A, Coronin-1C, Spectrin, Enigma, TCP-1-theta, Cavin-1/PTRF, TG2, Ku86, Lamin B1, and FLT-1.

1.2.4. Previously reported functions of the selected candidate proteins

Tenascin-C (TNC, gene *Tnc*, Uniprot ID P24821) is a extracellular matrix (ECM) glycoprotein that binds ECM components (e.g., fibronectin, collagen, proteoglycans of the lectin family), cell surface receptors (e.g., integrins, EGF receptor, TLR4), soluble factors (e.g., Wnt3a, TGFβ, VEGF), and pathogens (e.g., Streptococcus, HIV) [77–80]. With a controlled pattern of expression, it is expressed in the embryo in sites of tissue morphogenesis, and in the healthy adult tissue is most prominent in stem cell niches and tendons [77,80,81]. It is transiently re-expressed upon tissue injury, infection and inflammation [77,80,82]. TNC is also expressed in other pathological conditions such as cancer and chronic inflammation (e.g., rheumatoid arthritis), and in a variety of cardiac diseases [77–79,82]. TNC is a stress protein that modulates cell adhesion, migration and proliferation, with a context-specific mode of action and cell type response [77,79,82].

Calgranulin-A (S100A8 or MRP8, gene *S100a8*, UniProt ID P05109) is a calcium-binding protein found both intra- and extracellularly, and is induced in myeloid cells, dendritic cells, microvascular endothelial cells, epithelial cells and fibroblasts [83–85]. Intracellular S100A8 is implicated in myeloid and keratinocyte differentiation and exerts anti-inflammatory effects in a Ca^{2+}-dependent manner. The protein can form the heterodimer with calprotectin S100A9 (S100A8/A9), which is involved in cytoskeleton modulation. S100A8 and S100A8/A9 are damage-associated molecular pattern (DAMP) molecules. Released by activated or damaged cells during inflammatory processes, they initiate and modulate local inflammation and innate immune responses by binding to receptors like TLR4 and RAGE, and activating different signalling pathways (e.g., ERK, NF-kB) [84–87]. S100A8 has the capacity to induce expression of MUC5AC (the mucin in airway mucus) production in airway epithelial cells [86]. S100A8/A9 is chemotactic for neutrophils, has antimicrobial functions, and modulates cell proliferation, differentiation and apoptosis [84,87]. S100A8 and S100A8/A9 are upregulated in

inflammatory diseases and tumors [84,85]. S100A8/A9 is found with high circulating levels in patients with obesity, Alzheimer's disease and cystic fibrosis [84,87,88].

Coronin 1C (Coronin 3, gene *Coro1C*, UniProt ID Q9ULV4) is a type I coronin. Coronins are regulators of the actin cytoskeleton and are implicated in actin-based processes such as cell motility. Like other type I coronins, Coro1C binds to F-actin and associates with the Arp2/3 complex (which nucleates actin branching) [89,90]. Coro1C interacts as well with the GDP-bound form of Rab27a (a regulator of membrane trafficking) [91]. Coro1C regulates ER recruitment for ER-associated endosome fission, and Rac1 (a key regulator of the actin cytoskeleton and CFTR anchoring) distribution on the cell [54,92,93]. The protein is ubiquitously expressed and localizes to cytoskeleton and leading edge lamellipodia, and is associated to membranes [92–94].

βII Spectrin (Spectrin Beta chain, non-erythrocytic 1, gene *SPTBN1*, UniProt ID Q01082) is the β chain of Spectrin, a cytoskeletal protein involved in maintaining cell shape and integrity [95–97]. βII spectrin is expressed in all nucleated cells and localizes to the membrane, Golgi apparatus, ER, vesicles and nucleus [95,96,98]. βII spectrin can form a large polymer complex with ankyrin and actin that, functionally couples integral membrane proteins (ion channels, receptors, transporters) with the cytoskeletal infrastructure [99]. The protein is engaged in biogenesis of the lateral membrane domains of epithelial cells, and compaction and accumulation of e-cadherin in the epithelial cell-cell contact [100,101]. βII Spectrin participates in delivery of proteins and phospholipids to the membrane, serves as a major scaffolding protein, and participates in cell cycle regulation by involvement in TGFβ signalling [95,98–100]. It is also involved in neuronal development and function, and is implicated in neurological disorders [102]. Defects in the protein have been associated with cardiac pathologies, and knockdown in epithelial cells results in loss of the lateral membrane and changes in cell morphology [99,101].

Enigma (LMP-1, gene *PDLIM7*, UniProt ID Q9NR12) is a cytosolic protein with a PDZ domain and three LIM domains that function as protein-protein interaction domains [103,104]. Enigma binding partners include the insulin receptor (InsR), the receptor tyrosine kinase RET, PKC, β-tropomyosin (a component of actin filaments), and YAP (yes associated protein) [103,105–108]. Enigma is also a ubiquitin E3 ligase that inhibits NF-κB mediated inflammatory responses, by controlling nuclear p65 protein levels [109]. In addition, it was shown that Enigma is involved in bone formation [104,110].

TCP-1-theta (T-complex protein 1 subunit theta, gene *CCT8*, UniProt ID P50990) is the θ subunit of the chaperonin CCT (chaperonin containing T-complex polypeptide 1, TRiC) [111]. The chaperone, abundant in eukaryotic cytosol, facilitates the folding of actin and tubulin, GAPDH, TCAB1 (telomerase cofactor), and other proteins, several of which are involved in cell cycle progression [111,112]. Actin and tubulin are obligate folding substrates of CCT [113]. Via its substrates, CCT is involved in cell cycle progression, cytoskeletal organization, and telomere maintenance [113,114]. TCP-1-theta was shown have a role in progression of tumors. It is overexpressed in several types of tumors, and facilitates migration and invasion of tumor cells by regulation of actin and tubulin [115,116]. TCP-1-theta has also been identified as in vitro microtubule-associated protein [117].

PTRF (polymerase I and transcript release factor or cavin-1, gene *CAVIN1*, UniProt ID Q6NZI2) is a protein found in the nucleus, cytosol, microsome and PM of the cell [118,119]. In the nucleus, PRTF is a cellular factor required for RNA Polymerase I (Pol I) transcription termination [120]. In the PM, PTRF is a component of caveolae (specialized invaginations of the PM), and is required for the formation and organization of caveolae, stabilizing and anchoring the structure to the cytoskeleton [118,119]. The protein is also a regulator of oxidative stress-induced premature senescence [121]. Mutations in PTRF have been

reported in patients with muscular dystrophy accompanied by congenital generalized lipodystrophy. Additional abnormalities include insulin resistance, dyslipidemia, and cardiac anomalies [122].

Transglutaminase 2 (TG2, gene *TGM2*, UniProt ID P21980), with ubiquitous tissue expression, is a predominantly cytosolic protein. TG2 catalyses Ca^{2+}-dependent post-translational modification of proteins that includes transamidation, esterification and hydrolysis [123,124]. And, with no requirement for Ca^{2+}, the protein has GTPase, ATPase, protein kinase, and protein disulfide isomerase activities, and mediates signal transduction through G protein-couple receptors [124,125]. TG2 can also be secreted, being involved in the assembly, remodelling and stabilization of the ECM by crosslinking of several proteins (such as fibronectin, proteoglycans, collagen V). In addition, it contributes to the covalent modification and activation of several growth factors including TGFß [123,124]. TG2 mediates cell-matrix interactions that affect cell spreading, migration, and are important for wound healing, promotes tissue mineralization and stabilizes dermo-epidermal junctions [124]. Other functions include regulation of cytoskeleton, cell adhesion and cell death. While there is no known disease associated to *TGM2*, TG2 is an autoantigen in celiac disease and in several inflammatory and fibrotic conditions transglutaminase activity is increased [123,124,126].

Ku86 (X-ray repair cross-complementing protein 5, gene *XRCC5*, UniProt ID P13010) is a subunit of Ku protein, a heterodimer of Ku70 and Ku86 subunits [127,128]. Ku is an abundant, mostly nuclear protein, with the ability to bind DNA and RNA, and with ssDNA-dependent ATPase and ATP-dependent DNA helicase activities. Ku protein is the regulatory subunit of the DNA-dependent protein kinase (DNA-PK) that phosphorylates many proteins, including SV40 large T antigen, p53, RNA-polymerase II, hsp90 (heat shock protein), and several transcription factors [127–129]. As such, Ku protein has been implicated, directly or indirectly, in DNA replication, transcription regulation, DNA double strand repair, V(D)J recombination of immunoglobulins and T-cell receptor genes, immunoglobulin isotype switching, regulations of heat shock-induced responses, and regulation of telomeric termini.

Lamin B1 (gene *LMNB1*, UniProt ID P20700) is a component of the nuclear lamina, a meshwork of filaments that underlines the inner nuclear membrane, and maintains nuclear shape, size and mechanical stability [130–132]. Lamin B1 is necessary for chromatin organization, participates in chromosome condensation and distribution of heterochromatin, and has a role in DNA repair and replication [131–133]. The protein participates as well in regulation of gene expression and splicing [132,133]. The protein expression is suggested to play an important role in the maintenance of cell proliferation [131,133]. Lamin B1 is constitutively expressed in all mammalian somatic cells and in undifferentiated embryonic stem (ES) cells [130,131]. A duplication of the gene *LMNB1* leads to adult-onset autosomal dominant leukodystrophy (ADLD), a demyelinating disorder [134]. Loss of function mutations have been linked to neural tube defects as susceptibility factors in humans, suggesting that this protein is essential for proper brain development and function [135].

Flt-1 (vascular endothelial growth factor receptor-1/VEGFR-1, gene *flt-1*, UniProt ID P17948) is a tyrosine kinase cell-surface receptor expressed almost exclusively at vascular endothelial cells [136]. Flt-1 binds to the angiogenic factors: vascular endothelial growth factor (VEGF)-A, VEGF-B, and placenta growth factor (PIGF) [137,138]. By binding and trapping VEGF-A, Flt-1 is a negative regulator for angiogenesis at embryogenesis [138,139]. In adulthood, Flt-1 is also expressed in macrophages, with its expression is upregulated in activated macrophages. Flt-1 is described as a positive regulator of macrophage functions, stimulating inflammation, cancer metastasis and atherosclerosis via the activation/migration of macrophage-lineage cells, and via its kinase ability [139]. It is involved in the progression of rheumatoid arthritis, and Flt-1 is upregulated when in the recovery from ischemia [139,140].

Flt-1 gene (*flt-1*) expresses one full-length receptor and a soluble short protein known as soluble VEGFR-1 (sFlt-1), the last one is generated by alternative splicing and is secreted [141]. sFlt-1 is a VEGF-A antagonist. Overexpression of sFlt-1 in the placenta of preeclamptic patients is also indicated to cause hypertension and renal dysfunction [139,142].

2. Objectives

The main objective of this dissertation project is to analyse and validate the effect of 11 candidate CFTR-interacting proteins on the pharmacological rescue ofPhe508del-CFTR.

To complete the proposed objectives the following experimental plan was carried out:

1) Culture of human bronchial epithelial cells and optimization of candidate protein depletion by RNA interference;

2) Investigation of the effects of depleting each of the candidate proteins on wt- and pharmacologically rescued Phe508del-CFTR using:

- Western blot (WB) of whole cell lysates to monitor CFTR steady-state levels;
- Cell surface protein biotinylation assays coupled to WB to evaluate CFTR PM abundance;
- RT-PCR to assess steady-state levels of CFTR mRNA.

3. Materials and Methods

3.1. Cell Culture

Cell culture refers to the isolation of cells from an animal, microbe or plant and their subsequent *in vitro* maintenance. It is a tool exploited in many different ways, as it provides model systems for the study of physiology and biochemistry of cells, or it can used for drug screening and development [143].

There are two types of cell culture, primary and continuous. Whereas primary cultures are cells derived directly from tissues and have a limited life span, continuous cell lines consist of a single cell type that has gain the ability for infinity growth. Though the process of transformation, spontaneous or either chemically or virally induced, cells lose their growth regulation ability (senescence), acquiring the ability to divide indefinitely, becoming immortalised [143]. The cell lines used in this work are derived from CFBE41o-, a well-known cystic fibrosis human cell line. The parental cells were isolated from bronchial epithelial cells and immortalized with the origin-of-replication defective SV40 plasmid (pSVori-) from a CF patient, homozygous for the Phe508del CFTR mutation. This cell line displays the ion transport traits typical of CF pathophysiology: a defective cAMP-dependent chloride transport and an intact calcium-dependent chloride transport [**144]. In this work, we used two subclones of CFBE41o- cells engineered to stably express wild-type- and Phe508del-CFTR, respectively. These cells were a kind gift from JP Clancy, University of Alabama, USA, and were selected through a puromycin antibiotic resistance gene, incorporated together with the CFTR transgenes [145].

Culture conditions vary for each cell type, but always consists of an appropriate container with a substrate or medium that supplies the essential nutrients (amino acids, carbohydrates, vitamins, minerals), growth factors, hormones, and gases (O_2, CO_2), and regulates the physiochemical milieu (pH, osmotic pressure, temperature) [††]. Both CFBE41o- cell clones (hence forward designated wt-CFBE e and Phe508del-CFBE) were cultured in T75 flasks (VWR) and maintained with minimal essential medium (MEM) supplemented with 10% (v/v) foetal bovine serum (FBS), and 2 μg/mL puromycin (all reagents were from Gibco, Life Technologies), to ensure transgene expression. All cell lines were grown at 37°C in 5% CO_2 and regularly checked for the absence of mycoplasma infection.

Like most cells from epithelial origin, CFBE cells form adherent monolayers, and when the cells capture all the available substrate and have no room for expansion, cell proliferation is greatly reduced or ceases. Cells reach a stationary phase (confluence) and is necessary to divide the culture and transferer the cells to a new vessel with fresh growth medium (subculturing/passing), keeping an optimal cell density and enabling further propagation of the cell line [143]. Therefore, maintenance of the cultured cell lines was done every 4-5 days as follows: growth medium was removed and cells were rinsed and incubated for 10 min with PBS 0.05% EGTA (Gibco, Life Technologies), to wash medium remains and, as these cells are very tightly packed, to gently disrupt adherent junctions between cells by chelating Ca^{2+} ions necessary for the interaction of cadherins in adjacent cells. Next, cell adhesions to the substrate were enzymatically digested with trypsin for 7 min and cells harvested and resuspended in complete growth medium to inactivate the trypsin.

[**] https://www.sigmaaldrich.com/deepweb/assets/sigmaaldrich/product/documents/420/525/scc151ds.pdf
Site accessed at 7th May 2020

[††] https://www.thermofisher.com/content/dam/LifeTech/Documents/PDFs/PG1563-PJT1267-COL31122-Gibco-Cell-Culture-Basics-Handbook-Global-FLR.pdf
Site accessed at 29th January 2021

Cell culture was done under sterile conditions to keep cells free from contamination by microorganisms such as bacteria, fungi and viruses. Such organisms outgrow the cells being cultured, eventually killing them due to the release of toxins and/or depletion of nutrients from the culture medium. Even low-level contamination can cause cellular stress. The sources of contamination can be nonsterile supplies, media, reagents, airborne particles, unclean incubators and dirty work surfaces. As such, good aseptic techniques were used and cells, as well as all culture material and reagents, were handled in a cell culture hood that provides an sterile work area and reduces contamination from airborne particles and aerosols[143].

3.2. Reverse Transfection

Down-regulation of a target protein can be achieved by short interference RNA (siRNA), a method used to downregulate gene expression by cleaving the target mRNA, preventing translation. siRNAs are short, double-stranded RNA molecules, normally 21 to 23 nucleotides long. Inside the cell, siRNAs interact with the multi-component RNA-induced silencing complex (RISC), unwinding the siRNA duplex and breaking down the sensed strand, leaving the antisense strand associated. The siRNA antisense strand is able to bind to a complementary mRNA target, which is cleaved at a single site by the RISC complex. The target mRNA is dismantled while the antisense strand remains associated with RISC, enabling direct cleavage of further mRNA target molecules, leading to the downregulation of protein expression [146].

Given that there is an electrostatic repulsion between the siRNA molecules and the cellular membranes, as both present a negative net charge under normal physiological conditions, the delivery of siRNAs to cells requires transfection methodologies [147]. These are laboratory procedures that introduce foreign nucleic acids into cells by biologic, physical, or chemical approaches [148]. Lipofectamine 2000 is a cationic liposome based reagent used for chemical transfection, that forms positive charged complexes with nucleic acid molecules, allowing siRNAs to overcome the electrostatic repulsion of the cell membrane and be taken up by the cell [147]. Transfection of adherent cells can be standard, where the siRNA-lipid complexes are added on top of pre-seeded cells, or reversed where the cells in suspension are added to the siRNA-lipid complex mix on the plate. The latter approach increases the efficiency of transfection of epithelial cells, since the cell's spheroid from when in suspension increases the membrane area exposed to the complexes [149].

In this work we used the Lipofectamine-mediated transfection of specific siRNAs to downregulate the expression of 11 proteins of interest. First, we optimized the siRNA transfection conditions to determine the best siRNA concentrations and cell incubation times. Cells were reversed transfected according to recommendations from Invitrogen, as follows: for each 35 mm petri dish we prepared two transfection mixtures, the first composed of 110 or 220 ρmol of siRNA diluted in 125 µL of OptiMEM (Gibco, Life Technologies), and the second of 9 µL of lipofectamine 2000 (Invitrogen) diluted in 125 µL of OptiMEM, both incubated for 5 min at room temperature. Following incubation, both solutions were mixed and further incubated for 20 min at room temperature, after which the mixture was added to the respective 35 mm dishes. In parallel, confluent cells were trypsinized and resuspended in MEM supplemented with 10% (v/v) FBS. $2x10^6$ cells in suspension were then added to each 35 mm petri dish containing the transfection mixture. Cells were cultured for 24 h or 48 h at 37°C with 5% CO_2, after which, cells were lysed and RNA was extracted to be analysed by RT-PCR (see below). The siRNAs used were all from commercial sources: Calgranulin A siRNA (h): sc-43342; Coronin 1C siRNA (h): sc-44693; Enigma siRNA (h): sc-77273; Flt-1 siRNA (h): sc-29319; Ku86 siRNA (h): sc-29384; Lamin B1 siRNA (h): sc-29386; PTRF siRNA (h): sc-76293; Spectrin β II siRNA (h): sc-36551; TCP-1 θ siRNA (h): sc-43451; Tenascin-C siRNA (h): sc-43186; TGase2

siRNA (h): sc-37514, all from Santa Cruz Biotechnology. Oligo control siRNA against firefly luciferase (siLuc) from Thermo Scientific.

3.3. Cell Lysis and RNA Extraction

RNA extraction is the purification of RNA from a biological sample. And typically, the protocol follows three steps: (1) cell lysis to release the nucleic acid; (2) purification to remove proteins and other cellular debris; and (3) isolation of the purified nucleic acid [150].

Cell lysis depends on factors such as the specimen type or what we want to isolate, being DNA, RNA, proteins or organelles, and the downstream application of the extract. As such, lysis can be either mechanical disruption (e.g. sonification or homogenization) or non- mechanical disruption (e.g. detergents, chaotropic salt solutions, or enzymatic digestion) [150]. Protocols for the isolation of RNA can use two different buffers for cellular lysis: (1) non-ionic detergents and hypotonic buffers, that gently solubilize the plasma membrane while maintaining nuclear and other organelle integrity; or (2) buffers that consist of harsh chaotropic agents, such as the guanidium salts, sodium dodecyl sulphate (SDS) or phenol, which disrupt the PM and subcellular organelles and which simultaneously inactivate RNases [151]. These chaotropic salts act by disrupting the water's structure and promoting solubility of nonpolar substances like proteins in polar solvents like water [150].

After lysis, purification can be achieved by either organic or nonorganic methods [150]. In this work it was used a nonorganic method based on silica binding. Silica binding is currently the most popular method for small-scale RNA isolation. It is efficient, rapid, easy, eliminates the use of the organic solvents and it is commercially available by kits [150,151]. The method is based on the high affinity that nucleic acids have for the silica compound, in the presence of high salt concentration produced by chaotropic salts like guanidine isothiocyanate (GITC). GITC can be used for cell lysis as well as to promote adsorption of nucleic acids to silica columns. The modified silica surfaces are designed to work with optimized binding and wash buffers, which aid in the separation of nucleic acids from cellular components. Nucleic acid can be eluted from the silica using a low concentration, non-chaotropic salt buffer [150,151].

In this work, RNA was extracted from CFBE cells to confirm the efficiency of siRNA-mediated knockdown of all candidate protein transcripts by RT-PCR (see below), enabling the optimization of the reverse-transfection conditions. For that, cells were first washed with PBS++ (PBS pH 8.0 containing 0.1 mM $CaCL_2$ and 0.5 mM $MgCl_2$) and lysed with RA1 buffer from NucleoSpin RNA Kit. RNA was extracted using the kit instructions for "RNA purification from cultured cells and tissue". Extracted RNA was quantified, and its purity assessed on a NanoDrop One spectrophotometer (Thermo Scientific). RNA was stored at -80°C until used for RT-PCR (see below).

3.4. Semi-Quantitative Reverse Transcription-Polymerase Chain Reaction

Reverse transcription-polymerase chain reaction (RT-PCR) is a technic that allows amplification of a short-defined sequence of complementary DNA (cDNA) in a highly specific and sensitive manner [152]. RT-PCR is used when the starting material is RNA, and is divided in two steps: conversion of RNA into cDNA by a reverse transcriptase enzyme; and conventional PCR and analysis.

3.4.1. Reverse Transcription (RT)

Following the RNA extraction, cDNA was synthesized using qScript XLT cDNA SuperMix (Quanta bio). This commercial mix contains an engineered M-MLV reverse transcriptase mutant with reduced

RNase H^+ activity and improved yield and temperature stability, as well an optimized reaction buffer already containing the necessary concentrations of $MgCl_2$, dATP, dCTP, dGTP, and dTTP. It also contains titrated concentrations of random hexamer and oligo(dT) primer that allows an efficient reverse transcription by hybridizing with virtually all RNA molecules in the sample, and priming cDNA polymerization. Synthesis reactions were carried out according to manufacturer's instructions, using 1 μg of total RNA.

3.4.2. PCR Method

The PCR assay is composed of a reaction mixture containing the template DNA, primers, nucleotides (adenine, tyrosine, cytosine, guanine), a DNA polymerase and a reaction buffer. The primers are a set of two oligonucleotide sequences that can be chemically synthetised to be complementary to the 3' side of the opposite strands of the target DNA, flanking the region of interest that we want to amplify [143]. The primers also serve as an extension point for the DNA polymerase, that uses the nucleotides in the mixture to synthetise the new DNA strand. The PCR procedure consists in a series of 30 to 40 cycles, each consisting of three sequential steps with defined times and temperatures: (1) denaturation, (2) annealing, (3) extension. First, denaturation of the double stranded DNA occurs by raising the temperature above 90℃. Next, with the DNA strands separated, the temperature is lowered and the primers can bind (anneal) to the complementary target DNA, flanking the sequence to amplify. The temperature for this step is dependent of the sequence and GC content of the primers used and is usually mathematically estimated and then experimentally optimized. For the final step, the primers provide a free 3'end for the DNA polymerase extension, the duration of which depends on the fragment size and the optimal temperature usually varies between 60-72℃, depending on the polymerase used. After the PCR reaction, the product can be analysed by agarose gel electrophoresis (see below).

All PCR amplifications were performed in C1000 Touch Thermal Cycler (Bio-Rad). For each reaction we used 2 μL of cDNA (synthesized as above), and 23 μL of reaction mixture: 21.9 μL of PCR buffer (50 mM KCl, 10 mM Tris-HCl pH 9, 1.5 mM $MgCl_2$, 0.01% gelatin, 0.2 mM of each dNTP), 0.1 μL (0,5 U) GoTaq G2 Flexi DNA Polymerase (Promega) and 0.5 μL of reverse and forward primer (10 μM). The PCR program structure was similar for all the primers used: first the reaction was heated to 94˚C for 5 min; then, according to the total number of cycles for each PCR system, three steps were repeated, (1) the mixture was heated for 30 sec at 94˚C, (2) cooled to annealing temperature (Ta) for 15 sec, (3) and heated to 72˚C for 30 sec; after all cycles the mixture stayed at 72˚C for 5 min. The number of cycles and Ta values for each primer pair are described in Table 3.1.

Table 3.1 - Description of primer sequence and its targets, and specific cycling parameters for each primer pair: annealing temperature and number of cycles.

Target	Primer Name: Sequence 5'→3'	Ta (℃)	Number of Cycles
Calgranulin A	S100A8- F: TTCAGGTGGGGCAAGTCCG	62	36
	S100A8-R: ACGTCTGCACCCTTTTTCCTGAT		
Lamin B1	LMNB1-F: GCGAAGAAGAGAGGTTGAAGCTG	62	25
	LMNB1-R: GTGGCTGAGGCGGAATGAGA		
Enigma	PDLIM7-F: CCACCATGCTATGACGTGCG	62	26
	PDLIM7-R: TCTTCTCATAGTCTCGCTCGCAA		
PTRF	CAVIN1-F: CGTCAACGTGAAGACCGTGC	62	26
	CAVIN1-R: GGCAGCTTCACTTCATCCTGGT		
Spectrin β II	SPTBN1-F: CGCAACAGACGGGGAAGGTTA	62	25
	SPTBN1-R: GGGACTCTTCCAGACGGGC		
TGase2	TGM2-F: TCGGCCCATGACCAGAACAG	62	26

	TGM2-R: GCAGTACGTCCCTTCGCTCT		
Ku86	XRCC5-F: CAAGTCGGCGTGGCTTTTCC	62	26
	XRCC5-R: TTCAACTGTGCCTCGGTGGG		
TCP-1 theta	CCT8-F: GGCCTGTCAGTTTCAGAGGTCA	62	26
	CCT8-R: TGGAGGTACGAAGTAGAGATGAGAC		
Tenascin-C	TNC -F: AGTAACGGTGGTGGATTCTGGG	62	31
	TNC -R: ACTTCCGGTTCGGCTTCTGT		
Coronin 1C	CORO1C -F: GGTCATTGCCAGCGGTTCAG	62	29
	CORO1C -R: GGCATTATCACAGCCTGCACT		
FLT-1	FLT1-F: GCCACCTCCATGTTTGATGACT	62	40
	FLT1-R: CTCAGCGTGGTCGTAGGTGA		
CFTR	CFTR-F: CTTCTGGGAGGAGGGATTTGG	60	23
	CFTR-R: TCCAGCAACCGCCAACAAC		
QPol2	QPol2-F: CGCAATGAGCAGAACGGCGC	62	26
	QPol2-R: TCTGCATGGCACGGGGCAAG		

3.4.3. Semi-Quantitative RT-PCR analysis

To estimate the efficiency of knockdown of the targeted transcripts we applied a semi-quantitative approach. Briefly, the control siRNA sample (siLuc) is designated as the reference sample, with the intensity of its RT-PCR product assigned a value of 1.0 and, the intensity of the targeted siRNA samples is compared to this baseline value. This semiquantitative method also requires the parallel amplification of a housekeeping gene in all samples [153]. Housekeeping genes are characteristically expressed constitutively and are chosen because their expression patterns show none to minimal variations in the experimental conditions used. As such, they can be used as internal standards to normalize for the total RNA (converted to cDNA) among the various samples, allowing meaningful comparisons between experimental conditions [153,154]. In this work, the housekeeping gene used for normalization of the samples was the RNA polymerase II (QPol2) transcript.

3.4.4. Primer Design

The primers used for the internal standard, polymerase II, were already available in the host lab, all other primers were designed with the primer-blast program available at the National Center for Biotechnology Information (NCBI) website ‡‡. The mRNA complete sequence for the transcripts of interest was selected from the NCBI nucleotide database and the *in* site tool "pick primers" was used setting the primer selection parameters as follows: PCR product size between 150 and 300 bases and a range of 58˚C to 65˚C primer melting temperature (Tm). In addition, the option "Primer must span an exon-exon junction" was selected, to ensure that any contaminant of genomic origin in the cDNA would not be efficiently amplified. When needed, the range of the primers in the mRNA sequence was constricted. All other optional parameters were kept at default settings. The optimal pair of primers was selected from the program output list considering the best combination of product length, Tm and a minimum of self-complementarity. Primer synthesis was procured from Thermo Fisher (Invitrogen) and the ideal PCR conditions (Ta and number of cycles) were then optimized for each primer pair. The primers stock solutions (100 μM) were prepared in sterile TE buffer (10 mM Tris pH 8, 1 mM EDTA).

3.4.5. Agarose Gel Electrophoresis

Electrophoresis is the migration of a charged particle under the influence of an electric field [143]. The technic uses a polymerized gel-matrix, where the DNA molecules of the analysed samples are

‡‡ https://www.ncbi.nlm.nih.gov/

separated. The migration of these molecules can be influenced by: (1) the size, shape, charge, and chemical composition of the molecules; (2) the gel-matrix density and structure; and (3) the applied electric field; as represented in Equation 3.1:

Equation 3.1

$$v = \frac{Eq}{f}$$

where:

E = electric field in volts/cm
q = net charge of the molecule
f = frictional coefficient, dependent on the mass and shape of the molecule and the gel-matrix properties
v = velocity of the molecule

For molecules with similar conformation, like PCR products, and under constant-voltage conditions, the movement of the charged molecule will not vary with shape, and as such, molecules migrate at a rate proportional to their charge-to-mass ratio [155]. DNA molecules migrate towards the anode of the electrophoretic setup, due to the negative charge phosphates along the DNA backbone [156]. Because charge per unit length is the same for different DNA fragments, the separation of these molecules occurs because of resistance caused by the matrix, with the largest molecules having more difficulty passing through the gel-matrix and the smallest molecules moving faster [143]. Agarose gels can be used in both protein and nucleic acids electrophoresis. The gels are made by dissolving agarose in a conductive buffer like Tris-Borate with EDTA (TBE). The concentration of agarose dictates the density of the gel matrix structure, with higher concentrations producing denser matrixes. As such, gel concentrations are chosen according to the size range of the molecules to be separated. For electrophoresis of DNA, the gel is placed in the electrophoresis tank and submerged in the conductive buffer [143]. Samples are then mixed with a loading solution containing sucrose, glycerol or Ficoll (to increase sample density and allow deposition in the gel wells) and a tracking dye (to estimate migration of the DNA molecules), and loaded in to the gel. After electrophoresis, the migration of the DNA bands can be visualized by staining with a dye, like ethidium bromide, that intercalates with DNA and fluoresces red orange (560 nm) under UV lights [143].

In this work, all PCR products [20 µL of the reaction mixed with 5ul of 5X Green GoTaq Flexi Buffer (loading solution from Promega)] were analysed in 2% - 2.5% (w/v) agarose gels stained with 0.5 µg/ml of ethidium bromide (Sigma-Aldrich). Electrophoresis were ran at 80V in TBE buffer (89 mM Tris-borate, 2 mM EDTA at pH 8.3). A DNA ladder (1 Kb DNA Ladder from Invitrogen) was loaded to every gel to confirm expected molecular weight of the amplification products. Images of the ethidium bromide-stained gels were acquired using the digital image acquisition system, Fire Reader (Progen Scientific).

3.5. Cell Surface Protein Biotinylation

The chemical modification of molecules (proteins, DNA, RNA, *etc.*) with biotin is one of the most useful tools in biochemical and biomedical research. Biotin is a water-soluble vitamin that can bind strongly to the proteins avidin and streptavidin (SA) [157]. The high affinity and specificity of the interactions biotin-avidin and biotin-SA makes biotinylated molecules easily detected with streptavidin derivates or efficiently captured on avidin/streptavidin-coated solid supports [158,159]. *In*

vivo, biotinylation occurs when biotin is covalent linked to an amino acid or carbohydrate moiety of the protein [157]. One application of this approach is the identification and purification of cell surface proteins [160]. The chemical reagent used for protein biotinylation is made up of: (1) a biotin moiety, that interacts with avidin/SA reagents; (2) a spacer, with sufficient length to allow protein capture by avidin/SA; and (3) a reactive moiety for the covalent binding of biotin to the protein, being the most used the reactive esters like the N-hydroxysuccinimide (NHS) group that targets α- or ε-amino groups of lysine residues or the proteins' N-terminus. The NHS group is widely used due to most proteins having numerous lysine residues that usually occupy an accessible position of the protein, and that lysine residues are usually not directly involved or has little effect in the biological activity of the protein [157,159]. NHS-esters of biotin are essentially water-insoluble, but a sulfonate group on the NHS ring (sulfo-NHS-esters) conveys solubility to the compound and makes these reagents less membrane permeable, making sulfo-NHS-esters of biotin the most frequently used as cell surface biotinylation reagents. Cleavable spacers groups can be added to the reagent to facilitate the release of biotinylated proteins after capture, the most common being a disulphide bridge that can be broken by reducing agents like b-mercaptoethanol or DTT (dithiothreitol) [159]. Biotinylation of cell surface proteins allows the selective study plasma membrane protein composition. For this approach the reagent Sulfosuccinimidyl-2-(biotinamido) ethyl-1,3-dithiopropionate (sulfo-NHS-SS-biotin) is the most commonly used. After biotinylation of the proteins at the cell surface, cells can be lysed and membrane proteins purified on a SA-coated support. Other protein contaminants can be removed by a series of washing procedures and biotinylated proteins can be eluted by reducing the disulphide bridge of the cleavable linker and further analysed [161].

In this study we used the cell surface protein biotinylation technique to assess the effect of the siRNA-mediated knockdown of our selected proteins on the levels of CFTR at the PM of CFBE cells. Phe508del-CFBE and wt- CFBE cells were reverse transfected in 35 mm petri dishes with 220 ρmol of siRNA as described above (see Reverse Transfection). Cells were either transfected with siRNAs for the proteins of interest or siLuc (as control), and treated with 5 μM VX-809 (Vertex Pharmaceuticals), a chemical chaperon drug that corrects Phe508del-CFTR folding and partially rescues its PM expression, or with the vehicle DMSO (Honeywell), and incubated for 48 h at 37°C, 5% CO_2 [29]. Additionally, CFBE cells treated with DMSO but not transfected or exposed to the biotinylation reagent were used to control for potential contaminations of precipitates with endogenous unbiotinylated proteins [160].

After the 48 h, cells were washed vigorously with RPMI medium 1640 (Gibco, Life Technologies) to remove medium contaminants and dead cells. Afterwards, cells were placed on ice and washed five times with ice cold PBS-CM (PBS pH 8.0 containing 0.1 mM $CaCl_2$ and 1 mM $MgCl_2$) to further remove contaminants and arrest endocytosis. Cells were incubated for 15 min with 1 mL of ice-cold PBS-CM with 0.5 mg/mL of Sulfo-NHS-SS-Biotin (Santa Cruz Biotechnology) per well, to label all cell surface proteins. Next, cells were rinsed twice and incubated for 15 min with 2 mL of ice-cold Tris-Q (100 mM Tris/HCl pH 8.0, 150 mM NaCl, 0.1 mM $CaCl_2$, 1 mM $MgCl_2$, 10 mM glycine, 1% (w/v) BSA) to quench the reaction. Tris and glycine contain primary amines, and BSA competes for the reaction with biotin. Cells were then washed three times with cold PBS-CM. After, PBS-CM was removed and each well was lysed in 250 μL of ice-cold pull-down buffer (50 mM Tris/HCl pH 7.5, 100 mM NaCl, 10% (v/v) glycerol, 1% (v/v) NP40, 1% (v/v) of Protease inhibitor cocktail (Sigma-Aldrich)) with the help of a scraper and always on ice. From this point on, all samples were also handled on ice. Cell lysates were collected and centrifuged (Eppendorf Centrifuge 5418 R) at 10000x rpm for 10 min at 4˚C. For each lysate sample, 20 μL of the supernatant was collected and added to 20 μL of 2x Sample Buffer (62.5 mM Tris-HCl pH 6.8, 3% (v/v) SDS, 10% (v/v) Glycerol, 0.02% (v/v)

Bromophenol Blue), representing whole cell lysate. Approximately 180 µL of supernatant was added to 30 µl of G-protein agarose beads (Roche) slurry (1:1, beads:pull-down-buffer) to perform a pre-clearing of the cell lysate, removing proteins that bind to the beads in a non-specific way. The remaining 50 µL of supernatant and pellet were resuspended in 350 µL of RA1 buffer for RNA extraction (as described above). The lysates added to G-protein agarose beads were rotated for 1 h at 4˚C and centrifuged for 1 min at 6000x rpm. All of the 180 µL of supernatant was recovered and the beads were discarded. The pre-cleared lysate were added to 40 µl streptavidin-agarose beads (Sigma) slurry (1:1, beads:pull-down-buffer), previously incubated for 1 h in 1 ml cold pull-down buffer containing 2% (w/v) milk, and washed three times in pull-down buffer. Lysate and beads were rotated for 1 h at 4˚C, where biotinylated proteins were captured by the streptavidin-agarose beads allowing purification. Lysates and beads were centrifuged for 1 min at 6000x rpm, supernatant was discarded and beads were washed five times in cold wash buffer (100 mM Tris/HCl pH 7.5, 300 mM NaCl, 1% (v/v) Triton X-100). Beads were dried with the help of a needle and the captured proteins were recovered in 20 µl of 2x Sample Buffer with 100 mM DTT (BioRad).

Proteins samples, either whole cell lysates or surface membrane proteins, were further analysed by SDS-Page and Western Blotting (see below) to evaluate CFTR protein levels and candidate protein knockdown efficiency, when antibodies were available. RT-PCR was performed to confirm knockdown and mRNA expression levels of proteins for which a specific antibody was not available. PCR was also used to evaluate the effect of the protein knockdown on the levels of CFTR mRNA.

3.6. SDS-Page and Western Blotting

Sodium dodecyl sulphate – polyacrylamide gel electrophoresis (SDS-PAGE) is an electrophoretic method used for analysis of protein mixtures in the presence of SDS, and is based on the separation of proteins according to size. The protein mixture is treated with a sample buffer that usually contains either mercaptoethanol or DTT, to reduce disulphide bridges and break the protein tertiary structure [143]. The buffer also contains SDS that further breaks the protein structure, producing linear polypeptide chains, and that binds to the denaturated protein in a constant ratio, conferring it a negative net charge, a constant charge/mass ratio and an uniform shape. As such, in an electrophoresis, the proteins move towards the anode, and separate according to their molecular weight, where the smaller proteins pass through the gel-matrix more easily [143,155]. In addition, the buffer also has a tracking dye to monitor the electrophoretic run, like bromophenol blue, and sucrose or glycerol to give the sample density to settle at the bottom of the loading wells of the gel.[143] SDS-PAGE uses a polyacrylamide gel formed by polymerization of acrylamide and the cross-liking agent N,N'-methylyne-bis-bis-acrylamide. Much like in a agarose gel, the concentrations of acrylamide and bis-acrylamide will determine the resolving power and molecular size range of a gel, where lower concentrations give gels more open matrixes, allowing analysis of molecules with higher molecular weight [155]. The gel is usually a vertical slab, prepared between two glass plates separated by spacers. To make the sample wells, a plastic comb is inserted into the top of the slab gel and removed after polymerization. SDS-PAGE can be a discontinuous gel electrophoresis, where the gel has two layers, a lower or resolving gel and an upper or stacking gel. The samples are loaded to the stacking gel to concentrate the protein sample into a sharp band before it enters the separating gel. Proteins are concentrated because the buffers used to prepare the two gel layers are of different ionic strengths and pH, and the stacking gel has a lower acrylamide concentration, so its pore sizes are larger. Thus the proteins enter the resolving gel at the same time, and start to separate according to their molecular weight [143,155].

Western blotting is a technic that allows individual separated proteins to be analysed after SDS-PAGE. It consists of the electrophoretic transfer (electroblotting) of the separated proteins from a

polyacrylamide gel to a sheet of a nitrocellulose or polyvinylidene fluoride (PVDF) membrane. The transferred membrane (blot) strongly binds and immobilizes the proteins, making them more accessible to chemical or biochemical reagents for further analysis [143,155]. In this method, the gel and the membrane are compressed like a sandwich in a cassette and immersed in a buffer between two parallel electrodes. The current passes at right angles to the gel, causing the proteins to migrate out of the gel and into the blot membrane [143]. The blot membrane can be probed with an antibody for detection of specific proteins. First, the membrane is incubated in a 5% (w/v) non-fat dried milk to block protein-binding sites on the membrane that are not occupied by blotted proteins to prevent unspecific binding of membrane-antibody. Following, the blot is incubated overnight with a dilution of a primary antibody (immunoglobulin G, IgG) directed against the protein of interest. To visualize the interaction protein-primary antibody, the blot can be further incubated in a dilution of a secondary antibody directed against the the species that provided the primary antibody. The second antibody is labelled (conjugated) usually to an enzyme so that the interaction of the second antibody with the primary antibody produces a visual signal, and one of the most used enzymes is horseradish peroxidase (HRP). To detect horseradish peroxidase, one can use the method enhanced chemiluminescence (ECL). In the presence of hydrogen peroxidase and the chemiluminescent substrate luminol, the enzyme oxidises the luminol with a concomitant production of light, detected by exposing the blot to a photographic film [143,155].

Thus, in this study, protein samples obtain through biotinylation were fractionated by SDS-PAGE and further analysed by WB. SDS-PAGE gels used were of a 0.75 mm thickness, containing a 10 mm stacking layer of 4% polyacrylamide gel on top of a 30 mm layer of 9% polyacrylamide resolving gel. Each gel was prepared by mixing: distilled water; Tris-HCL buffer (Tris-HCl 0.5 M pH 6.8 for the stacking gel and Tris-HCl 1.5 M pH 8.8 for the resolving gel); 40% acrylamide/bis-acrylamide (Merck Millipore); SDS 10% (w/v) (Sigma-Aldrich) and glycerol 100% (Sigma-Aldrich) in the quantities described in Table 3.2. 10% (v/v) ammonium persulfate (APS, Sigma-Aldrich) and tetramethylenediamine (TEMED, Panreac Applichem) were added to the mixture to activate polymerization. After polymerization, the gel was set in the electrode assembly, placed in the electrophoresis chamber and submerged in 1x SDS-PAGE running buffer (25 mM Tris, 192 mM glycine, 0.1% (w/v) SDS). The samples were loaded into the gel together with a protein ladder marker (Precision Plus Proteins™ All Blue Standards, Bio-Rad), which contains proteins of known molecular weight to help monitoring the migration rate during the run and estimate the size of proteins detected afterwards by WB. The electrophoresis was ran under 150V, at 4˚C, for approximately 1 h and 15 min.

Table 3.2 - Recipe for one polyacrylamide gel.

	Resolving gel	**Stacking gel**
Polyacrylamide %	9%	4%
ddH2O (mL)	2.25	1.45
Tris-HCl buffer (mL)	1.15	0.25
40% Acrylamide/bis (mL)	1.00	0.20
100% Glycerol (mL)	0.045	0.020
10% SDS (mL)	0.045	0.020
10% APS (µL)	67.5	30
TEMED (µL)	5	3.25

Following SDS-PAGE, the gel was removed from the cassette and the stacking layer was discarded. Proteins in the resolving layer of the gel were transferred onto a PVDF membrane (BioRad) previously activated with methanol and hydrated with double-distillate water. The gel and membrane

were placed in a cassette between blot filter paper and foam pads and set on a block in a Wet/Tank Blotting System Mini Trans-Blot® Cell (Bio-Rad) with transfer buffer (20% (v/v) methanol, 0.3% (w/v) Tris, 1.44% (w/v) glycine) for 90 min at 300 mA, on ice. After transfer, in order to confirm the loading of correct amount of proteins in all lanes, blot membranes were stained with Coomassie Blue (0.25% (w/v), Sigma), 45% (v/v) methanol, 10% (v/v) acetic acid) and washed two times, under agitation, with distain solution (45% (v/v) methanol, 10% (v/v) acetic acid, to remove unbound background dye from the membrane and fixate the protein to the membrane. Under agitation, the membrane was washed three times for 5 min with TBST (0.5 mM Tris, 0.67 mM NaCl, 0.28% (v/v) HCl 37% and 0.05% (v/v) Triton x-100 (0,05% (v/v)), pH 7.6) and incubated with a blocking solution (5% (w/v) non-fat milk in TBST). After blocking, the membrane was cut according to the molecular weight of the selected proteins to detect, and each piece was probed overnight, under agitation at 4˚C, with the appropriate dilution of primary antibody in blocking solution. Primary antibodies directed against the proteins of interest were all purchased from Santa Cruz Biotechnology, and the dilutions used are as follow: 1:750 mouse α-Enigma clone H-12 (sc-398100), 1:3000 mouse α-Ku-86 clone B-1 (sc-5280), 1:100 mouse α-Lamin B1 clone A-11 (sc-377000), 1:300 mouse α-PTRF clone 4a (sc-517589), 1:1500 mouse α-spectrin β II clone F-7 (sc-515592), 1:250 mouse α-TCP-1 θ clone E-7 (sc-377261), 1:3000 mouse α-TGase2 clone E-3 (sc-48387). The protein Tubulin was detected using mouse α-βTubulin (Sigma Aldrich) with a dilution of 1:200 000, both as a loading control in all cell lysates and as a control for contamination with cytosolic proteins in the cell surface protein biotinylation samples. An alternative loading control used was β-catenin, detected using mouse α-β-catenin (Abcam) with a dilution of 1:4000, whenever the molecular size of the proteins of interest was close to that of tubulin. To CFTR detection a mouse α-CFTR clone 596 (CFF) antibody was used, with dilutions described in Table 3.3.

Table 3.3 - Dilutions used for α-CFTR antibody.

Cell line	Lysate	Antibody Dilution
CFBE Phe508del-CFTR	Membrane Protein	1:1 500
	Whole cell lysate	1:5 000
CFBE wild type-CFTR	Membrane Protein	1:20 000
	Whole cell lysate	1:60 000

Next, always under agitation, the membranes parts were washed three times for 10 min with TBST, incubated for 1h with 1:3000 secondary antibody conjugated with HRP, (α-mouse IgG, sc-1706516, Bio-Rad) and washed again three times with TBST for 10 min. The chemiluminescent method to visualize the proteins of interest was performed in a dark chamber, where membranes were incubated with a mixture of two solutions for 1 min: (solution 1) 0.1 M Tris-HCL pH 8.8, 2 mM Luminol, 0.2 mM p-coumaric acid; (solution 2) 0.1 M Tris-HCL pH 8.8, 2.5 mM hydrogen peroxide. The chemiluminescent reaction between HRP and luminol was detected by making multiple exposures of the membrane to x-ray films (Fujifilm) in an appropriated cassette. The exposed x-ray films were processed in a X-Omat 2000 automatic developer (Kodak).

When necessary, membranes were stripped and reblotted as follows. WB membranes were washed three times with double-distillate water and incubated for 5 min with NaOH 0.25 M. Next, membranes were washed three times with double-distillate water and TBST and incubated for 30 min with blocking solution, followed by overnight incubation with the primary antibody. The rest of the WB procedure was as described above.

3.7. Data Analysis

Densitometric analysis of band intensities in digitalized WB films and RT-PCR gel images were performed using ImageJ software (NIH).

For semi-quantitative analysis of RT-PCR bands, a calibration curve was included in all PCR reactions, made from serial (1:2) dilutions of control cDNAs. The corresponding band intensities were fitted using linear regression, and the equation obtained used to estimate the relative DNA concentration corresponding to the intensity of each sample band in the same PCR assay. To account for variations in RNA concentration during cDNA preparation, the values obtained for each transcript of interest were first normalized to the values similarly obtained for the RNA polymerase II transcript amplified in parallel from the same cDNA samples (internal housekeeping control). Next, of the corrected densitometric values obtained for the transcripts of interest in each siRNA assay were expressed in fold change to the values obtained for the siLuc control the same assay (considered as reference sample). Afterwards a t-student test was applied to compare data sets of replicate control (siLuc) vs. transcript of interest knockdown, and differences were considered significant when p-value < 0.05.

Analogous to DNA analysis, for WB normalization, the ratio between the protein of interest and tubulin or β-catenin (loading controls) was done. Afterwards, protein abundance was determined by calculating the ratio between the protein of interest in a condition with siRNA and the control condition with siLuc. This ratio expresses the change of protein levels with respect to the control. Similarly, t-student tests were applied to compare replicate datasets of control (siLuc) vs. protein of interest knockdown and differences were considered significant when p-value < 0.05.

4. Results

To analyse the effect of the candidate proteins on pharmacologically rescued Phe508del-CFTR (rPhe508del-CFTR) we used an RNA interference approach. We depleted the candidate proteins and observed the effect it had on rPhe508del-CFTR overall and PM abundance through cell surface protein biotinylation assays and Western Blot (WB) analysis.

To begin, we tested the efficiency of siRNA-mediated depletion on each of the candidate proteins transcripts, in CFBE cells. We tested different siRNA quantities and different incubation time points post-transfection, and used RT-PCR to monitor transcript levels for each candidate protein. We chose to use 220 ρmol of siRNA followed by an incubation time of 48 h as the optimal conditions to obtain the significant reduction in expression of the targeted transcripts (see example in Figure 4.1 B) The monitoring of depletion efficiencies required the design of specific primers and optimization of optimal RT-PCR conditions for each candidate transcript (see 3. Materials and Methods).

When specific antibodies were available, target protein levels were also assessed by WB, after siRNA-mediated depletion.

4.1. Tenascin-C

We started our study by depleting candidate protein Tenascin-C (TNC) After transfection, Phe508del-CFBE cells were incubated for 48 h with either 5μM of the VX-809 corrector or with DMSO (vehicle used as control). We then performed a cell surface protein biotinylation assay, where proteins at the cell surface are labelled with non-permeable EZ link Sulfo-NHS-SS-Biotin and captured with streptavidin beads (described in 3. Materials and Methods). We recovered surface proteins and collected whole cell lysates for protein and RNA analysis. To control this assay, on one condition we did not apply biotin, and thus expected to recover no surface proteins. The recovered proteins fractions were then analysed through SDS-PAGE and WB. The protein tubulin was used as a loading control and to assess contamination of the biotinylation assay with intracellular proteins from permeable cells. The same methodology was applied for each one of the candidate proteins. In WB analysis rPhe508del-CFTR, when comparing the siLuc control cells treated with DMSO to treatment with VX-809, we can confirm the pharmacologic rescue of CFTR, both in whole cell steady-state levels (WCL), with an increase in abundance of CFTR band C (full glycosylated protein), and at the PM (surface) fraction (see Figure 4.1 A).

WB analysis of PM proteins shows that TNC downregulation, appears to decrease PM expression of rPhe508del-CFTR when compared to “siLuc + VX-809” control cells (Figure 4.1 A). Quantification of membrane CFTR signals corroborates this trend. Cells treated with siTNC present rPhe508del-CFTR with a mean of 0.21 at the PM, opposed to the control, with a given value of 1. Because of covid restrictions, we were only able to conclude two replicates of this experiment (n = 2), and thus, this analysis is qualitative, and the result is not statistically significant. More replicates would be needed to confirm this tendency. Noticeably, TNC knockdown does not appear to alter the overall abundance of rPhe508del-CFTR, but further assays would be needed to corroboration. Altogether, these results may indicate that TNC knockdown interferes with CFTR abundance at the plasma membrane, but not total CFTR on the cell. We propose that CFTR stability at the PM may be affected.

We used the RNA fraction (after biotinylation) to extract RNA, and through PCR, analyse the quantity of TNC transcript and confirm TNC knockdown. Figure 4.1 B is a representation of the PCR confirming that the transfection reduced TNC mRNA.

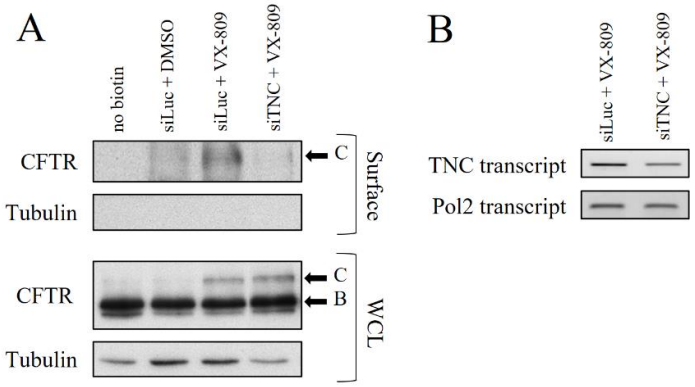

Figure 4.1 - TNC downregulation appears to reduce plasma membrane CFTR. (A) Western Blot analysis of Phe508del-CFTR in biotinylated cell surface proteins (Surface) and in whole cell lysates (WCL). Phe508del-CFBE cells were non-transfected, transfected with 220 ρmol of either siLuc or siTNC. Phe508del-CFTR was rescued to the PM by 48 h incubation with 5 μM VX-809 at 37°C. Non-transfection cells were used as a control for biotinylation, DMSO was used as a control for rescue with VX-809, and Tubulin was used as a loading control. Arrows indicate immature (band B) and fully glycosylated (band C) Phe508del-CFTR. (B) Representative semi-quantitative PCR for efficiency assessment of TNC siRNA-mediated knockdown. RNA Polymerase II (Pol2) was used as reference. The figure shows representative images of two replicate assays (n = 2).

4.2. Coronin 1C

Following the same procedure described above for TNC, we evaluated the effect of Coronin 1C downregulation on rPhe508del-CFTR abundance. Using a specific Coronin 1C siRNA we downregulated the protein transcript in Phe508del-CFTR CFBE cells to approximately 41% of its normal levels (control, siLuc + VX-809). The efficiency was determined through semi-quantitative PCR, see Figure 4.2 B.

Using surface biotinylation assay, we found that Coronin 1C knockdown led to a marked decrease of rPhe508del-CFTR at the cell surface when compared to control, see Figure 4.2 A. Analysis of WCL, reveals that there is also a slight reduction of the levels of fully glycosylated form of rPhe508del-CFTR, while the immature form of the protein appears to be the same. Quantification of CFTR levels of the WB membranes confirms statistical relevance in the reduction of surface and total mature rPhe508del-CFTR, to ≈ 31% and ≈ 79%, respectively (see Figure 4.3). These results show that Coronin 1C knockdown decreases mature rPhe508del-CFTR abundance and suggest a role for Coronin 1C in CFTR traffic to the cell surface and in its stability at the membrane, not excluding CFTR ER-Golgi trafficking [89,91,93].

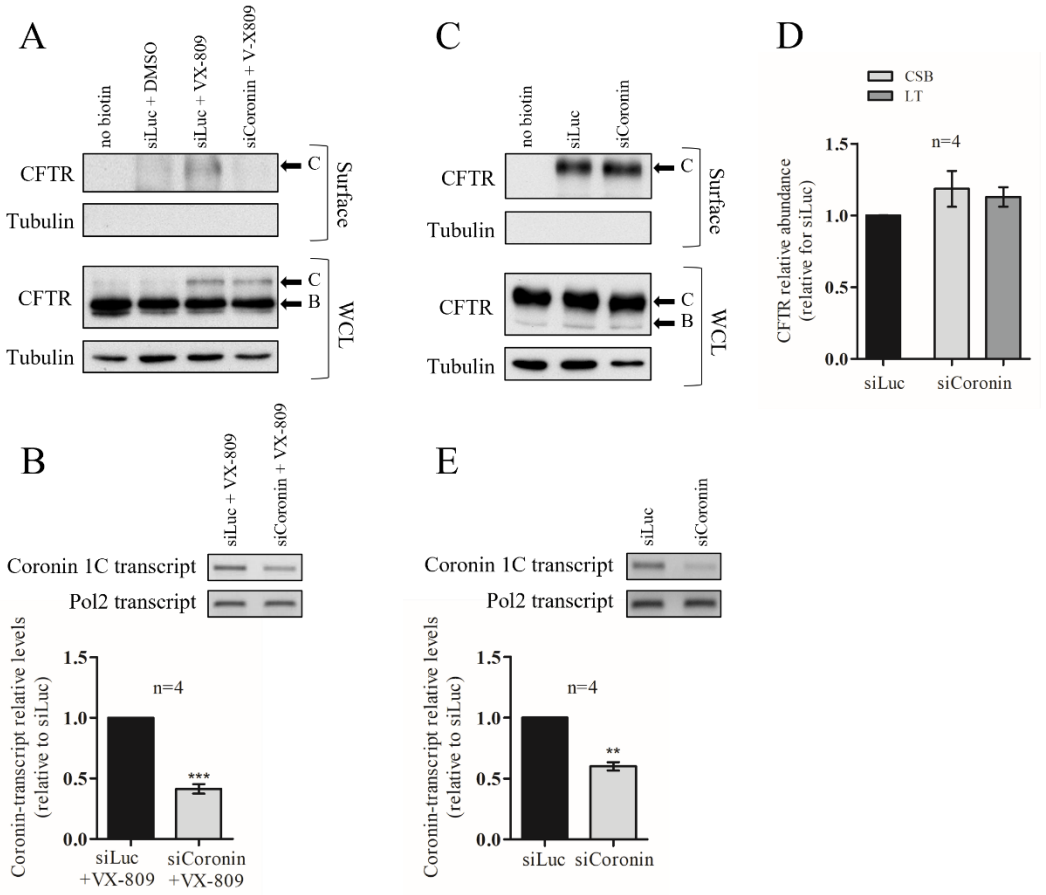

Figure 4.2 - Coronin 1C knockdown reduces VX-809-rescued Phe508del-CFTR but not wt-CFTR. (A) Biotinylation of cell surface proteins. Phe508del-CFTR CFBE cells were non-transfected or, transfected with 220 ρmol of either siLuc or siCoronin, followed by 48 h incubation at 37°C with VX-809 (5 μM) or DMSO. Shown are representative WBs of Phe508del-CFTR from recovered biotinylated cell surface proteins (Surface) and whole cell lysates (WCL). Arrows indicate immature (band B) and fully glycosylated (band C) CFTR. Membranes were further stained for α-Tubulin as a loading control. (B) Representative semi-quantitative PCR and graphic representation of band intensity for Coronin 1C mRNA levels in Phe508del-CFTR CFBE cells. Cells treated as described in (A). RNA Polymerase II (Pol2) was used as reference. Graphic data are means ± SEM, compared to siLuc + VX-809, significance was tested using unpaired, two-tailed, t-test. *** is $\rho < 0.001$. (C) Surface biotinylation assay in wt-CFTR CFBE cells and (D) graphic representation of CFTR band intensity from recovered biotinylated cell surface proteins and whole cell lysates. Cells were transfected with 220 ρmol of siLuc (control) or siCoronin and incubated for 48 h at 37°C. Tubulin was used as a loading control. In (D) Data are means ± SEM relative to siLuc [analysis of variance (Anova) followed by t-test]. (E) Representative semi-quantitative PCR and graphic representation of band intensity for Coronin 1C mRNA levels in wt-CFTR CFBE cells. Cells treated as described in (C). RNA Polymerase II (Pol2) was used as reference. Graphic data are means ± SEM, compared to siLuc + VX-809, significance was tested using unpaired, two-tailed, t-test. ** is $\rho < 0.01$.

Next, we checked if the downregulation of Coronin 1C in wt CFBE cells had the same effect. wt-CFBE cells were transfected with siLuc or siCoronin and incubated for 48 h at 37°C. Afterwards, it was performed a cell surface protein biotinylation assay, where cell surface proteins, whole cell lysates and RNA fraction were recovered. Coronin 1C downregulation was controlled by PCR. Coronin 1C transcripts levels were reduced to 60% compared to normal levels in cells treated with siLuc, see Figure 4.2 E. Analysis and quantification of WB membranes reveal that there is no significant alteration of the abundance of wt CFTR on the PM or in whole cell after Coronin 1C knockdown (see Figure 4.2 C). Suggesting that the effect we see on Phe508del-CFBE cells is specific to the phe508del-CFTR interactome.

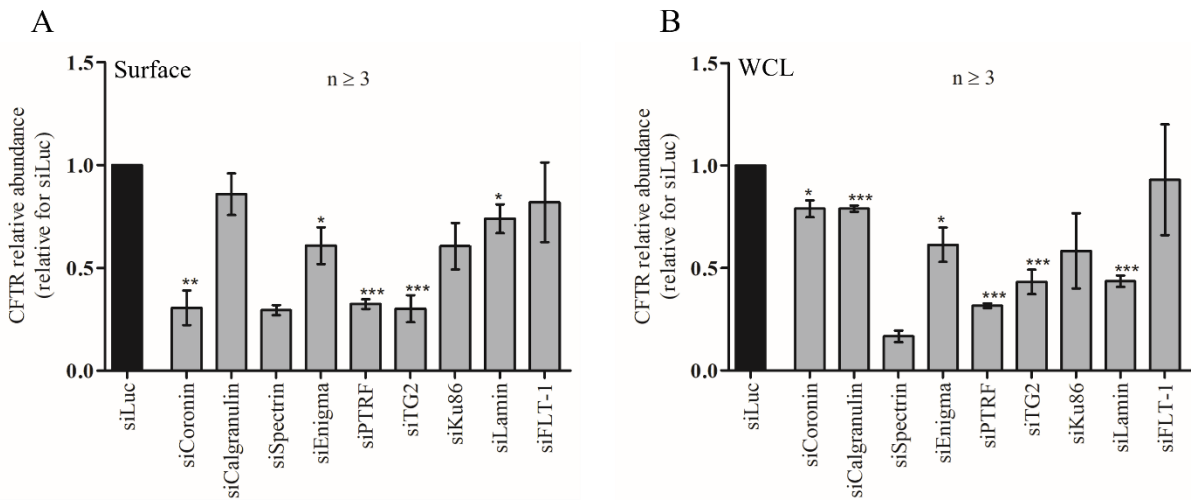

Figure 4.3 - Summary of Surface and WCL CFTR band C levels quantification. Quantification by WB densitometry of CFTR band C levels from (A) isolated biotinylated surface proteins and (B) WCL, in Phe508del-CFTR CFBE cells. Cells transfected with 220 ρmol of protein-specific siRNA (siLuc, siCoronin, siCalgranulin, siSpectrin, siEnigma, siPTRF, siTG2, siKu86, siLamin or siFLT-1) and incubated for 48 h at 37°C with VX-809 (5 μM). Data are means ± SEM, compared to siLuc + VX-809 (control), * is $\rho < 0.05$, ** is $\rho < 0.01$, and *** is $\rho < 0.001$. Analysis of variance (Anova) was followed by t-test.

4.3. Calgranulin

Calgranulin is a protein found in high circulating levels in CF patients [88]. So, to check if the protein has a direct effect on CFTR abundance at the PM is of great interest. Using siRNA specific for Calgranulin, we reduced the protein transcript to ≈ 45% of its normal levels (control, siLuc + VX-809). The efficiency was determined through semi-quantitative PCR, see figure 4.4 B.

WB analysis shows that Calgranulin knockdown does not promote any difference in abundance of rPhe508del-CFTR at the PM. In whole cell lysates, band C appears to be slightly reduced, while band B remains unchanged. Quantification of the membranes confirms a statistic reduction, albeit modest, of ≈ 20% of the abundance of band C from WCL (Figure 4.3 B). It suggests that Calgranulin downregulation does not affect CFTR synthesis or stability at the PM, but it may interfere with ER-Golgi trafficking. The same way we used the RNA fraction of the biotinylation assay to see the Calgranulin transcript levels, we perform a PCR to confirm that Calgranulin knockdown does not affect CFTR transcripts levels. The analysis does not reveal any statistically significant change of the levels of CFTR transcript, confirming that the observed effects were not caused by changes in CFTR synthesis (Figure 4.4 C and Figure 4.5).

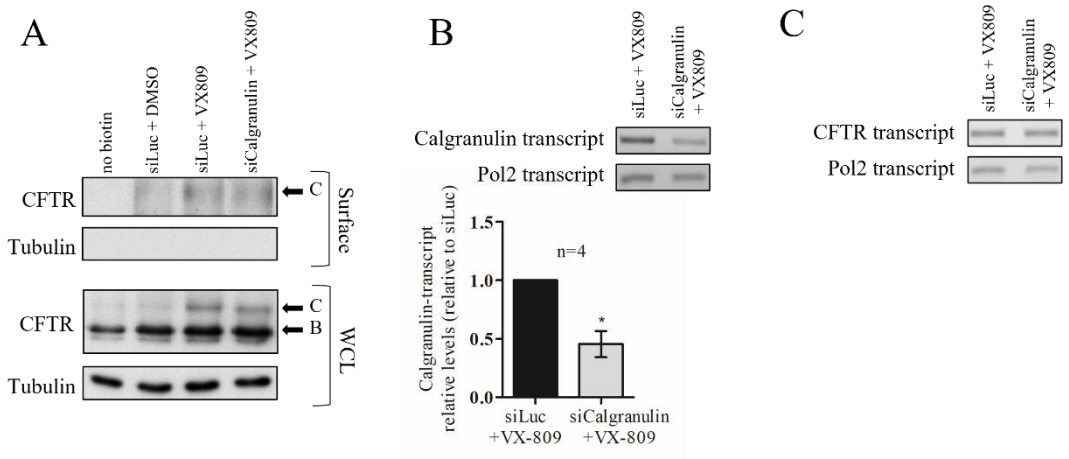

Figure 4.4 - Calgranulin downregulation does not affect rPhe508del-CFTR stability at the PM. (A) WB analysis of biotinylation assay in Phe508del-CFTR CFBE cells. Cells were non-transfected or, transfected with 220 ρmol of either siLuc or siCalgranulin, followed by 48 h incubation at 37℃ with VX-809 (5 μM) or DMSO. Recovered biotinylated cell surface proteins (Surface) and whole cell lysates (WCL), arrows indicate immature (band B) and fully glycosylated (band C) rPhe508del-CFTR. Tubulin used as a loading control. (B) Representative semi-quantitative PCR and graphic representation of band intensity for Calgranulin mRNA levels in Phe508del-CFTR CFBE cells. Cells treated as described in (A). RNA Polymerase II (Pol2) was used as reference. Graphic data are means ± SEM, compared to siLuc + VX-809, significance was tested using unpaired, two-tailed, t-test. * is $\rho < 0.05$ (C) Assessment of CFTR mRNA levels in Phe508del-CFTR CFBE cells by semi-quantitative PCR. Cells treated as described in (A). RNA Polymerase II (Pol2) was used as reference. Shown are representative images of at least 3 replicate assays (n > 3).

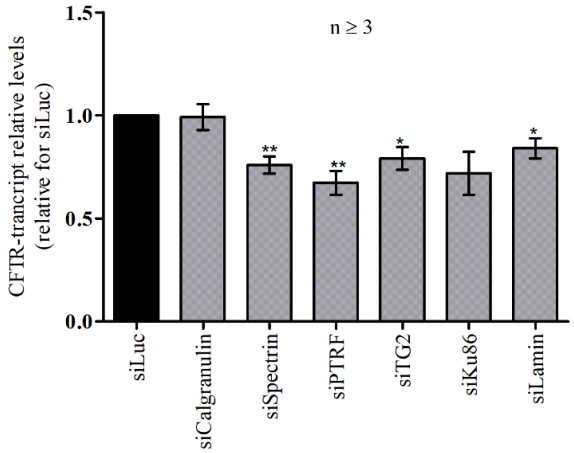

Figure 4.5 - Summary of CFTR transcript analysis. Quantification of CFTR mRNA bands from semi-quantitative PCR. Phe508del-CFTR CFBE cells were transfected with 220 ρmol of protein-specific siRNA (siLuc, siCoronin, siCalgranulin, siSpectrin, siEnigma, siPTRF, siTG2, siKu86, siLamin or siFLT-1) and incubated for 48 h at 37℃ with VX-809 (5 μM). Cells were used in the biotinylation assay and RNA fraction was recuperated for use in a semi-quantitative PCR. Data are means ± SEM, compared to siLuc + VX-809 (control), * is $\rho < 0.05$, and ** is $\rho < 0.01$. Analysis of variance (Anova) was followed by t-test.

4.4. βII Spectrin, Enigma

βII Spectrin and Enigma proteins were downregulated in Phe508del-CFTR CFBE cells to approximately 18% and 12%, respectively, of their normal cell levels (control, siLuc + VX-809). The efficiency of the siRNA's, siSpectrin and siEnigma, mediated knockdown was determined through quantitative analysis of the proteins' levels in WB membranes (see Figure 4.6 A and B). Following the same procedure used for the other candidate proteins, cells were then treated with DMSO or VX-809 (for Phe508del-CFTR rescue), and used for biotinylation assay and WB analysis. Analysis of the WB membrane from the first assay revealed DNA contamination. The first step of the protein purification was not done properly, and the resulting blotting presents blurry protein bands that could not be accurately quantified. As such, we only have one valid assay for Spectrin, with three replicates.

However, the visual analysis of this contaminated WB membrane is in agreement with that of the valid assay. The assessment of WB membranes and its quantification shows that, cells treated with siSpectrin and siEnigma, have a clear reduction of surface rPhe508del-CFTR levels and band C from whole cell lysates (Figure 4.3 and Figure 4.6 A). A reduction of the band B levels in WCL, was only observed with βII Spectrin knockdown (Figure 4.6 A).

βII Spectrin is a cytoskeleton protein, present in the membrane, Golgi, ER vesicles and nucleus [95–98]. Its functions and importance to cell viability explain why after cell treatment with siSpectrin it was observed more cell death than with other siRNAs. Taking in account its functions, and that the levels of rPhe508del-CFTR were reduced, not only at the PM but in whole cell lysates, we suggest that βII Spectrin knockdown interferes with synthesis and/or processing of CFTR protein. To understand if CFTR synthesis was affected, we proceeded to test RNA levels. Like before, RNA fraction of cells treated with "siLuc + VX809" (control) and "siSpectrin + VX-809" were recovered after biotinylation, and used to produce cDNA and do a semi-quantitative PCR followed by agarose electrophoresis to ascertain CFTR RNA levels. Analysis and quantification of the agarose gels indicates that, when compared to control, βII Spectrin knockdown reduces only modestly CFTR RNA levels, approximately 14% (see Figure 4.6 C and Figure 4.5). This result supports that βII Spectrin could be implicated in CFTR synthesis.

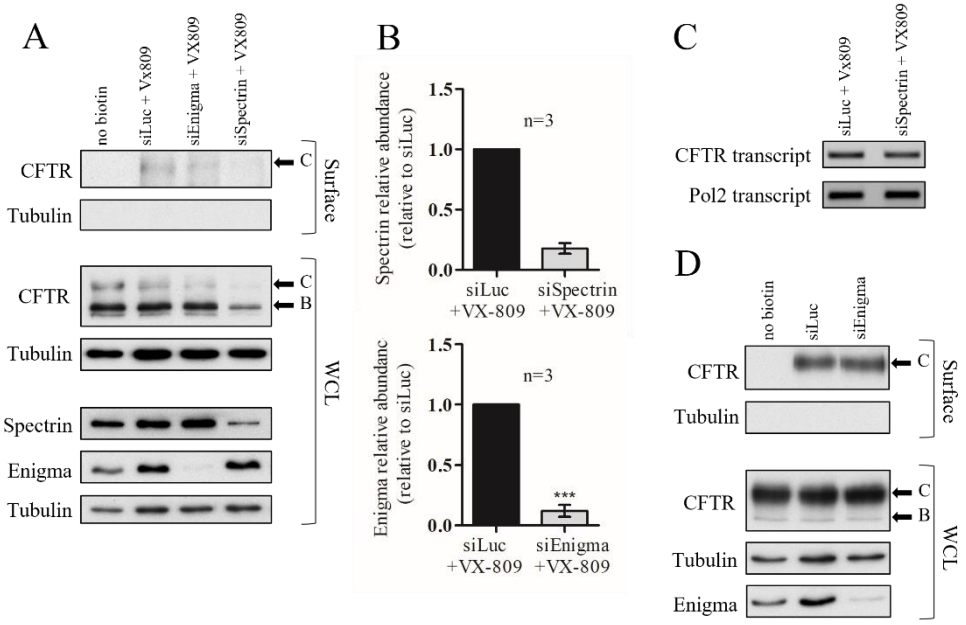

Figure 4.6 - βII Spectrin and Enigma downregulation can affect Phe508del-CFTR processing and/or synthesis. (A) Analysis of surface protein biotinylation assay in Phe508del-CFTR CFBE cells. Cells were non-transfected or, transfected with 220 ρmol of either siLuc, siSpectrin or siEnigma, followed by 48 h incubation at 37°C with VX-809 (5 μM) or DMSO. Shown are representative WBs of Phe508del-CFTR protein in the surface protein fraction (Surface) and correspondent whole cell lysates (WCL). Arrows indicate immature (band B) and fully glycosylated (band C) rPhe508del-CFTR. Membranes were further stained for α-Spectrrin, α-Enigma and α-Tubulin, the last as a loading control. (B) Determination of Spectrin and Enigma knockdown efficiency. Quantification by WB densitometry of Spectrin and Enigma protein levels in WCL like described in (A). Data are means ± SEM, compared to siLuc + VX-809, significance was tested using unpaired, two-tailed, t-test. *** is $\rho < 0.001$. (C) Representative semi-quantitative PCR for CFTR mRNA levels in Phe508del-CFTR CFBE cells treated with siSpectrin, as described in A. RNA Polymerase II (Pol2) was used as reference. (D) WB analysis of wt-CFTR levels in biotinylation assay. wt CFBE cells were transfected with 220 ρmol of siLuc (control) or siEnigma, and incubated for 48 h at 37°C. Membrane was further probed with antibodies to Enigma and Tubulin, the last used as a loading control. Recovered biotinylated cell surface proteins (Surface) and whole cell lysates (WCL). Arrows indicate immature (band B) and fully glycosylated (band C) wt-CFTR.

Enigma knockdown resulted in CFTR band C reduction (with statistic relevance), both in the PM and WCL, to approximately 61 % of control cell levels (siLuc + VX809, see Figure 4.3). Based on these findings, it appears that Enigma downregulation may interfere with CFTR processing, and given that there is no band B accumulation, the transport of CFTR from the ER to Golgi apparatus does not appear to be affected.

We also tested if wt CFBE cells would present the same behaviour with Enigma knockdown. The procedure applied is the same as described for Coronin-1C. Briefly, wt CFBE cells were either transfected with siLuc or siEnigma, and incubated for 48 h, followed by biotinylation essay, where surface, whole cell lysate and RNA fraction were recovered. Western Blot analysis of Surface and WCL fractions reveals no apparent increment of CFTR protein in the PM, nor in the WCL (Figure 4.6 D). The difference between results obtained by wt and Phe508del-CFTR cells indicates that Enigma may have different roles depending on mutated and wt-CFTR interactome.

4.5. TCP-1-Theta

Following we tested the effect of TCP-1-Theta depletion on rPhe508del-CFTR levels. Efficiency of TCP-1-Theta siRNA mediated knockdown was assessed by quantitative analysis of the protein levels in WB membranes. TCP-1-Theta was downregulated to approximately 39% of its normal cell levels (control, siLuc + VX-809), see Figure 4.7 A and D.

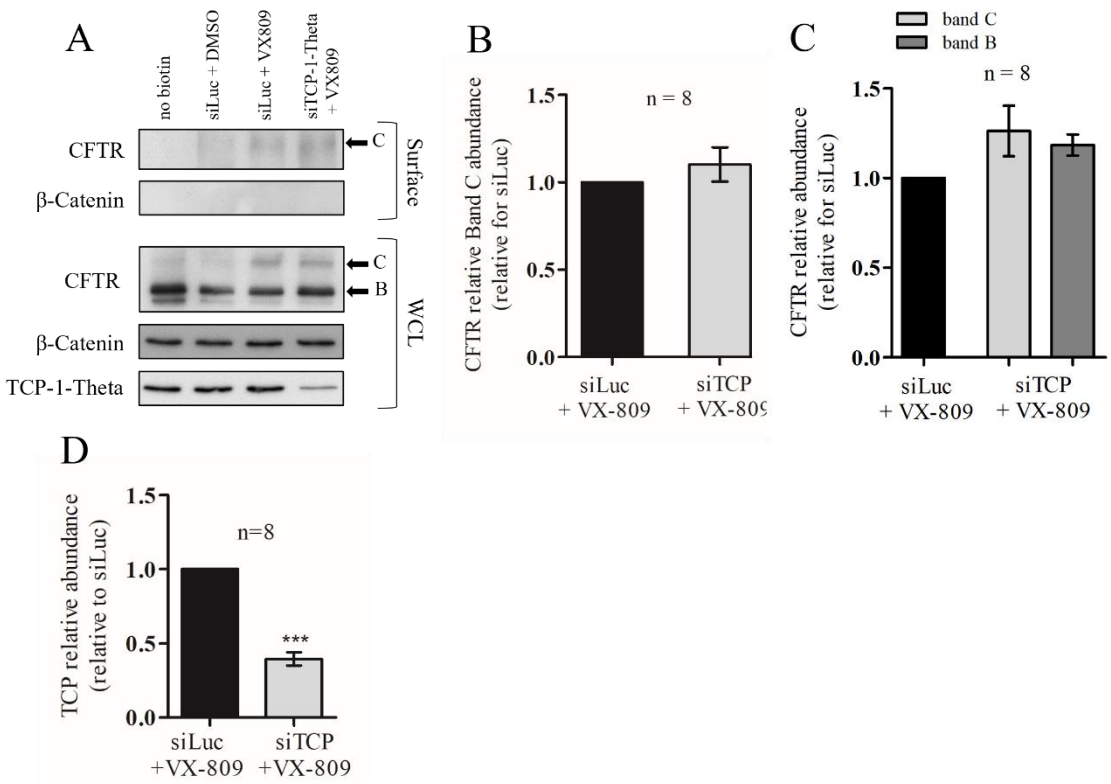

Figure 4.7 - TCP-1-Theta knockdown does not affect CFTR levels. (A) WB analysis of biotinylation assay in Phe508del-CFTR CFBE cells. Cells were non-transfected or, transfected with 220 ρmol of either siLuc or siTCP-1-Theta, followed by treatment with VX-809 (5 μM) or DMSO for 48 h at 37°C. Recovered biotinylated cell surface proteins (Surface) and whole cell lysates (WCL), arrows indicate immature (band B) and fully glycosylated (band C) rPhe508del-CFTR. Membranes were further stained for α-TCP-1-Theta and α-β-Catenin, the last as a loading control. Blots are representative of four independent assays. (B) Graphic representation of Surface CFTR, (C) WCL CFTR and (D) TCP relative abundance (relative to control, siLuc + VX-809), values normalized to β-Catenin. The data are presented as means ± SEM and significance was tested using unpaired, two-tailed t-tests comparing siTCP-1-Theta to siLuc + VX-809 for (B) and (D), and one-way Anova followed by t-test for (C), *** is $\rho < 0.001$.

WB analysis of the biotinylation assay shows a slight enrichment of surface rPhe508del-CFTR levels. On WCL, the abundance of CFTR band C and B appears to remain unchanged. Quantification of the membranes does not give significance to the apparent increment of CFTR surface abundance. Therefore, we suggest that TCP-1-Theta downregulation does not interfere with CFTR overall abundance.

4.6. PTRF and TG2

The same procedure was followed once more for PTRF and TG2 proteins. The efficiency of protein knockdown by siRNA-specific for PTRF and TG2 in Phe508del-CFTR CFBE cells was assessed by quantitative analysis of the protein levels in WB membranes. PTRF and TG2 were downregulated to approximately 13% and 7%, respectively, of their normal levels (control, siLuc + VX-809), see Figure 4.8 A and B. Following the treatment with DMSO or VX-809 (for Phe508del-CFTR rescue), cells were then used in biotinylation assays for WB analysis.

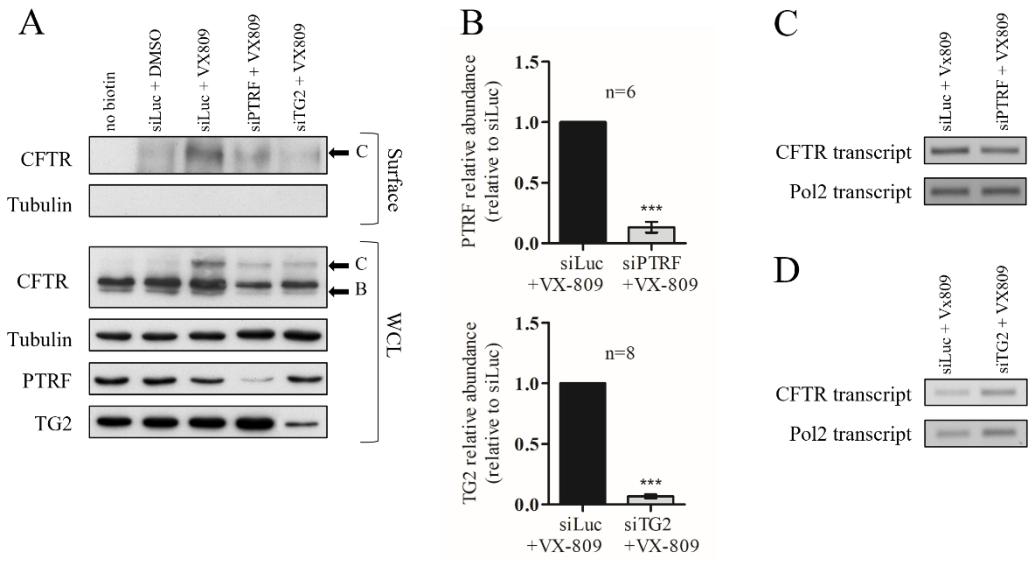

Figure 4.8 - PTRF and TG2 proteins downregulation reduces Phe508del-CFTR protein and RNA levels. (A) Analysis of CFTR levels. Phe508del-CFTR CFBE cells were non-transfected or, transfected with 220 ρmol of either siLuc, siPTRF or siTG2, and incubated with DMSO or VX-809 (5 μM) for 48 h at 37°C. Shown are representative WBs of biotinylated CFTR at the cell surface (Surface) or in whole cell lysates (WCL). Arrows indicate immature (band B) and fully glycosylated (band C) rPhe508del-CFTR. Further staining of the membrane for α-PTRF, α-TG2 and α-Tubulin, the last as a loading control. (B) Graphic representation of PTRF and TG2 relative abundance (relative to control, siLuc + VX-809). The data are presented as means ± SEM and significance was tested using unpaired, two-tailed t tests, *** is $\rho < 0.001$. (C) and (D) Representative semi-quantitative PCR for CFTR mRNA levels in Phe508del-CFTR CFBE cells treated with siPTRF or siTG2, as described in (A). RNA Polymerase II (Pol2) was used as reference. Images are representative of at least three independent assays.

Analysis of CFTR abundance in WB membranes and its quantification reveals that cells treated with siPTRF and siTG2 have a significant depletion of the amount of surface Phe508del-CFTR rescued by VX-809 and WCL CFTR, band C and B. At the PM, and when compared to control cell levels, rPhe508del-CFTR is down to ≈ 30%, for both knockdown conditions. In WCL, band C is reduced to ≈ 32% and ≈ 43% of control levels, respectively, for PTRF and TG2, while band B is decreased approximately 50% in either knockdown (Figure 4.3 and Figure 4.9). Since CFTR protein abundance is reduced not only at the PM but in the whole cell lysates, the results indicate that PTRF and TG2 knockdown can perhaps interfere with Phe508del-CFTR synthesis and/or processing. To assess this, we used RNA fraction recovered after biotinylation to monitor CFTR RNA levels. We used RNA fraction of cells treated with "siLuc + VX809" (control) and either "siPTRF + VX-809" or "siTG2 + VX-809" to produce cDNA and do a semi-quantitative PCR followed by agarose electrophoresis.

Analysis and quantification of the agarose gels indicates that when compared to control, PTRF and TG2 downregulation reduces (with statistic relevance) CFTR mRNA levels to approximately 67% and 79%, respectively (see Figure 4.5 and Figure 4.8 C and D). This result indicates that PTRF and TG2 may both interfere with CFTR gene translation or the stability of its mRNA synthesis.

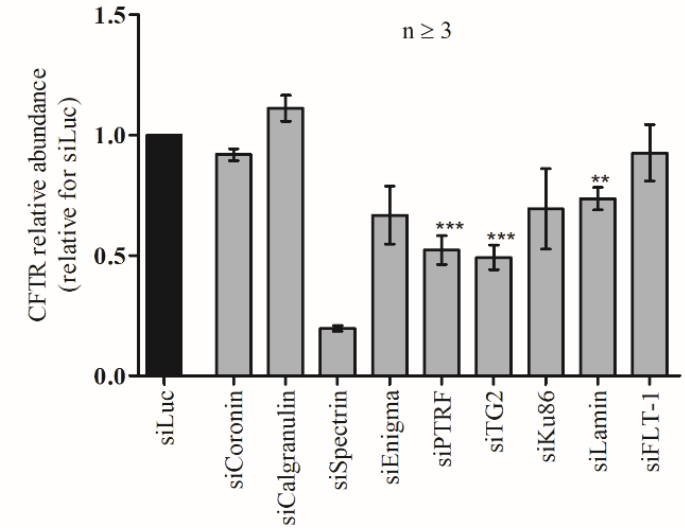

Figure 4.9 - Summary of CFTR band B level quantification in WCL. Quantification by WB densitometry of CFTR band B levels from WCL in Phe508del-CFTR CFBE cells. Cells transfected with 220 ρmol of protein-specific siRNA (siLuc, siCoronin, siCalgranulin, siSpectrin, siEnigma, siPTRF, siTG2, siKu86, siLamin or siFLT-1) and incubated for 48 h at 37°C with VX-809 (5 μM). Data are means ± SEM, compared to siLuc + VX-809 (control), ** is $\rho < 0.01$, and *** is $\rho < 0.001$. Analysis of variance (Anova) was followed by t-test.

4.7. Ku86 and Lamin

Following the transfection of Phe508del-CFTR CFBE cells with siRNA, siKu86 or siLamin, and treatment with DMSO or VX-809, cells were used in biotinylation assay for WB analysis. The proteins' downregulation was first assessed by quantitative analysis of the protein levels in WB membranes (Figure 4.10 A-D). Ku86 and Lamin were downregulated to approximately 15% and 9%, respectively, of their normal cell levels (control, siLuc + VX-809).

CFTR WB analysis displays a reduction of rPhe508del-CFTR abundance in surface proteins after Ku86 and Lamin knockdown. The following quantification of the protein bands, both knockdowns reduced CFTR abundance at the PM in 30-40%, although only the Lamin knockdown reached statistical significance (Figure 4.3 A). In WCL, we see also a reduction of rPhe508del-CFTR, band C and B, albeit only significant for Lamin depletion (Figure 4.3 B and Figure 4.9).

Both Ku86 and Lamin proteins can have nuclear localization, so as above we investigated if CFTR transcript is also affected by their knockdown [127,130]. Analysis and quantification of the RT-PCRs showed only small reductions of CFTR mRNA in either condition (Figure 4.5 and Figure 4.10 E and F), albeit significant for lamin knockdown. Although this transcript reductions could contribute to the observed decrease in CFTR protein levels, additional assays are needed to confirm this hypothesis.

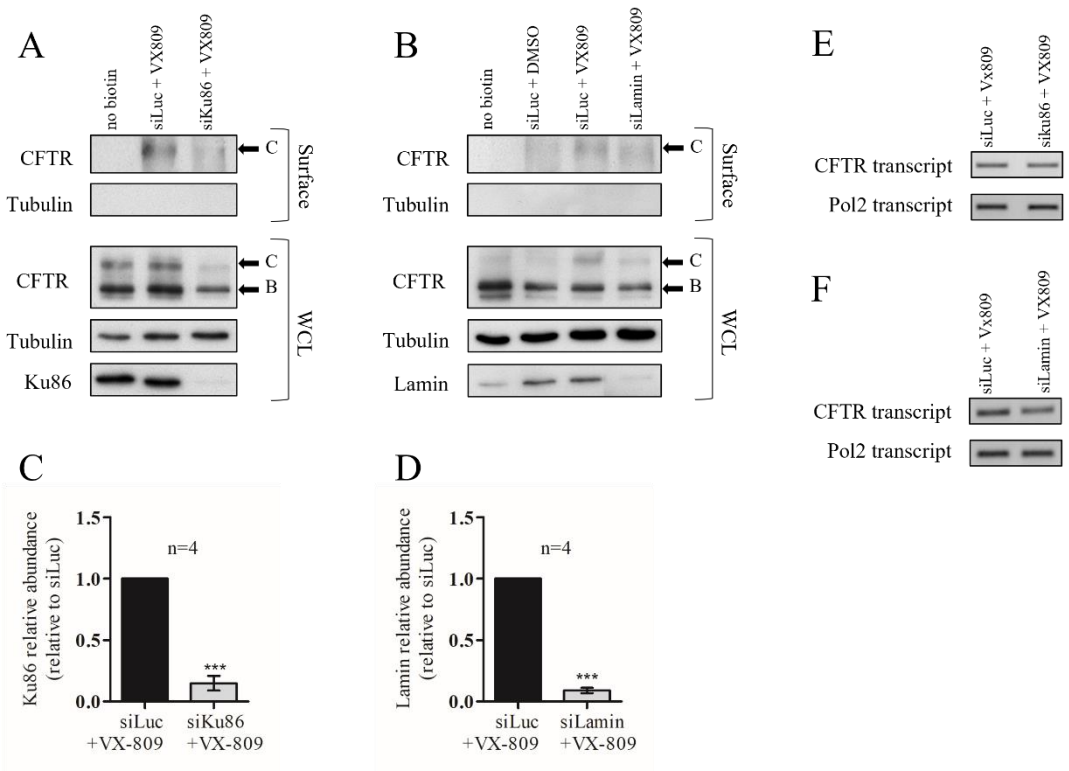

Figure 4.10 - Phe508del-CFTR protein and RNA levels are reduced in Ku86 and Lamin knockdown conditions. (A) WB analysis of biotinylation of CFTR at the cell surface (Surface) and whole cells lysates (WCL) in Phe508del-CFTR CFBE cells. Cells were non-transfected, or transfected with 220 ρmol of either siLuc (control), siKu86 or siLamin (B), followed by 48 h incubation at 37°C with VX-809 (5 μM) or DMSO. Arrows indicate immature (band B) and fully glycosylated (band C) Phe508del-CFTR. Membranes were further stained for α-Ku86, α-Lamin and α-Tubulin, the last as a loading control. Blots are representative of at least 3 independent assays. (C) Graphic representation of Ku86 and (D) Lamin relative abundance (relative to control, siLuc + VX-809). The data are presented as means ± SEM and significance was tested using unpaired, two-tailed t tests, *** is $\rho < 0.001$. (E) Representative semi-quantitative PCR for CFTR mRNA levels in Phe508del-CFTR CFBE cells treated with siKu86 or siLamin (F), as described in (A) and (B). RNA Polymerase II (Pol2) was used as reference.

4.8. FLT-1

In the biotinylation assays testing the effect of FLT-1 knockdown, this protein downregulation was controlled through mRNA levels, since antibody against the protein was not available. Using siFLT-1, we were able to reduce FLT-1 transcript to approximately 61% of its normal cell levels (control, siLuc + VX-809). The efficiency was determined through semi-quantitative PCR, see Figure 4.11 B. In the biotinylation essay, analysis of WB of both surface proteins and WCL, show that the abundance of rPhe508del-CFTR appears to be close to control. Quantification of WB membrane confirms the observation (Figure 4.3). The results show that FLT-1 knockdown does not seem to affect either the steady-stated or PM levels of Phe508del-CFTR rescued by VX-809.

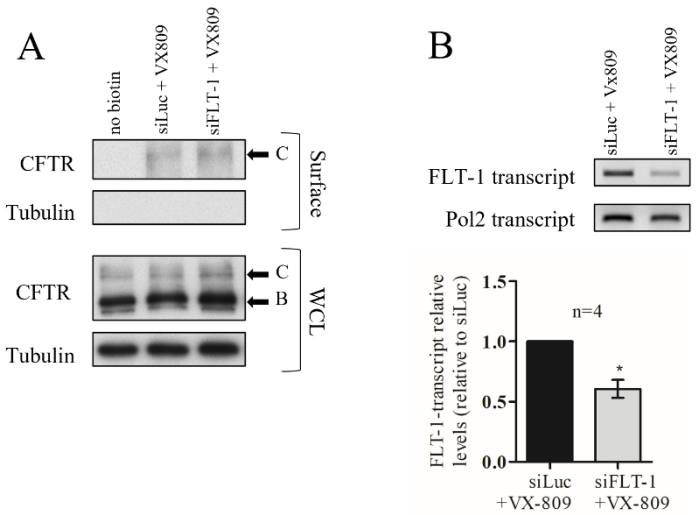

Figure 4.11 - FLT-1 downregulation does not interfere with rPhe508-CFTR but reduces wt-CFTR. (A) WB analysis of biotinylation assay in Phe508del-CFTR CFBE cells. Cells were non-transfected or, transfected with 220 ρmol of either siLuc, or siFLT-1, and treated with DMSO or VX-809 (5 μM) for 48 h at 37°C. Recovered biotinylated cell surface proteins (Surface) and whole cell lysates (WCL), arrows indicate immature (band B) and fully glycosylated (band C) Phe508del-CFTR. Membrane was further stained for α-Tubulin. (B) Assessment of FLT-1 siRNA-mediated knockdown efficiency. Analysis of semi-quantitative PCR and graphic representation of band quantification for FLT-1 mRNA levels in Phe508del-CFTR cells, treated as described in (A). RNA Polymerase II (Pol2) was used as reference. Graphic data are means ± SEM, compared to siLuc + VX-809 (control), * is $\rho < 0.05$, Shown are images representative of four replicate experiments (n=4).

5. Discussion

In this dissertation project we investigated the effect of the suppression of the endogenous expression of 11 candidate proteins on the PM abundance of Phe508del-CFTR pharmacologically rescued with the VX-809 corrector drug [30]. About these proteins, we observed that when comparing with control levels (siLuc + VX-809), Calgranulin, TCP-1-Theta and Flt-1 knockdown did not affect rPhe508-CFTR abundance at the cell surface.

The protein Calgranulin (S100A8) was of great interest to study. Calgranulin is a protein that can be found as a homodimer, or heterodimer with S100A9 [162]. Both protein dimers have diverse cellular functions, that include inducing expression of the mucin MUC5AC in airway mucus, and modulating inflammation and immune processes [85,86,163]. The S100A8-S100A9 dimer is present with high circulating levels in patients with Cystic Fibrosis and can be considered a biomarker of the disease [87,163]. With downregulation of Calgranulin we found, with surprise, that that the abundance of rescued Phe508del-CFTR at the cell surface was not affected. However, a modest reduction of ≈ 21% of CFTR band C was seen in WCL. We confirmed CFTR transcript levels, and this reduction is not caused by changes in CFTR gene expression. As such, since CFTR band B levels remained unaltered, Calgranulin downregulation might interfere with CFTR ER-Golgi trafficking or its maturation at the Golgi but not the abundance of the channel at the PM. Others already suggested, that S100A8 high levels in CF patients are a consequence of the clinical manifestations of the disease and not the cause [164,165]. Our observations are in accordance to this, the results do not show a direct effect of Calgranulin downregulation on the abundance of rescued Phe508del-CFTR (at the PM). Nonetheless, further analysis would be necessary to check if the activity of the chloride channel at the PM is not affected with Calgranulin downregulation. It was suggested that Calgranulin is a mediator linking neutrophil-dominant airway inflammation to mucin hyperproduction [86]. Therefore, in continuation of this work, it would also be interesting to verify changes in inflammation regulation and mucin production in a more complex CF disease model and where Calgranulin is downregulated.

TCP-1-Theta is another protein which knockdown did not impact the abundance of rescued Phe508del-CFTR at the cell surface. TCP-1-Theta is a subunit of the chaperonin CCT, that facilitates actin and tubulin folding [111]. In fact, actin and tubulin are obligate substrates of CTT, and we confirmed by western blot that following TCP-1-Theta knockdown tubulin is downregulated (result not shown) [113]. The same result was already seen for tubulin as well as for actin [116]. Therefore, tubulin could not be used for protein loading control in the western blot, instead we used β-catenin. Actin cytoskeleton participates in CFTR anchorage to the plasma membrane, so we initially expected TCP-1-Theta knockdown by siRNA would lead to a decrease of rPhe508del-CFTR levels at the PM as a direct consequence of actin protein levels decrease. However, after the cell surface biotinylation assay, western blot quantification revealed no alteration of rPhe508del-CFTR in the recuperated biotinylated surface proteins and whole cell lysates. TCP-1-Theta protein levels were reduced to ≈ 39% when compared to control levels. Is the remaining protein enough for actin folding and subsequent CFTR anchoring to the PM? We observed no changes in the overall CFTR protein levels, neither band B or band C, which is expected since the chloride channel is not a substrate of the chaperonin CCT [115]. Given the results, we propose that TCP-1-Theta does not impact on rPhe508del-CFTR overall abundance or at the PM levels.

Like the proteins discussed before we found no significant change in the abundance of VX-809 rescued Phe508del-CFTR at the cell surface after FLT-1 knockdown. Western blot analysis also shows that the abundance of rPhe508del-CFTR, in WCL, is close to control. Flt-1 is a tyrosine kinase cell-surface receptor that can bind the angiogenic factors VEGF-A, VEGF-B and PIGF [136–138]. Its gene can

also express a soluble short protein, sFlt-1, that is VEGF-A antagonist [141]. The results do not show a relation between Flt-1 expression and CFTR levels, which is in accordance to Flt-1 known functions. However, it was reported that Flt-1 tyrosine kinase activity signalling promotes pulmonary fibrosis and that blocking the signal may be useful in the treatment of pulmonary fibrosis [166,167]. Relative to CF subjects it was only reported an increase of VEGFA levels in the serum and that CFTR dysfunction induces VEGFA synthesis in airway epithelium [168]. Thus, we suggest that Flt-1 expression does not affect Phe508del-CFTR abundance in the PM or its overall levels. Whether it can play a role in the pathophysiology of CF, this is something that can be further investigated.

Following Ku86 knockdown, we observed in the WB a reduction in the abundance of surface rPhe508del-CFTR and its overall band C and B levels, on average to approximately 60% of control levels. However, the high variability among replicates removed statistical significance from these observations. Additional experimental replicates would be useful to clarify the significance of this reduction, but unfortunately these could not be carried out due to time constrains. Ku86 is a subunit of the Ku protein that found in the nucleus of the cell. And Ku protein is also a subunit of the DNA-PK (DNA repair enzyme), thus Ku86 is involved, among other function, in DNA replication and transcription regulation [127–129]. Taking in account Ku86 functions we investigated if CFTR transcript was affected. We observed a slight reduction of CFTR RNA, however also without statistic relevance. While this could explain the overall decrease in CFTR protein levels, without addidional replicates we cannot reach a precise conclusion on the effects of Ku86 knockdown on the overall and PM abundance of rPhe508del-CFTR.

Tenascin-C knockdown and cell surface biotinylation assay could only be performed once, giving a small data set of two replicates. Even so we did a qualitative analysis of the western blot membrane that shows a marked decrease in rPhe508del-CFTR at the PM when compared to control cells (siLuc + VX-809). In WCL, Tenascin-C knockdown does not change the overall abundance of rPhe508del-CFTR in WCL. Tenascin-C is a extracellular matrix protein that binds ECM components, surface receptors, soluble factors and pathogens [77–80]. As such, it is plausible that this protein can have a role in the stabilization of CFTR in the membrane. Again, more replicates of the assay would be needed to corroborate the results. It would also be interesting to investigate Tenascin-C levels in CF patients, since its expression is tightly regulated in adult tissue, and is expressed de novo during wound healing and pathological conditions like chronic inflammation. In fact, persistent Tenascin-C expression has been correlated with matrix deposition in patients with fibrotic lung disorders [80].

Regarding Coronin 1C and Enigma, depletion of either protein resulted in the reduction of rPhe508del-CFTR band C at the PM and in WCL, but with no change in band B levels. After Coronin 1C knockdown, the biotinylation assay revealed the statistically significant reduction of rPhe508del-CFTR at the cell surface, to ≈ 31% when compared to control. While in WCL, band C was reduced to ≈ 79%, while the abundance of immature form of CFTR is close to control. Coronin 1C is an ubiquitously expressed protein that can bind F-actin and participates in actin-dependent processes, and that it can be found associated to the cytoskeleton and membranes [89]. It is found to also bind GDP-bound form of Rab27a, a regulator of membrane trafficking, and be its effector in insulin-secreted cell lines [91]. In fact, it was also shown that Rab27a can interact with CFTR, restraining its localization to intracellular compartments, and thus limiting the channel expression at the PM [169,170]. Is the action of Rab27a on CFTR affected by Coronin 1C knockdown? Coronin 1C has been identified to interact with Rac1 as well, and mediate its redistribution from lateral to protruding membrane where its activated [93]. It was already identified that CFTR anchors to apical actin cytoskeleton, via Ezrin, upon activation of Rac1 signalling [54]. Is Coronin 1C knockdown reducing Rac1 levels at the PM of these cells? And is that the reason the reduction of rPhe508del-CFTR levels is more pronounced at the membrane?

Taking all data into consideration, we wondered whether Coronin 1C might be a key participant in conventional CFTR trafficking to the PM, and not only modulating the abundance of the rescued channel at the PM. Thus, we tested what effect downregulating Coronin 1C protein levels had in the abundance of wt CFTR in CFBE cells. It was with surprise that we did not observe any alteration of wt CFTR protein levels at the cell surface, nor in WCL. Is the difference between mutant and wt CFTR because of the depletion of Coronin 1C was more efficient in Phe508del-CFTR-expressing cells? Also, does the levels of wt CFTR protein being higher than what a pharmacological rescued of Phe508del-CFTR can achieve, downplay the effects of Coronin 1C knockdown? In continuation of the work, it would be interesting to try and answer these questions.

Enigma knockdown resulted in a reduction of rPhe508del-CFTR at the PM and band C on WCL to ≈ 60% of control cells, suggesting that post-ER trafficking of Phe508del-CFTR might be affected. Enigma is a cytosolic protein with PDZ and LIM domains that function as protein-protein interaction domains. Can Enigma binding partners be responsible by the reduction of rPhe508del-CFTR levels? In fact, a few of enigma binding partners are F-actin and YAP, the later found recently to bind Phe508del-CFTR and be a mediator for fibrotic/epithelial-mesenchymal transition processes in CF [105,171]. For Enigma studies, we also used wt-CFTR cell line and downregulated Enigma. While we had opportunity to make only one biotinylation assay, qualitative analysis of western blot membrane appears to show no clear variation in wt-CFTR at the PM but or in WCL. More assays repetitions are needed to give a trustworthy result. However, if the tendency is confirmed it might indicate that enigma is an exclusive interactor of rescued Phe508del-CFTR, regulating post-ER- trafficking or stability.

The other four proteins in study, βII Spectrin, PTRF, TG2 and Lamin, show the same result when downregulated – They caused rPhe508del-CFTR band C reduction, not only at the PM, but in WCL, as well as band B, indicating an interference in the CFTR overall production. Starting with βII Spectrin knockdown, WB analysis revealed a noticeable reduction in rPhe508del-CFTR levels and band B, when compared to control. We went further and analysed CFTR transcript levels. CFTR RNA levels were reduced to ≈ 76%, indicating that βII Spectrin could be required for proper CFTR gene expression. However, the mechanism leading to this effect is unclear. βII Spectrin is a cytoskeletal protein and a subunit of Spectrin protein, involved in maintaining cell architecture, morphology, and membrane stability. Spectrin has been implicated in protein transport from the ER to the Golgi, and can also interact with the Golgi apparatus and affect cell secretion [95,97]. βII Spectrin can bind to actin and ankyrin forming large protein complex with actin and ankyrin, that couples membrane proteins with the cytoskeleton structure [99,115]. This suggests that Spectrin may also interfere with proper rPhe508del-CFTR trafficking and processing, reducing banc C levels. Altogether, the results suggest that βII Spectrin knockdown might affect synthesis and processing of Phe508del-CFTR and thus its abundance at the PM.

PTRF knockdown produced a relevant reduction of rPhe508-CFTR abundance in the membrane, to approximately 30% of control cell levels. In fact, the same was observed for overall CFTR levels in the cell. In WCL, band C and B were reduced to ≈ 30% and 50% respectively. Since band B is also reduced, PTRF knockdown may affect not only CFTR processing but also its synthesis. Thus, we assessed CFTR transcript levels. CFTR mRNA levels were reduced to ~70%, suggesting an impairment in CFTR gene expression. This result goes in accordance with PTRF function as a cellular factor required for Pol I transcription termination [120], however other mechanisms must be in place to produce the pronounced decrease in CFTR overall abundance observed. Such mechanisms will require further investigation in the future.

TG2 knockdown also produced promounced reduction in rPhe508-CFTR abundance in the PM, to ≈ 30% of control cell levels. This was accompanied by the decrease in band C and B, in WCL, to ≈ 40% and ≈ 50%, respectively. Interestingly, TG2 depletion only reduced CFTR mRNA in ≈ 20%. TG2 is an inducible transamidating acyltransferase that catalyzes Ca(2+)-dependent protein modifications. In addition to being an enzyme, TG2 also serves as a G protein for several seven transmembrane receptors and acts as a co-receptor for integrin β1 and β3 integrins distinguishing it from other members of the transglutaminase family. TG2 is ubiquitously expressed in almost all cell types and all cell compartments. TG2 has been associated with various human diseases including inflammation and fibrosis [123–125]. Thus, the depletion of TG2 may act to hinder the synthesis and processing of Phe508del-CFTR along the secretory pathway reducing its overall and PM. However, and contrary to our results, it has been demonstrated that the use of cysteamine, that can inhibit TG2 transamidating activity, improves the trafficking of Phe508del-CFTR [172–175]. These discrepancies will require further investigation in the future.

Lamin B1 is a component of the nuclear lamina, participating in chromatin organization and DNA repair and replication [130–133]. Given Lamin B1 functions, its presence at rPhe508del-CFTR complexes captured from the PM was unexpected. Hence we included this protein as a control for hit protein specificity. It was surprising to find that although, it had a modest impact in decreasing CFTR mRNA levels, it had a very significant impact in steady-state CFTR band C levels, indicating a pronounced interference with the late processing or stability of the rescued mutant protein. This result strengthens the robustness of the candidate proteins identified in complex with rPhe508del-CFTR at the PM, but also indicates that Lamin B1 may have important functions outside the nucleus that are as of yet unrecognized.

6. Conclusion

Through this work we investigated the effects of depleting each of 11 proteins putatively interacting with pharmacological rescued Phe508del-CFTR at the PM. We evaluated how this depletion would influence both the channel's overall abundance and its localization on the cell's surface. We found that while several of the candidate proteins were clearly involved in maintaining rPhe508del overall and PM levels none appear to constitute a good target to improve the pharmacological rescue of Phe508del-CFTR or its retention at the PM. However, one should not disregard future studies to understand the mechanism by which many of these proteins seem to affect the channel's abundance. One important point is to find if the candidate proteins, or their dysregulation, is somehow involved in CF disease ethology, or whether their function could contribute for the differential response to CFTR modulator drugs from patients with equivalent CFTR genotypes [25,27,30]. Extending the investigation, can also bring light into other interactions of Phe508del-CFTR that might be of interest to the discover of new CFTR modulators.

7. References

(1) Fong, P.; Gray, M. A. Orchestration of Vectorial Chloride Transport by Epithelia. In *Advances in Molecular and Cell Biology*; Elsevier, 2006; Vol. 38, pp 329–368. https://doi.org/10.1016/S1569-2558(06)38012-5.

(2) Frizzell, R. A.; Hanrahan, J. W. Physiology of Epithelial Chloride and Fluid Secretion. *Cold Spring Harbor Perspectives in Medicine* **2012**, *2* (6), a009563–a009563. https://doi.org/10.1101/cshperspect.a009563.

(3) Guggino, W. B.; Stanton, B. A. New Insights into Cystic Fibrosis: Molecular Switches That Regulate CFTR. *Nat Rev Mol Cell Biol* **2006**, *7* (6), 426–436. https://doi.org/10.1038/nrm1949.

(4) Dransfield, D. T. Ezrin Is a Cyclic AMP-Dependent Protein Kinase Anchoring Protein. *The EMBO Journal* **1997**, *16* (1), 35–43. https://doi.org/10.1093/emboj/16.1.35.

(5) Riordan, J. R.; Rommens, J. M.; Kerem, B.-S.; Alon, N.; Rozmahel, R.; Grzelczak, Z.; Zielenski, J.; Lok, S.; Plavsic, N.; Chou, J.-L.; Drumm, M. L.; Iannuzzi, M. C. Identification of the Cystic Fibrosis Gene: Cloning and Characterization of Complementary DNA. *Science* **1989**, *245*, 8. https://doi.org/10.1126/science.2475911.

(6) Scotet, V.; L'Hostis, C.; Férec, C. The Changing Epidemiology of Cystic Fibrosis: Incidence, Survival and Impact of the CFTR Gene Discovery. *Genes* **2020**, *11* (6), 589. https://doi.org/10.3390/genes11060589.

(7) Brian P O'Sullivan; Steven D Freedman. Cystic Fibrosis. *Lancet 2009; 373: 1891–904* 14. https://doi.org/10.1016/S01406736(09)60327-5.

(8) Elborn, J. S. Cystic Fibrosis. *The Lancet* **2016**, *388* (10059), 2519–2531. https://doi.org/10.1016/S0140-6736(16)00576-6.

(9) De Boeck, K.; Zolin, A.; Cuppens, H.; Olesen, H. V.; Viviani, L. The Relative Frequency of CFTR Mutation Classes in European Patients with Cystic Fibrosis. *Journal of Cystic Fibrosis* **2014**, *13* (4), 403–409. https://doi.org/10.1016/j.jcf.2013.12.003.

(10) Riordan, J. R. CFTR Function and Prospects for Therapy. *Annual Review of Biochemistry* **2008**, *Vol. 77:701-726*, 29. https://doi.org/10.1146/annurev.biochem.75.103004.142532.

(11) Sheppard, D. N.; Welsh, M. J. Structure and Function of the CFTR Chloride Channel. *Physiological Reviews* **1999**, *79* (1), S23–S45. https://doi.org/10.1152/physrev.1999.79.1.S23.

(12) Rowe, S. M.; Miller, S.; Sorscher, E. J. Cystic Fibrosis. *N Engl J Med* **2005**, *352* (19), 1992–2001. https://doi.org/10.1056/NEJMra043184.

(13) Farinha, C. M.; Matos, P.; Amaral, M. D. Control of Cystic Fibrosis Transmembrane Conductance Regulator Membrane Trafficking: Not Just from the Endoplasmic Reticulum to the Golgi. *FEBS J* **2013**, *280* (18), 4396–4406. https://doi.org/10.1111/febs.12392.

(14) Hwang, T.-C.; Yeh, J.-T.; Zhang, J.; Yu, Y.-C.; Yeh, H.-I.; Destefano, S. Structural Mechanisms of CFTR Function and Dysfunction. *Journal of General Physiology* **2018**, *150* (4), 539–570. https://doi.org/10.1085/jgp.201711946.

(15) Sohma, Y.; Hwang, T.-C. Cystic Fibrosis and the CFTR Anion Channel. In *Handbook of Ion Channels*; Zheng, J., Trudeau, M., Eds.; CRC Press, 2015; pp 627–648. https://doi.org/10.1201/b18027-48.

(16) Guggino, W. B.; Stanton, B. A. New Insights into Cystic Fibrosis: Molecular Switches That Regulate CFTR. *Nat Rev Mol Cell Biol* **2006**, *7* (6), 426–436. https://doi.org/10.1038/nrm1949.

(17) Marianna M Sockrider; Thomas W Ferko. Twenty Facts About Cystic Fibrosis. *American Journal of Respiratory and Critical Care Medicine 196(12)*, P23–P24. https://doi.org/10.1164/rccm.19612P23.

(18) Sheppard, M. N.; Nicholson, A. G. The Pathology of Cystic Fibrosis. *Current Diagnostic Pathology* **2002**, *8* (1), 50–59. https://doi.org/10.1054/cdip.2001.0088.
(19) Grossman, S.; Grossman, L. C. Pathophysiology of Cystic Fibrosis: Implications for Critical Care Nurses. *Critical Care Nurse* **2005**, *25* (4), 46–51. https://doi.org/10.4037/ccn2005.25.4.46.
(20) Ehre, C.; Ridley, C.; Thornton, D. J. Cystic Fibrosis: An Inherited Disease Affecting Mucin-Producing Organs. *The International Journal of Biochemistry & Cell Biology* **2014**, *52*, 136–145. https://doi.org/10.1016/j.biocel.2014.03.011.
(21) Kreda, S. M.; Davis, C. W.; Rose, M. C. CFTR, Mucins, and Mucus Obstruction in Cystic Fibrosis. *Cold Spring Harbor Perspectives in Medicine* **2012**, *2* (9), a009589–a009589. https://doi.org/10.1101/cshperspect.a009589.
(22) Quinton, P. M. Cystic FIbrosis: Impaired Bicarbonate Secretion and Mucoviscidosis. *Lancet* **2008**, *372*, 415–417. https://doi.org/10.1016/S0140-6736(08)61162-9.
(23) Lemke, A. Reproductive Issues in Adults with Cystic Fibrosis: Implications for Genetic Counseling. *J Genet Counsel* **1992**, *1* (3), 211–218. https://doi.org/10.1007/BF00961582.
(24) Ahmad, A.; Ahmed, A.; Patrizio, P. Cystic Fibrosis and Fertility: *Current Opinion in Obstetrics and Gynecology* **2013**, *25* (3), 167–172. https://doi.org/10.1097/GCO.0b013e32835f1745.
(25) Fonseca, C.; Bicker, J.; Alves, G.; Falcão, A.; Fortuna, A. Cystic Fibrosis: Physiopathology and the Latest Pharmacological Treatments. *Pharmacological Research* **2020**, 105267. https://doi.org/10.1016/j.phrs.2020.105267.
(26) Amaral, M. D. Novel Personalized Therapies for Cystic Fibrosis: Treating the Basic Defect in All Patients. *J Intern Med* **2015**, *277* (2), 155–166. https://doi.org/10.1111/joim.12314.
(27) De Boeck, K.; Amaral, M. D. Progress in Therapies for Cystic Fibrosis. *The Lancet Respiratory Medicine* **2016**, *4* (8), 662–674. https://doi.org/10.1016/S2213-2600(16)00023-0.
(28) Collins, F. Cystic Fibrosis: Molecular Biology and Therapeutic Implications. *Science* **1992**, *256* (5058), 774–779. https://doi.org/10.1126/science.1375392.
(29) Farinha, C. M.; Matos, P. Repairing the Basic Defect in Cystic Fibrosis - One Approach Is Not Enough. *FEBS J* **2016**, *283* (2), 246–264. https://doi.org/10.1111/febs.13531.
(30) Lopes-Pacheco, M. CFTR Modulators: The Changing Face of Cystic Fibrosis in the Era of Precision Medicine. *Front. Pharmacol.* **2020**, *10*, 1662. https://doi.org/10.3389/fphar.2019.01662.
(31) Amaral, M. D.; Kunzelmann, K. Molecular Targeting of CFTR as a Therapeutic Approach to Cystic Fibrosis. *Trends in Pharmacological Sciences* **2007**, *28* (7), 334–341. https://doi.org/10.1016/j.tips.2007.05.004.
(32) Xue, X.; Mutyam, V.; Tang, L.; Biswas, S.; Du, M.; Jackson, L. A.; Dai, Y.; Belakhov, V.; Shalev, M.; Chen, F.; Schacht, J.; J. Bridges, R.; Baasov, T.; Hong, J.; Bedwell, D. M.; Rowe, S. M. Synthetic Aminoglycosides Efficiently Suppress Cystic Fibrosis Transmembrane Conductance Regulator Nonsense Mutations and Are Enhanced by Ivacaftor. *Am J Respir Cell Mol Biol* **2014**, *50* (4), 805–816. https://doi.org/10.1165/rcmb.2013-0282OC.
(33) Leubitz, A.; Frydman-Marom, A.; Sharpe, N.; van Duzer, J.; Campbell, K. C. M.; Vanhoutte, F. Safety, Tolerability, and Pharmacokinetics of Single Ascending Doses of ELX-02, a Potential Treatment for Genetic Disorders Caused by Nonsense Mutations, in Healthy Volunteers. *Clinical Pharmacology in Drug Development* **2019**, *8* (8), 984–994. https://doi.org/10.1002/cpdd.647.
(34) Li, C.; Naren, A. P. Macromolecular Complexes of Cystic Fibrosis Transmembrane Conductance Regulator and Its Interacting Partners. *Pharmacology & Therapeutics* **2005**, *108* (2), 208–223. https://doi.org/10.1016/j.pharmthera.2005.04.004.

(35) Li, C.; Naren, A. P. CFTR Chloride Channel in the Apical Compartments: Spatiotemporal Coupling to Its Interacting Partners. *Integr. Biol.* **2010**, *2* (4), 161. https://doi.org/10.1039/b924455g.

(36) Wang, S.; Li, M. Molecular Studies of CFTR Interacting Proteins. *Pfluegers Archiv European Journal of Physiology* **2001**, *443* (0), S62–S64. https://doi.org/10.1007/s004240100646.

(37) Cheng, J.; Moyer, B. D.; Milewski, M.; Loffing, J.; Ikeda, M.; Mickle, J. E.; Cutting, G. R.; Li, M.; Stanton, B. A.; Guggino, W. B. A Golgi-Associated PDZ Domain Protein Modulates Cystic Fibrosis Transmembrane Regulator Plasma Membrane Expression. *Journal of Biological Chemistry* **2002**, *277* (5), 3520–3529. https://doi.org/10.1074/jbc.M110177200.

(38) Cheng, J.; Wang, H.; Guggino, W. B. Modulation of Mature Cystic Fibrosis Transmembrane Regulator Protein by the PDZ Domain Protein CAL. *Journal of Biological Chemistry* **2004**, *279* (3), 1892–1898. https://doi.org/10.1074/jbc.M308640200.

(39) Reczek, D.; Bretscher, A. The Carboxyl-Terminal Region of EBP50 Binds to a Site in the Amino-Terminal Domain of Ezrin That Is Masked in the Dormant Molecule. *Journal of Biological Chemistry* **1998**, *273* (29), 18452–18458. https://doi.org/10.1074/jbc.273.29.18452.

(40) Short, D. B.; Trotter, K. W.; Reczek, D.; Kreda, S. M.; Bretscher, A.; Boucher, R. C.; Stutts, M. J.; Milgram, S. L. An Apical PDZ Protein Anchors the Cystic Fibrosis Transmembrane Conductance Regulator to the Cytoskeleton. *Journal of Biological Chemistry* **1998**, *273* (31), 19797–19801. https://doi.org/10.1074/jbc.273.31.19797.

(41) Sun, F.; Hug, M. J.; Bradbury, N. A.; Frizzell, R. A. Protein Kinase A Associates with Cystic Fibrosis Transmembrane Conductance Regulator via an Interaction with Ezrin. *Journal of Biological Chemistry* **2000**, *275* (19), 14360–14366. https://doi.org/10.1074/jbc.275.19.14360.

(42) Sun, F.; Hug, M. J.; Lewarchik, C. M.; Yun, C.-H. C.; Bradbury, N. A.; Frizzell, R. A. E3KARP Mediates the Association of Ezrin and Protein Kinase A with the Cystic Fibrosis Transmembrane Conductance Regulator in Airway Cells. *Journal of Biological Chemistry* **2000**, *275* (38), 29539–29546. https://doi.org/10.1074/jbc.M004961200.

(43) Moyer, B. D.; Duhaime, M.; Shaw, C.; Denton, J.; Reynolds, D.; Karlson, K. H.; Pfeiffer, J.; Wang, S.; Mickle, J. E.; Milewski, M.; Cutting, G. R.; Guggino, W. B.; Li, M.; Stanton, B. A. The PDZ-Interacting Domain of Cystic Fibrosis Transmembrane Conductance Regulator Is Required for Functional Expression in the Apical Plasma Membrane. *Journal of Biological Chemistry* **2000**, *275* (35), 27069–27074. https://doi.org/10.1016/S0021-9258(19)61481-X.

(44) Haggie, P. M.; Kim, J. K.; Lukacs, G. L.; Verkman, A. S. Tracking of Quantum Dot-Labeled CFTR Shows Near Immobilization by C-Terminal PDZ Interactions□D □V. *Molecular Biology of the Cell* **2006**, *17*, 9.

(45) Reczek, D.; Berryman, M.; Bretscher, A. Identification of EBP50: A PDZ-Containing Phosphoprotein That Associates with Members of the Ezrin-Radixin-Moesin Family. *Journal of Cell Biology* **1997**, *139* (1), 169–179. https://doi.org/10.1083/jcb.139.1.169.

(46) Wang, S.; Raab, R. W.; Schatz, P. J.; Guggino, W. B.; Li, M. Peptide Binding Consensus of the NHE-RF-PDZ1 Domain Matches the C-Terminal Sequence of Cystic Fibrosis Transmembrane Conductance Regulator (CFTR). *FEBS Letters* **1998**, *427* (1), 103–108. https://doi.org/10.1016/S0014-5793(98)00402-5.

(47) Cushing, P. R.; Fellows, A.; Villone, D.; Boisguérin, P.; Madden, D. R. The Relative Binding Affinities of PDZ Partners for CFTR: A Biochemical Basis for Efficient Endocytic Recycling. *Biochemistry* **2008**, *47* (38), 10084–10098. https://doi.org/10.1021/bi8003928.

(48) Bhattacharya, S.; Dai, Z.; Li, J.; Baxter, S.; Callaway, D. J. E.; Cowburn, D.; Bu, Z. A Conformational Switch in the Scaffolding Protein NHERF1 Controls Autoinhibition and Complex Formation. *Journal of Biological Chemistry* **2010**, *285* (13), 9981–9994. https://doi.org/10.1074/jbc.M109.074005.

(49) Li, J.; Callaway, D. J. E.; Bu, Z. Ezrin Induces Long-Range Interdomain Allostery in the Scaffolding Protein NHERF1. *Journal of Molecular Biology* **2009**, *392* (1), 166–180. https://doi.org/10.1016/j.jmb.2009.07.005.

(50) Guggino, W. B.; Stanton, B. A. New Insights into Cystic Fibrosis: Molecular Switches That Regulate CFTR. 11.

(51) Loureiro, C. A.; Matos, A. M.; Dias-Alves, Â.; Pereira, J. F.; Uliyakina, I.; Barros, P.; Amaral, M. D.; Matos, P. A Molecular Switch in the Scaffold NHERF1 Enables Misfolded CFTR to Evade the Peripheral Quality Control Checkpoint. *Sci. Signal.* **2015**, *8* (377). https://doi.org/10.1126/scisignal.aaa1580.

(52) Bretscher, A.; Chambers, D.; Nguyen, R.; Reczek, D. ERM-Merlin and EBP50 Protein Families in Plasma Membrane Organization and Function. *Annu. Rev. Cell Dev. Biol.* **2000**, *16* (1), 113–143. https://doi.org/10.1146/annurev.cellbio.16.1.113.

(53) Gary, R.; Bretscher, A. Ezrin Self-Association Involves Binding of an N-Terminal Domain to a Normally Masked C-Terminal Domain That Includes the F-Actin Binding Site. *Molecular Biology of the Cell* **1995**, *6* (8), 1061–1075. https://doi.org/10.1091/mbc.6.8.1061.

(54) Moniz, S.; Sousa, M.; Moraes, B. J.; Mendes, A. I.; Palma, M.; Barreto, C.; Fragata, J. I.; Amaral, M. D.; Matos, P. HGF Stimulation of Rac1 Signaling Enhances Pharmacological Correction of the Most Prevalent Cystic Fibrosis Mutant F508del-CFTR. *ACS Chem. Biol.* **2013**, *8* (2), 432–442. https://doi.org/10.1021/cb300484r.

(55) Fievet, B. T.; Gautreau, A.; Roy, C.; Del Maestro, L.; Mangeat, P.; Louvard, D.; Arpin, M. Phosphoinositide Binding and Phosphorylation Act Sequentially in the Activation Mechanism of Ezrin. *Journal of Cell Biology* **2004**, *164* (5), 653–659. https://doi.org/10.1083/jcb.200307032.

(56) Simons, P. C.; Pietromonaco, S. F.; Reczek, D.; Bretscher, A.; Elias, L. C-Terminal Threonine Phosphorylation Activates ERM Proteins to Link the Cell's Cortical Lipid Bilayer to the Cytoskeleton. *Biochemical and Biophysical Research Communications* **1998**, *253* (3), 561–565. https://doi.org/10.1006/bbrc.1998.9823.

(57) Matsui, T.; Maeda, M.; Doi, Y.; Yonemura, S.; Amano, M.; Kaibuchi, K.; Tsukita, S.; Tsukita, S. Rho-Kinase Phosphorylates COOH-Terminal Threonines of Ezrin/Radixin/Moesin (ERM) Proteins and Regulates Their Head-to-Tail Association. *Journal of Cell Biology* **1998**, *140* (3), 647–657. https://doi.org/10.1083/jcb.140.3.647.

(58) Ng, T.; Parsons, M.; Hughes, W. E.; Monypenny, J.; Zicha, D.; Gautreau, A.; Arpin, M.; Gschmeissner, S.; Verveer, P. J.; Bastiaens, P. I. H.; Parker, P. J. Ezrin Is a Downstream Effector of Trafficking PKC-Integrin Complexes Involved in the Control of Cell Motility. 19.

(59) McClure, M. L.; Barnes, S.; Brodsky, J. L.; Sorscher, E. J. Trafficking and Function of the Cystic Fibrosis Transmembrane Conductance Regulator: A Complex Network of Posttranslational Modifications. *American Journal of Physiology-Lung Cellular and Molecular Physiology* **2016**, *311* (4), L719–L733. https://doi.org/10.1152/ajplung.00431.2015.

(60) Estabrooks, S.; Brodsky, J. L. Regulation of CFTR Biogenesis by the Proteostatic Network and Pharmacological Modulators. *IJMS* **2020**, *21* (2), 452. https://doi.org/10.3390/ijms21020452.

(61) Sharma, M.; Pampinella, F.; Nemes, C.; Benharouga, M.; So, J.; Du, K.; Bache, K. G.; Papsin, B.; Zerangue, N.; Stenmark, H.; Lukacs, G. L. Misfolding Diverts CFTR from Recycling to Degradation. *Journal of Cell Biology* **2004**, *164* (6), 923–933. https://doi.org/10.1083/jcb.200312018.

(62) Okiyoneda, T.; Barrière, H.; Bagdány, M.; Rabeh, W. M.; Du, K.; Höhfeld, J.; Young, J. C.; Lukacs, G. L. Peripheral Protein Quality Control Removes Unfolded CFTR from the Plasma Membrane. *Science* **2010**, *329* (5993), 805–810. https://doi.org/10.1126/science.1191542.

(63) Jensen, T. J.; Loo, M. A.; Pind, S.; Williams, D. B.; Goldberg, A. L.; Riordan, J. R. Multiple Proteolytic Systems, Including the Proteasome, Contribute to CFTR Processing. *Cell* **1995**, *83* (1), 129–135. https://doi.org/10.1016/0092-8674(95)90241-4.

(64) Farinha, C. M.; Gentzsch, M. Revisiting CFTR Interactions: Old Partners and New Players. *IJMS* **2021**, *22* (24), 13196. https://doi.org/10.3390/ijms222413196.

(65) Prince, L. S.; Workman, R. B.; Marchase, R. B. Rapid Endocytosis of the Cystic Fibrosis Transmembrane Conductance Regulator Chloride Channel. *Proc. Natl. Acad. Sci. U.S.A.* **1994**, *91* (11), 5192–5196. https://doi.org/10.1073/pnas.91.11.5192.

(66) Bertrand, C. A.; Frizzell, R. A. The Role of Regulated CFTR Trafficking in Epithelial Secretion. *American Journal of Physiology-Cell Physiology* **2003**, *285* (1), C1–C18. https://doi.org/10.1152/ajpcell.00554.2002.

(67) Lukacs, L. G.; Segal, G.; Kartner, N.; Grinstein, S.; Zhang, F. Constitutive Internalization of Cystic Fibrosis Transmembrane Conductance Regulator Occurs via Clathrin-Dependent Endocytosis and Is Regulated by Protein Phosphorylation. *Biochemical Journal* **1997**, *328* (2), 353–361. https://doi.org/10.1042/bj3280353.

(68) Bradbury, N. A.; Cohn, J. A.; Venglarik, C. J.; Bridges, R. J. Biochemical and Biophysical Identification of Cystic Fibrosis Transmembrane Conductance Regulator Chloride Channels as Components of Endocytic Clathrin-Coated Vesicles. *Journal of Biological Chemistry* **1994**, *269* (11), 8296–8302. https://doi.org/10.1016/S0021-9258(17)37192-2.

(69) Gentzsch, M.; Chang, X.-B.; Cui, L.; Wu, Y.; Ozols, V. V.; Choudhury, A.; Pagano, R. E.; Riordan, J. R. Endocytic Trafficking Routes of Wild Type and deltaF508 Cystic Fibrosis Transmembrane Conductance Regulator. *Molecular Biology of the Cell* **2004**, *15*, 13. https://doi.org/10.1091/mbc.e04-03-0176.

(70) Weixel, K. M.; Bradbury, N. A. The Carboxyl Terminus of the Cystic Fibrosis Transmembrane Conductance Regulator Binds to AP-2 Clathrin Adaptors. *Journal of Biological Chemistry* **2000**, *275* (5), 3655–3660. https://doi.org/10.1074/jbc.275.5.3655.

(71) Okiyoneda, T.; Lukacs, G. L. Cell Surface Dynamics of CFTR: The Ins and Outs. *Biochimica et Biophysica Acta (BBA) - Molecular Cell Research* **2007**, *1773* (4), 476–479. https://doi.org/10.1016/j.bbamcr.2007.01.004.

(72) Picciano, J. A.; Ameen, N.; Grant, B. D.; Bradbury, N. A. Rme-1 Regulates the Recycling of the Cystic Fibrosis Transmembrane Conductance Regulator. *American Journal of Physiology-Cell Physiology* **2003**, *285* (5), C1009–C1018. https://doi.org/10.1152/ajpcell.00140.2003.

(73) Swiatecka-Urban, A.; Brown, A.; Moreau-Marquis, S.; Renuka, J.; Coutermarsh, B.; Barnaby, R.; Karlson, K. H.; Flotte, T. R.; Fukuda, M.; Langford, G. M.; Stanton, B. A. The Short Apical Membrane Half-Life of Rescued ΔF508-Cystic Fibrosis Transmembrane Conductance Regulator (CFTR) Results from Accelerated Endocytosis of ΔF508-CFTR in Polarized Human Airway Epithelial Cells. *Journal of Biological Chemistry* **2005**, *280* (44), 36762–36772. https://doi.org/10.1074/jbc.M508944200.

(74) Wang, X.; Venable, J.; LaPointe, P.; Hutt, D. M.; Koulov, A. V.; Coppinger, J.; Gurkan, C.; Kellner, W.; Matteson, J.; Plutner, H.; Riordan, J. R.; Kelly, J. W.; Yates, J. R.; Balch, W. E. Hsp90 Cochaperone Aha1 Downregulation Rescues Misfolding of CFTR in Cystic Fibrosis. *Cell* **2006**, *127* (4), 803–815. https://doi.org/10.1016/j.cell.2006.09.043.

(75) Pankow, S.; Bamberger, C.; Calzolari, D.; Martínez-Bartolomé, S.; Lavallée-Adam, M.; Balch, W. E.; Yates, J. R. ΔF508 CFTR Interactome Remodelling Promotes Rescue of Cystic Fibrosis. *Nature* **2015**, *528* (7583), 510–516. https://doi.org/10.1038/nature15729.

(76) Loureiro, C. A.; Santos, J. D.; Matos, A. M.; Jordan, P.; Matos, P.; Farinha, C. M.; Pinto, F. R. Network Biology Identifies Novel Regulators of CFTR Trafficking and Membrane Stability. *Front. Pharmacol.* **2019**, *10*, 619. https://doi.org/10.3389/fphar.2019.00619.

(77) Midwood, K. S.; Chiquet, M.; Tucker, R. P.; Orend, G. Tenascin-C at a Glance. *Journal of Cell Science* **2016**, jcs.190546. https://doi.org/10.1242/jcs.190546.

(78) Midwood, K. S.; Hussenet, T.; Langlois, B.; Orend, G. Advances in Tenascin-C Biology. *Cell. Mol. Life Sci.* **2011**, *68* (19), 3175–3199. https://doi.org/10.1007/s00018-011-0783-6.

(79) Orend, G. Potential Oncogenic Action of Tenascin-C in Tumorigenesis. *The International Journal of Biochemistry & Cell Biology* **2005**, *37* (5), 1066–1083. https://doi.org/10.1016/j.biocel.2004.12.002.

(80) Midwood, K. S.; Orend, G. The Role of Tenascin-C in Tissue Injury and Tumorigenesis. *J. Cell Commun. Signal.* **2009**, *3* (3–4), 287–310. https://doi.org/10.1007/s12079-009-0075-1.

(81) Chiquet-Ehrismann, R.; Mackie, E. J.; Pearson, C. A.; Sakakura, T. Tenascin: An Extracellular Matrix Protein Involved in Tissue Interactions during Fetal Development and Oncogenesis. *Cell* **1986**, *47* (1), 131–139. https://doi.org/10.1016/0092-8674(86)90374-0.

(82) Chiquet-Ehrismann, R.; Chiquet, M. Tenascins: Regulation and Putative Functions during Pathological Stress: Tenascins in Pathological Stress. *J. Pathol.* **2003**, *200* (4), 488–499. https://doi.org/10.1002/path.1415.

(83) Odink, K.; Cerletti, N.; Brüggen, J.; Clerc, R. G.; Tarcsay, L.; Zwadlo, G.; Gerhards, G.; Schlegel, R.; Sorg, C. Two Calcium-Binding Proteins in Infiltrate Macrophages of Rheumatoid Arthritis. *Nature* **1987**, *330* (6143), 80–82. https://doi.org/10.1038/330080a0.

(84) Donato, R.; Cannon, B. R.; Sorci, G.; Riuzzi, F.; Hsu, K.; Weber, D. J.; Geczy, C. L. Functions of S100 Proteins. *Current Molecular Medicine* **2013**, *13 (1)*, 24–57.

(85) Foell, D.; Wittkowski, H.; Vogl, T.; Roth, J. S100 Proteins Expressed in Phagocytes: A Novel Group of Damage-Associated Molecular Pattern Molecules. *Journal of Leukocyte Biology* **2007**, *81* (1), 28–37. https://doi.org/10.1189/jlb.0306170.

(86) Kang, J. H.; Hwang, S. M.; Chung, I. Y. S100A8, S100A9 and S100A12 Activate Airway Epithelial Cells to Produce MUC5AC via Extracellular Signal-Regulated Kinase and Nuclear Factor- *κ* B Pathways. *Immunology* **2015**, *144* (1), 79–90. https://doi.org/10.1111/imm.12352.

(87) Wang, S.; Song, R.; Wang, Z.; Jing, Z.; Wang, S.; Ma, J. S100A8/A9 in Inflammation. *Front. Immunol.* **2018**, *9*, 1298. https://doi.org/10.3389/fimmu.2018.01298.

(88) Dorin, J. R.; Novak, M.; Hill, R. E.; Brock, D. J. H.; Secher, D. S.; van Heyningen, V. A Clue to the Basic Defect in Cystic Fibrosis from Cloning the CF Antigen Gene. *Nature* **1987**, *326* (6113), 614–617. https://doi.org/10.1038/326614a0.

(89) Uetrecht, A. C.; Bear, J. E. Coronins: The Return of the Crown. *Trends in Cell Biology* **2006**, *16* (8), 421–426. https://doi.org/10.1016/j.tcb.2006.06.002.

(90) Rosentreter, A.; Hofmann, A.; Xavier, C.-P.; Stumpf, M.; Noegel, A. A.; Clemen, C. S. Coronin 3 Involvement in F-Actin-Dependent Processes at the Cell Cortex. *Experimental Cell Research* **2007**, *313*, 878–895. https://doi.org/10.1016/j.yexcr.2006.12.015.

(91) Kimura, T.; Kaneko, Y.; Yamada, S.; Ishihara, H.; Senda, T.; Iwamatsu, A.; Niki, I. The GDP-Dependent Rab27a Effector Coronin 3 Controls Endocytosis of Secretory Membrane in Insulin-Secreting Cell Lines. *Journal of Cell Science* **2008**, *121* (18), 3092–3098. https://doi.org/10.1242/jcs.030544.

(92) Hoyer, M. J.; Chitwood, P. J.; Ebmeier, C. C.; Striepen, J. F.; Qi, R. Z.; Old, W. M.; Voeltz, G. K. A Novel Class of ER Membrane Proteins Regulates ER-Associated Endosome Fission. *Cell* **2018**, *175* (1), 254-265.e14. https://doi.org/10.1016/j.cell.2018.08.030.

(93) Williamson, R. C.; Cowell, C. A. M.; Hammond, C. L.; Bergen, D. J. M.; Roper, J. A.; Feng, Y.; Rendall, T. C. S.; Race, P. R.; Bass, M. D. Coronin-1C and RCC2 Guide Mesenchymal Migration by Trafficking Rac1 and Controlling GEF Exposure. *Journal of Cell Science* **2014**, 16.

(94) Spoerl, Z.; Stumpf, M.; Noegel, A. A.; Hasse, A. Oligomerization, F-Actin Interaction, and Membrane Association of the Ubiquitous Mammalian Coronin 3 Are Mediated by Its Carboxyl Terminus. *Journal of Biological Chemistry* **2002**, *277* (50), 48858–48867. https://doi.org/10.1074/jbc.M205136200.

(95) Machnicka, B.; Grochowalska, R.; Bogusławska, D. M.; Sikorski, A. F.; Lecomte, M. C. Spectrin-Based Skeleton as an Actor in Cell Signaling. *Cell. Mol. Life Sci.* **2012**, *69* (2), 191–201. https://doi.org/10.1007/s00018-011-0804-5.

(96) Winkelmann, J. C.; Forget, B. G. Erythroid and Nonerythroid Spectrins. *Blood* **1993**, *81* (12), 3173–3185. https://doi.org/10.1182/blood.V81.12.3173.3173.

(97) Zhang, R.; Zhang, C.; Zhao, Q.; Li, D. Spectrin: Structure, Function and Disease. *Sci. China Life Sci.* **2013**, *56* (12), 1076–1085. https://doi.org/10.1007/s11427-013-4575-0.

(98) Bennett, V.; Baines, A. J. Spectrin and Ankyrin-Based Pathways: Metazoan Inventions for Integrating Cells Into Tissues. *Physiological Reviews* **2001**, *81* (3), 1353–1392. https://doi.org/10.1152/physrev.2001.81.3.1353.

(99) Smith, S. A.; Sturm, A. C.; Curran, J.; Kline, C. F.; Little, S. C.; Bonilla, I. M.; Long, V. P.; Makara, M.; Polina, I.; Hughes, L. D.; Webb, T. R.; Wei, Z.; Wright, P.; Voigt, N.; Bhakta, D.; Spoonamore, K. G.; Zhang, C.; Weiss, R.; Binkley, P. F.; Janssen, P. M.; Kilic, A.; Higgins, R. S.; Sun, M.; Ma, J.; Dobrev, D.; Zhang, M.; Carnes, C. A.; Vatta, M.; Rasband, M. N.; Hund, T. J.; Mohler, P. J. Dysfunction in the βII Spectrin–Dependent Cytoskeleton Underlies Human Arrhythmia. *Circulation* **2015**, *131* (8), 695–708. https://doi.org/10.1161/CIRCULATIONAHA.114.013708.

(100) Kizhatil, K.; Davis, J. Q.; Davis, L.; Hoffman, J.; Hogan, B. L. M.; Bennett, V. Ankyrin-G Is a Molecular Partner of E-Cadherin in Epithelial Cells and Early Embryos. *Journal of Biological Chemistry* **2007**, *282* (36), 26552–26561. https://doi.org/10.1074/jbc.M703158200.

(101) Kizhatil, K.; Yoon, W.; Mohler, P. J.; Davis, L. H.; Hoffman, J. A.; Bennett, V. Ankyrin-G and B2-Spectrin Collaborate in Biogenesis of Lateral Membrane of Human Bronchial Epithelial Cells. *Journal of Biological Chemistry* **2007**, *282* (3), 2029–2037. https://doi.org/10.1074/jbc.M608921200.

(102) Cousin, M. A.; Creighton, B. A.; Breau, K. A.; Spillmann, R. C.; Torti, E.; Dontu, S.; Tripathi, S.; Ajit, D.; Edwards, R. J.; Afriyie, S.; Bay, J. C.; Harper, K. M.; Beltran, A. A.; Munoz, L. J.; Falcon Rodriguez, L.; Stankewich, M. C.; Person, R. E.; Si, Y.; Normand, E. A.; Blevins, A.; May, A. S.; Bier, L.; Aggarwal, V.; Mancini, G. M. S.; van Slegtenhorst, M. A.; Cremer, K.; Becker, J.; Engels, H.; Aretz, S.; MacKenzie, J. J.; Brilstra, E.; van Gassen, K. L. I.; van Jaarsveld, R. H.; Oegema, R.; Parsons, G. M.; Mark, P.; Helbig, I.; McKeown, S. E.; Stratton, R.; Cogne, B.; Isidor, B.; Cacheiro, P.; Smedley, D.; Firth, H. V.; Bierhals, T.; Kloth, K.; Weiss, D.; Fairley, C.; Shieh, J. T.; Kritzer, A.; Jayakar, P.; Kurtz-Nelson, E.; Bernier, R. A.; Wang, T.; Eichler, E. E.; van de Laar, I. M. B. H.; McConkie-Rosell, A.; McDonald, M. T.; Kemppainen, J.; Lanpher, B. C.; Schultz-Rogers, L. E.; Gunderson, L. B.; Pichurin, P. N.; Yoon, G.; Zech, M.; Jech, R.; Winkelmann, J.; Undiagnosed Diseases Network; Genomics England Research Consortium; Beltran, A. S.; Zimmermann, M. T.; Temple, B.; Moy, S. S.; Klee, E. W.; Tan, Q. K.-G.; Lorenzo, D. N. Pathogenic SPTBN1 Variants Cause an Autosomal Dominant Neurodevelopmental Syndrome. *Nat Genet* **2021**, *53* (7), 1006–1021. https://doi.org/10.1038/s41588-021-00886-z.

(103) Wu, R. Y.; Gill, G. N. LIM Domain Recognition of a Tyrosine-Containing Tight Turn. *Journal of Biological Chemistry* **1994**, *269* (40), 25085–25090. https://doi.org/10.1016/S0021-9258(17)31502-8.

(104) Liu, Y.; Hair, G. A.; Boden, S. D.; Viggeswarapu, M.; Titus, L. Overexpressed LIM Mineralization Proteins Do Not Require LIM Domains to Induce Bone. *J Bone Miner Res* **2002**, *17* (3), 406–414. https://doi.org/10.1359/jbmr.2002.17.3.406.

(105) Guy, P. M.; Kenny, D. A.; Gill, G. N. The PDZ Domain of the LIM Protein Enigma Binds To. *Molecular Biology of the Cell* **1999**, *10 (6)*, 1973–1984. https://doi.org/10.1091/mbc.10.6.1973.

(106) Kuroda, S.; Tokunaga, C.; Kiyohara, Y.; Higuchi, O.; Konishi, H.; Mizuno, K.; Gill, G. N.; Kikkawa, U. Protein-Protein Interaction of Zinc Finger LIM Domains with Protein Kinase C. *Journal of Biological Chemistry* **1996**, *271* (49), 31029–31032. https://doi.org/10.1074/jbc.271.49.31029.

(107) Durick, K.; Wu, R.-Y.; Gill, G. N.; Taylor, S. S. Mitogenic Signaling by Ret/Ptc2 Requires Association with Enigma via a LIM Domain. *Journal of Biological Chemistry* **1996**, *271* (22), 12691–12694. https://doi.org/10.1074/jbc.271.22.12691.

(108) Elbediwy, A.; Vanyai, H.; Diaz-de-la-Loza, M.-C.; Frith, D.; Snijders, A. P.; Thompson, B. J. Enigma Proteins Regulate YAP Mechanotransduction. *Journal of Cell Science* **2018**, jcs.221788. https://doi.org/10.1242/jcs.221788.

(109) Jodo, A.; Shibazaki, A.; Onuma, A.; Kaisho, T.; Tanaka, T. PDLIM7 Synergizes With PDLIM2 and P62/Sqstm1 to Inhibit Inflammatory Signaling by Promoting Degradation of the P65 Subunit of NF-κB. *Front. Immunol.* **2020**, *11*, 1559. https://doi.org/10.3389/fimmu.2020.01559.

(110) Boden, S. D.; Liu, Y.; Hair, G. A.; Helms, J. A.; Hu, D.; Racine, M.; Nanes, M. S.; Titus, L. LMP-1, A LIM-Domain Protein, Mediates BMP-6 Effects on Bone Formation. *Endocrinology* **1998**, *139* (12), 5125–5134. https://doi.org/10.1210/endo.139.12.6392.

(111) Kubota, H.; Hynes, G.; Willison, K. The Eighth Cct Gene, Cctq, Encoding the Theta Subunit of the Cytosolic Chaperonin Containing TCP-1. *Gene* **1995**, *154* (2), 231–236. https://doi.org/10.1016/0378-1119(94)00880-2.

(112) Brackley, K. I.; Grantham, J. Activities of the Chaperonin Containing TCP-1 (CCT): Implications for Cell Cycle Progression and Cytoskeletal Organisation. *Cell Stress and Chaperones* **2009**, *14* (1), 23–31. https://doi.org/10.1007/s12192-008-0057-x.

(113) Grantham, J.; Brackley, K. I.; Willison, K. R. Substantial CCT Activity Is Required for Cell Cycle Progression and Cytoskeletal Organization in Mammalian Cells. *Experimental Cell Research* **2006**, *312* (12), 2309–2324. https://doi.org/10.1016/j.yexcr.2006.03.028.

(114) Freund, A.; Zhong, F. L.; Venteicher, A. S.; Meng, Z.; Veenstra, T. D.; Frydman, J.; Artandi, S. E. Proteostatic Control of Telomerase Function through TRiC-Mediated Folding of TCAB1. *Cell* **2014**, *159* (6), 1389–1403. https://doi.org/10.1016/j.cell.2014.10.059.

(115) Qiu, X.; He, X.; Huang, Q.; Liu, X.; Sun, G.; Guo, J.; Yuan, D.; Yang, L.; Ban, N.; Fan, S.; Tao, T.; Wang, D. Overexpression of CCT8 and Its Significance for Tumor Cell Proliferation, Migration and Invasion in Glioma. *Pathology - Research and Practice* **2015**, *211* (10), 717–725. https://doi.org/10.1016/j.prp.2015.04.012.

(116) Yang, X.; Ren, H.; Shao, Y.; Sun, Y.; Zhang, L.; Li, H.; Zhang, X.; Yang, X.; Yu, W.; Fu, J. Chaperonin-Containing T-complex Protein 1 Subunit 8 Promotes Cell Migration and Invasion in Human Esophageal Squamous Cell Carcinoma by Regulating α-Actin and β-Tubulin Expression. *Int J Oncol* **2018**. https://doi.org/10.3892/ijo.2018.4335.

(117) Roobol, A.; Sahyoun, Z. P.; Carden, M. J. Selected Subunits of the Cytosolic Chaperonin Associate with Microtubules Assembled in Vitro. *Journal of Biological Chemistry* **1999**, *274* (4), 2408–2415. https://doi.org/10.1074/jbc.274.6408.

(118) Liu, L.; Pilch, P. F. A Critical Role of Cavin (Polymerase I and Transcript Release Factor) in Caveolae Formation and Organization. *Journal of Biological Chemistry* **2008**, *283* (7), 4314–4322. https://doi.org/10.1074/jbc.M707890200.

(119) Aboulaich, N.; Vainonen, J. P.; Strålfors, P.; Vener, A. V. Vectorial Proteomics Reveal Targeting, Phosphorylation and Specific Fragmentation of Polymerase I and Transcript Release Factor (PTRF) at the Surface of Caveolae in Human Adipocytes. *Biochemical Journal* **2004**, *383* (2), 237–248. https://doi.org/10.1042/BJ20040647.

(120) Jansa, P. Cloning and Functional Characterization of PTRF, a Novel Protein Which Induces Dissociation of Paused Ternary Transcription Complexes. *The EMBO Journal* **1998**, *17* (10), 2855–2864. https://doi.org/10.1093/emboj/17.10.2855.

(121) Volonte, D.; Galbiati, F. Polymerase I and Transcript Release Factor (PTRF)/Cavin-1 Is a Novel Regulator of Stress-Induced Premature Senescence. *Journal of Biological Chemistry* **2011**, *286* (33), 28657–28661. https://doi.org/10.1074/jbc.C111.235119.

(122) Low, J.-Y.; Nicholson, H. D. Emerging Role of Polymerase-1 and Transcript Release Factor (PTRF/ Cavin-1) in Health and Disease. *Cell Tissue Res* **2014**, *357* (3), 505–513. https://doi.org/10.1007/s00441-014-1964-z.

(123) Fesus, L.; Piacentini, M. Transglutaminase 2: An Enigmatic Enzyme with Diverse Functions. *Trends in Biochemical Sciences* **2002**, *27* (10), 534–539. https://doi.org/10.1016/S0968-0004(02)02182-5.

(124) Lorand, L.; Graham, R. M. Transglutaminases: Crosslinking Enzymes with Pleiotropic Functions. *Nat Rev Mol Cell Biol* **2003**, *4* (2), 140–156. https://doi.org/10.1038/nrm1014.

(125) Király, R.; Demény, MátéÁ.; Fésüs, L. Protein Transamidation by Transglutaminase 2 in Cells: A Disputed Ca2+-Dependent Action of a Multifunctional Protein: Protein Transamidation by Transglutaminase 2 in Cells. *FEBS Journal* **2011**, *278* (24), 4717–4739. https://doi.org/10.1111/j.1742-4658.2011.08345.x.

(126) Mehta, K. Mammalian Transglutaminases: A Family Portrait. In *Progress in Experimental Tumor Research*; Mehta, K., Eckert, R., Eds.; KARGER: Basel, 2005; Vol. 38, pp 1–18. https://doi.org/10.1159/000084229.

(127) Gottlieb, T. M.; Jackson, P. The DNA-Dependent Protein Ki for DNA Ends and AssocWbn with Ku Ant. *Cell* **1993**, *72* (1), 131–142. https://doi.org/10.1016/0092-8674(93)90057-W.

(128) Dynan, W. S.; Yoo, S. Interaction of Ku Protein and DNA-Dependent Protein Kinase Catalytic Subunit with Nucleic Acids. *Nucleic Acids Research* **1998**, *26* (7), 1551–1559. https://doi.org/10.1093/nar/26.7.1551.

(129) Tuteja, R.; Tuteja, N. Ku Autoantigen: A Multifunctional DNA-Binding Protein. *Critical Reviews in Biochemistry and Molecular Biology* **2000**, *35* (1), 1–33. https://doi.org/10.1080/10409230091169177.

(130) Lin, F.; Worman, H. J. Structural Organization of the Human Gene (LMNB1) Encoding Nuclear Lamin B1. *Genomics* **1995**, *27* (2), 230–236. https://doi.org/10.1006/geno.1995.1036.

(131) Dechat, T.; Pfleghaar, K.; Sengupta, K.; Shimi, T.; Shumaker, D. K.; Solimando, L.; Goldman, R. D. Nuclear Lamins: Major Factors in the Structural Organization and Function of the Nucleus and Chromatin. *Genes Dev.* **2008**, *22* (7), 832–853. https://doi.org/10.1101/gad.1652708.

(132) Shimi, T.; Pfleghaar, K.; Kojima, S.; Pack, C.-G.; Solovei, I.; Goldman, A. E.; Adam, S. A.; Shumaker, D. K.; Kinjo, M.; Cremer, T.; Goldman, R. D. The A- and B-Type Nuclear Lamin Networks: Microdomains Involved in Chromatin Organization and Transcription. *Genes Dev.* **2008**, *22* (24), 3409–3421. https://doi.org/10.1101/gad.1735208.

(133) Camps, J.; Erdos, M. R.; Ried, T. The Role of Lamin B1 for the Maintenance of Nuclear Structure and Function. *Nucleus* **2015**, *6* (1), 8–14. https://doi.org/10.1080/19491034.2014.1003510.

(134) Padiath, Q. S.; Saigoh, K.; Schiffmann, R.; Asahara, H.; Yamada, T.; Koeppen, A.; Hogan, K.; Ptáček, L. J.; Fu, Y.-H. Lamin B1 Duplications Cause Autosomal Dominant Leukodystrophy. *Nat Genet* **2006**, *38* (10), 1114–1123. https://doi.org/10.1038/ng1872.

(135) Giacomini, C.; Mahajani, S.; Ruffilli, R.; Marotta, R.; Gasparini, L. Lamin B1 Protein Is Required for Dendrite Development in Primary Mouse Cortical Neurons. *MBoC* **2016**, *27* (1), 35–47. https://doi.org/10.1091/mbc.E15-05-0307.

(136) M Shibuya; S Yamaguchi; A Yamane; T Ikeda; A Tojo; H Matsushime; M Sato. Nucleotide Sequence and Expression of a Novel Human Receptor-Type Tyrosine Kinase Gene (Flt) Closely Related to the Fms Family. Oncogene April 1990. https://pubmed.ncbi.nlm.nih.gov/2158038/.

(137) Seetharam L; Gotoh N; Maru Y; Neufeld G; Yamaguchi S; Shibuya M. A Unique Signal Transduction from FLT Tyrosine Kinase, a Receptor for Vascular Endothelial Growth Factor VEGF. Oncogene January 5, 1995. https://pubmed.ncbi.nlm.nih.gov/7824266/#affiliation-1.

(138) Shibuya, M. Structure and Function of VEGF/VEGF-Receptor System Involved in Angiogenesis. *Cell Struct. Funct.* **2001**, *26* (1), 25–35. https://doi.org/10.1247/csf.26.25.

(139) Shibuya, M. Vascular Endothelial Growth Factor Receptor-1 (VEGFR-1/Flt-1): A Dual Regulator for Angiogenesis. *Angiogenesis* **2006**, *9* (4), 225–230. https://doi.org/10.1007/s10456-006-9055-8.

(140) Amano, H.; Kato, S.; Ito, Y.; Eshima, K.; Ogawa, F.; Takahashi, R.; Sekiguchi, K.; Tamaki, H.; Sakagami, H.; Shibuya, M.; Majima, M. The Role of Vascular Endothelial Growth Factor Receptor-1 Signaling in the Recovery from Ischemia. *PLoS ONE* **2015**, *10* (7), e0131445. https://doi.org/10.1371/journal.pone.0131445.

(141) Kendall, R. L.; Thomas, K. A. Inhibition of Vascular Endothelial Cell Growth Factor Activity by an Endogenously Encoded Soluble Receptor. *Proc. Natl. Acad. Sci. U.S.A.* **1993**, *90* (22), 10705–10709. https://doi.org/10.1073/pnas.90.22.10705.

(142) Shibuya, M. Vascular Endothelial Growth Factor and Its Receptor System: Physiological Functions in Angiogenesis and Pathological Roles in Various Diseases. *Journal of Biochemistry* **2013**, *153* (1), 13–19. https://doi.org/10.1093/jb/mvs136.

(143) *Wilson and Walker's Principles and Techniques of Biochemistry and Molecular Biology:*, 8th ed.; Hofmann, A., Clokie, S., Eds.; Cambridge University Press, 2018. https://doi.org/10.1017/9781316677056.

(144) Ehrhardt, C.; Collnot, E.-M.; Baldes, C.; Becker, U.; Laue, M.; Kim, K.-J.; Lehr, C.-M. Towards an in Vitro Model of Cystic Fibrosis Small Airway Epithelium: Characterisation of the Human Bronchial Epithelial Cell Line CFBE41o-. *Cell Tissue Res* **2006**, *323* (3), 405–415. https://doi.org/10.1007/s00441-005-0062-7.

(145) Hallows, K. R.; Fitch, A. C.; Richardson, C. A.; Reynolds, P. R.; Clancy, J. P.; Dagher, P. C.; Witters, L. A.; Kolls, J. K.; Pilewski, J. M. Up-Regulation of AMP-Activated Kinase by Dysfunctional Cystic Fibrosis Transmembrane Conductance Regulator in Cystic Fibrosis Airway Epithelial Cells Mitigates Excessive Inflammation. *Journal of Biological Chemistry* **2006**, *281* (7), 4231–4241. https://doi.org/10.1074/jbc.M511029200.

(146) Farrell, R. E. RNAi: Take a RSIC - Role the Dicer. In *RNA Methodologies*; Elsevier, 2010; pp 539–560.

(147) Dalby, B.; Cates, S.; Harris, A.; Ohki, E. C.; Tilkins, M. L.; Price, P. J.; Ciccarone, V. C. Advanced Transfection with Lipofectamine 2000 Reagent: Primary Neurons, siRNA, and High-Throughput Applications. *Methods* **2004**, *33*, 95–103. https://doi.org/10.1016/j.ymeth.2003.11.023.

(148) Kim, T. K.; Eberwine, J. H. Mammalian Cell Transfection: The Present and the Future. *Anal Bioanal Chem* **2010**, *397* (8), 3173–3178. https://doi.org/10.1007/s00216-010-3821-6.

(149) Almaça, J.; Dahimène, S.; Appel, N.; Conrad, C.; Kunzelmann, K.; Pepperkok, R.; Amaral, M. D. Functional Genomics Assays to Study CFTR Traffic and ENaC Function. In *Cystic Fibrosis*; Amaral, M. D., Kunzelmann, K., Eds.; Methods in Molecular Biology; Humana Press: Totowa, NJ, 2011; Vol. 742, pp 249–264. https://doi.org/10.1007/978-1-61779-120-8_15.
(150) Farkas, D. H.; Holland, C. A. Overview of Molecular Diagnostic Techniques and Instrumentation. In *Cell and Tissue Based Molecular Pathology*; Elsevier, 2009; pp 19–32. https://doi.org/10.1016/B978-044306901-7.50008-0.
(151) Farrell, R. E. RNA Isolation Strategies. *RNA Methodologies* 36.
(152) Garibyan, L.; Avashia, N. Polymerase Chain Reaction. *Journal of Investigative Dermatology* **2013**, *133* (3), 1–4. https://doi.org/10.1038/jid.2013.1.
(153) Farrell, R. E. Quantitative PCR Techniques. *RNA Methodologies* 41.
(154) Robert E. Farrell, Jr. RNA Methodologies A Laboratory Guide for Isolation and Characterization - Chapter 18 - RT-PCR: A Science and an Art Form. **2010**. https://doi.org/10.1016/B978-0-12-374727-3.00018-8.
(155) Boyer, R. F. *Biochemistry Laboratory: Modern Theory and Techniques*, 2nd ed.; Prentice Hall: Boston, 2012.
(156) Voytas, D. Agarose Gel Electrophoresis. In *Current Protocols in Molecular Biology*; Ausubel, F. M., Brent, R., Kingston, R. E., Moore, D. D., Seidman, J. G., Smith, J. A., Struhl, K., Eds.; John Wiley & Sons, Inc.: Hoboken, NJ, USA, 2001; p mb0205as51. https://doi.org/10.1002/0471142727.mb0205as51.
(157) Kohanski, R. A. Biotinylation of Proteins. In *Encyclopedia of Biological Chemistry*; Elsevier, 2013; pp 226–228. https://doi.org/10.1016/B978-0-12-378630-2.00168-7.
(158) Rybak, J.-N.; Scheurer, S. B.; Neri, D.; Elia, G. Purification of Biotinylated Proteins on Streptavidin Resin: A Protocol for Quantitative Elution. *Proteomics* **2004**, *4* (8), 2296–2299. https://doi.org/10.1002/pmic.200300780.
(159) Elia, G. Biotinylation Reagents for the Study of Cell Surface Proteins. *Proteomics* **2008**, *8* (19), 4012–4024. https://doi.org/10.1002/pmic.200800097.
(160) Luna, E. J. Biotinylation of Proteins in Solution and on Cell Surfaces. *Current Protocols in Protein Science* **1996**, *6* (1). https://doi.org/10.1002/0471140864.ps0306s06.
(161) Elia, G. Protein Biotinylation. *Current Protocols in Protein Science* **2010**, *60* (1). https://doi.org/10.1002/0471140864.ps0306s60.
(162) Heizmann, C. W.; Fritz, G.; Schäfer, B. W. S100 PROTEINS: STRUCTURE, FUNCTIONS AND PATHOLOGY. *Frontiers in Bioscience 7*, d1356-1368. https://doi.org/10.2741/A846.
(163) Sreejit, G.; Flynn, M. C.; Patil, M.; Krishnamurthy, P.; Murphy, A. J.; Nagareddy, P. R. S100 Family Proteins in Inflammation and Beyond. In *Advances in Clinical Chemistry*; Elsevier, 2020; Vol. 98, pp 173–231. https://doi.org/10.1016/bs.acc.2020.02.006.
(164) Murao, S.; Collart, F. R.; Huberman, E. A Protein Containing the Cystic Fibrosis Antigen Is an Inhibitor of Protein Kinases. *Journal of Biological Chemistry* **1989**, *264* (14), 8356–8360. https://doi.org/10.1016/S0021-9258(18)83189-1.
(165) Roth, J.; Teigelkamp, S.; Wilke, M.; Grün, L.; Tümmler, B.; Sorg, C. Complex Pattern of the Myelo-Monocytic Differentiation Antigens MRP8 and MRP14 during Chronic Airway Inflammation. *Immunobiology* **1992**, *186* (3–4), 304–314. https://doi.org/10.1016/S0171-2985(11)80259-7.
(166) Amano, H.; Matsui, Y.; Hatanaka, K.; Hosono, K.; Ito, Y. VEGFR1-Tyrosine Kinase Signaling in Pulmonary Fibrosis. *Inflamm Regener* **2021**, *41* (1), 16. https://doi.org/10.1186/s41232-021-00166-7.

(167) Amano, H.; Mastui, Y.; Ito, Y.; Shibata, Y.; Betto, T.; Eshima, K.; Ogawa, F.; Satoh, Y.; Shibuya, M.; Majima, M. The Role of Vascular Endothelial Growth Factor Receptor 1 Tyrosine Kinase Signaling in Bleomycin-Induced Pulmonary Fibrosis. *Biomedicine & Pharmacotherapy* **2019**, *117*, 109067. https://doi.org/10.1016/j.biopha.2019.109067.

(168) Martin, C.; Coolen, N.; Wu, Y.; Thévenot, G.; Touqui, L.; Prulière-Escabasse, V.; Papon, J.-F.; Coste, A.; Escudier, E.; Dusser, D. J.; Fajac, I.; Burgel, P.-R. CFTR Dysfunction Induces Vascular Endothelial Growth Factor Synthesis in Airway Epithelium. *Eur Respir J* **2013**, *42* (6), 1553–1562. https://doi.org/10.1183/09031936.00164212.

(169) Fukuda, M. Membrane Traffic in the Secretory Pathway: Regulation of Secretory Vesicle Traffic by Rab Small GTPases. *Cell. Mol. Life Sci.* **2008**, *65* (18), 2801–2813. https://doi.org/10.1007/s00018-008-8351-4.

(170) Saxena, S. K.; Kaur, S. Rab27a Negatively Regulates CFTR Chloride Channel Function in Colonic Epithelia: Involvement of the Effector Proteins in the Regulatory Mechanism. *Biochemical and Biophysical Research Communications* **2006**, *346* (1), 259–267. https://doi.org/10.1016/j.bbrc.2006.05.102.

(171) Quaresma, M. C.; Botelho, H. M.; Pankonien, I.; Rodrigues, C. S.; Pinto, M. C.; Costa, P. R.; Duarte, A.; Amaral, M. D. Exploring YAP1-Centered Networks Linking Dysfunctional CFTR to Epithelial–Mesenchymal Transition. *Life Sci. Alliance* **2022**, *5* (9), e202101326. https://doi.org/10.26508/lsa.202101326.

(172) Tosco, A.; De Gregorio, F.; Esposito, S.; De Stefano, D.; Sana, I.; Ferrari, E.; Sepe, A.; Salvadori, L.; Buonpensiero, P.; Di Pasqua, A.; Grassia, R.; Leone, C. A.; Guido, S.; De Rosa, G.; Lusa, S.; Bona, G.; Stoll, G.; Maiuri, M. C.; Mehta, A.; Kroemer, G.; Maiuri, L.; Raia, V. A Novel Treatment of Cystic Fibrosis Acting On-Target: Cysteamine plus Epigallocatechin Gallate for the Autophagy-Dependent Rescue of Class II-Mutated CFTR. *Cell Death Differ* **2016**, *23* (8), 1380–1393. https://doi.org/10.1038/cdd.2016.22.

(173) Luciani, A.; Villella, V. R.; Esposito, S.; Brunetti-Pierri, N.; Medina, D.; Settembre, C.; Gavina, M.; Pulze, L.; Giardino, I.; Pettoello-Mantovani, M.; D'Apolito, M.; Guido, S.; Masliah, E.; Spencer, B.; Quaratino, S.; Raia, V.; Ballabio, A.; Maiuri, L. Defective CFTR Induces Aggresome Formation and Lung Inflammation in Cystic Fibrosis through ROS-Mediated Autophagy Inhibition. *Nat Cell Biol* **2010**, *12* (9), 863–875. https://doi.org/10.1038/ncb2090.

(174) Stefano, D. D.; Villella, V. R.; Esposito, S.; Tosco, A.; Sepe, A.; Gregorio, F. D.; Salvadori, L.; Grassia, R.; Leone, C. A.; Rosa, G. D.; Maiuri, M. C.; Pettoello-Mantovani, M.; Guido, S.; Bossi, A.; Zolin, A.; Venerando, A.; Pinna, L. A.; Mehta, A.; Bona, G.; Kroemer, G.; Maiuri, L.; Raia, V. Restoration of CFTR Function in Patients with Cystic Fibrosis Carrying the F508del-CFTR Mutation. *Autophagy* **2014**, *10* (11), 2053–2074. https://doi.org/10.4161/15548627.2014.973737.

(175) Esposito, S.; Tosco, A.; Villella, V. R.; Raia, V.; Kroemer, G.; Maiuri, L. Manipulating Proteostasis to Repair the F508del-CFTR Defect in Cystic Fibrosis. *Mol Cell Pediatr* **2016**, *3* (1), 13. https://doi.org/10.1186/s40348-016-0040-z.